DESIGN AND ANALYSIS OF CONTROLLERS FOR MAGNETIC LEVITATION SYSTEMS

Thesis submitted to Andhra University
for the award of the Degree of

DOCTOR OF PHILOSOPHY

In

ELECTRICAL ENGINEERING

By

P. ANANTHABABU, M.E

Under the Guidance of

Dr. K. RAMA SUDHA, M.E., Ph.D.

Professor, Department of Electrical Engineering
Andhra University, Visakhapatnam – 03

DEPARTMENT OF ELECTRICAL ENGINEERING
COLLEGE OF ENGINEERING (AUTONOMOUS)
ANDHRA UNIVERSITY
VISAKHAPATNAM – 530 003
INDIA
2018

DECLARATION

I hereby declare that the thesis entitled **"DESIGN AND ANALYSIS OF CONTROLLERS FOR MAGNETIC LEVITATION SYSTEMS"** has been written by me and has not been submitted either in part or whole for the award of any degree, diploma or any other similar title to this or any other university.

Date: **(P. ANANTHABABU)**

COLLEGE OF ENGINEERING (A)
ANDHRA UNIVERSITY

CERTIFICATE

This is to certify that the thesis entitled "**DESIGN AND ANALYSIS OF CONTROLLERS FOR MAGNETIC LEVITATION SYSTEMS**" submitted by Mr. P. ANANTHABABU, in fulfilment of the requirement for the award of Ph.D. Degree in Electrical Engineering, College of Engineering (A), Andhra University, is a bonafide thesis work carried out by him under my guidance and supervision in the Department of Electrical Engineering, College of Engineering (A), Andhra University, Visakhapatnam. This work has not been submitted to any university for award of any degree.

Research Guide

Dr. K. Rama Sudha, *M.E., Ph.D*
Professor,
Department of Electrical Engineering,
Andhra University,
Visakhapatnam-530003,
 India.

ACKNOWLEDGEMENTS

I express my gratitude to my father Venkateswara Rao, my mother Kotiratnam, my wife Sirisha, my son Divija Karthik, my brother Venkata Krishna Rao for their encouragement and support during the period of this work.

Finally, I thank **everyone** who has directly or indirectly helped me during the course of this work.

<div align="right">

P. ANANTHABABU

</div>

ABSTRACT

Magnetic levitation (Maglev) has been a keen area of research, especially in the field of transportation. Maglev is used in order to reduce the maintenance cost, increase the efficiency and thereby to increase the useful life of the system. Maglev has numerous practical applications in research and industry where friction must be reduced or eliminated. Some of the more promising applications are transportation (low and high speed maglev), low friction bearings for gyroscopes and fly wheel energy storage. Other applications have been proposed, such as levitation melting of conductive metals. Applications such as eddy current braking and induction heating that involve similar physical processes as Maglev can be analyzed using similar or slightly modified solution techniques.

Eddy current damping is a key technique that improves levitation performance to increase the diversity of applications of Maglev systems. Eddy current damping is formed by a conductive plate placed below the levitating object, which is used to suppress vibrations and ensure stability. To understand the system behaviour, it is very important to derive the analytical relation for the eddy current based force. It is a function of the plate thickness and its distance to the permagnet. Position control of the Maglev system is not an easy task. Literature shows several authors have proposed different controllers to stabilise the position of the object in the air. The main drawback is that the controllers are designed by neglecting

the eddy current based force due to the motion of the levitated object. In the present work, Fractional order model reference adaptive controller, Backstepping fuzzy sliding mode controller, PID controller based on cuckoo search algorithm are designed for position tracking of Maglev system; each controller has its own importance in each case. Literature shows that, the Fractional Order Model Reference Adaptive Controller (FOMRAC) could make the entire control system perform better. This is due to FOMRAC controller satisfies five robustness criteria as compared with classical controller which has to satisfy three robustness criteria.

In first case, a FOMRAC controller is designed to reduce vibrations in the object as well as position tracking. The Model Reference Adaptive System (MRAS) is one of the main approaches to adaptive control, in which the desired performance is expressed in terms of a reference model and the parameters of the controller are adjusted based on the error between the reference model output and the system output. Using FOMRAC, Maglev system takes very short interval time to reach its desired position when compared with conventional controller and same has been shown in simulations.

In the second case, backstepping fuzzy sliding mode controller is designed for the position tracking of Maglev system. Backstepping fuzzy sliding mode control approach combines the fuzzy sliding mode control technique and the backstepping technique to achieve the position tracking of nonlinear Maglev system. A linear model that

represents the nonlinear dynamics of the Maglev system is derived by feedback linearization technique. Then backstepping fuzzy sliding mode control is derived from the proposed linear model based on the Lyapunov function approach, which is capable of handling nonlinear systems. Simulation results show the effectiveness of the backstepping fuzzy sliding mode control scheme for the position tracking of nonlinear Maglev system.

In third case, PID controller based on Cuckoo search algorithm is designed for the position tracking of real time Maglev system. The proportional-integral-derivative (PID) controller and its variants remain the controllers of choice in many applications, despite the efforts put in for the development of advanced control schemes over the past two decades. Maglev systems are highly nonlinear and unstable systems. In the present work, a noval method of global optimization algorithm, cuckoo search algorithm is proposed, to tune the parameters of PID controller. The proposed PID controller is tested on real time maglev system. Simulation results show the effectiveness of the cuckoo search based PID controller for position tracking of real time Maglev system.

Maglev is used in transportation system for high speed trains in which the vehicle is lifted from roadway by a magnetic field. LIM is usually preferred since it offers high precision and accuracy of the controlled acceleration and deceleration thereby reducing the maintenance cost. They are also used in a vast array of diverse

applications like industries. These applications require machines that can produce large forces, operate at high speeds and can be controlled precisely to meet performance requirements.

In the present work, parameters of single sided Linear Induction Motor (sLIM) are calculated based on rotary induction motor principle and same has been implemented in the design of prototype sLIM. A PID controller based on cuckoo search algorithm is designed for the speed control of sLIM. The computation results show that the proposed sLIM drive system is appropriate for driving maglev transportation prototype.

TABLE OF CONTENTS

LIST OF FIGURES

LIST OF TABLES

LIST OF ABBREVIATIONS

ABC	-	Artificial Bee Colony
BelM	-	Bearing less motors
BFNNC	-	Backstepping Fuzzy Neural Network Control
CARIMA	-	Controlled Auto Regressive Integrated Moving Average
CDM	-	Coefficient Diagram Method
CS	-	Cuckoo Search
CSA	-	Cuckoo Search Algorithm
DLIM	-	Double Sided Linear Induction Motor
DOF	-	Degree of Freedom
ECD	-	Eddy Current Damping
EDS	-	Electrodynamic Suspension
EMS	-	Electromagnetic Suspension
ES	-	Extremum Seeking
FEM	-	Finite Element Method
FIR	-	Finite Impulse Response
FODE	-	Fractional Order Differential Equation
FOPID	-	Fractional order Proportional –Integral – Derivative
GA	-	Genetic Algorithm
HTS	-	High Temperature Superconducting
IAE	-	Integral Absolute Error
IR	-	Infrared
ISE	-	Integral Square Error

ITAE	-	Integral Time Absolute Error
ITSE	-	Integral Time Square Error
KVL	-	Kirchhoff's Voltage Law
LabVIEW	-	Laboratory Virtual Instrument Engineering Workbench
LEE	-	Longitudinal End Effect
LIM	-	Linear Induction Motor
LQG	-	Linear Quadratic Gaussian
Maglev	-	Magnetic Levitation
MATLAB	-	Matrix Laboratory
MCLEVS	-	Microprocessor Controlled hybrid magnetic levitation and propulsion system
MIT	-	Massachusetts Institute of Technology
MIMO	-	Multi Input Multi Output
MLS	-	Magnetic Levitation System
MPC	-	Model Predictive Controller
MRAC	-	Model Reference Adaptive Controller
MRAS	-	Model Reference Adaptive System
NB	-	Negative Big
Nd	-	Neodymium
NM	-	Negative Medium
NMLS	-	Nonlinear Magnetic Levitation System
NS	-	Negative Small
PB	-	Positive Big
PFC	-	Parallel Feedforward Compensator

PID - Proportional- Integral-Derivative

PM - Permanent Magnet

PS - Positive Small

PSO - Particle Swarm optimization

RLS - Recursive Least Square

RMS - Root Mean Square

SISO - Single Input Single Output

sLIM - single sided Linear Induction Motor

SMC - Sliding Mode Control

SoS - Sum of Squares

TLIM - Tabular Linear Induction Motor

Z - Zero

LIST OF SYMBOLS /ACRONYMS

(For Maglev System)

λ — Order of Integrator

μ — Order of differentiator

K_P — Proportional gain

K_I — Integral gain

K_D — Derivative gain

D — Differentiation

μ_r — Relative permeability

F_{PM} — Force due to Permanent Magnet

M — Mass of the permagnet

c — Magnetic Force constant

g — Gravitational constant

A — Magnetic Vector Potential

σ — Conductivity of the Plate

μ_0 — Permeability of the free space

h — Height of the levitated object from plate

v — Velocity of the permanent Magnet

m — Magnetic dipole moment

r — Radius of the coil

w — Width of the plate

J — Current density

B_{eddy} — Eddy current damping coefficient

γ - Adaptation gain

α - order of derivative

f - Electromagnet force

L - Inductance

k_i - Current amplification gain

k_1 - Control voltage gain

k_2 - Sensor gain

y - Position of the levitated object

i - Current in the electromagnet

LIST OF SYMBOLS /ACRONYMS

(For Linear Induction Motor)

p	- Number of poles
f	- Frequency
V_s	- Synchronous velocity
V_r	- Rotor speed
s	- slip
R	- Stator radius of the rotary induction motor
τ	- Pole pitch
L_s	- Length of the stator
J_m	- Current sheet strength
m	- Number of phases
k_w	- Winding factor
N_c	- Number of turns per slot
I_1	- RMS Value of the stator Current
k_p	- pitch factor
k_d	- Distribution factor
θ_p	- Coil span
α	- Slot angle
q_1	- Slots-per-pole-per-phase
V_1	- RMS input phase voltage
$\cos \emptyset$	- Power factor
P_i	- Input power
P_0	- Mechanical output power

F_s	- Electromagnetic thrust
η	- Efficiency
N	- Number of turns
ϕ	- Flux
ϕ_p	- Flux linkage per pole
e	- Induced voltage per turn
E_1	- RMS value of induced voltage
B_{gavg}	- Average air-gap magnetic flux density
W_s	- Width of the stator iron core
$B_{g\,max}$	- Maximum air-gap flux density
g_e	- Effective air-gap
g_m	- Physical air-gap
g_0	- Magnetic air-gap
d	- Thickness of the conducting sheet
k_c	- Carter's Coefficient
λ	- Slot pitch
w_s	- Slot width
w_t	- Tooth width
$w_{t\,min}$	- Minimum value of tooth width
$B_{t\,max}$	- Maximum tooth flux density
h_s	- Slot depth
A_s	- Cross-sectional area of slot
A_w	- Area of cross-section of conductor
J_1	- Stator current density

h_y	- Yoke height of the stator core
V_c	- Linear speed of the rotor
R_1	- per-phase stator resistance
ρ_w	- Resistivity of the copper wire
l_w	- Length of the copper wire per phase
A_{wt}	- Cross-sectional area of the wire
l_{w1}	- Mean length of the one turn per phase
l_{ce}	- Length of end connection
X_1	- per-phase stator slot leakage reactance
X_m	- per-phase magnetizing reactance
R_2	- per-phase rotor resistance
G	- Goodness factor
ρ_r	- Resistivity of the rotor conductor outer layer
I_2	- Rotor phase current
i_{ds}	- d-axis primary current
i_{qs}	- q-axis primary current
V_{ds}	- d-axis primary voltage
V_{qs}	- q-axis primary voltage
$\emptyset_{dr}$	- d-axis secondary flux
$\emptyset_{qr}$	- q-axis secondary flux

Chapter – I

INTRODUCTION

1.1. Introduction

The Magnetic levitation (Maglev) system is an example of nonlinear, open loop unstable system with fast dynamics, which makes the modelling and design of controller difficult [1]. However, Magnetic levitation has numerous practical applications in research and industry where friction must be reduced or eliminated. Some of the more promising applications are transportation [2], [3] (low and high speed Maglev), low friction bearings for gyroscopes [4] and fly wheel energy storage [5]. Magnetic levitation is a method by which an object is suspended with no support other than magnetic fields. Magnetic force is used to counteract the effects of the gravitational force and any other forces. The two primary issues involved in magnetic levitation are (i) Lifting forces: providing an upward force sufficient to counteract gravity, and (ii) Stability: ensuring that the system does not spontaneously slide or flip into a configuration where the lift is neutralized.

Eddy currents are induced when a nonmagnetic, conductive material is moving as the result of being subjected to a magnetic field, or if it is placed in a time-varying magnetic field. These currents circulate in the conductive material causing a repulsive force between the magnet and the conductor. With this concept, eddy current

damping can be used as a form of viscous damping. The eddy current generates heat which is utilized in various applications like brazing, hardening and induction furnaces etc., and also used in non-destructive testing of conductive materials

Kwak et al. [6] investigated the effects of an eddy current damper on a cantilever beam and their experimental results showed that an eddy current damper can be an effective device for vibration suppression. Jae-Sung Bae et al. [7] conducted experiment to study the characteristics of eddy current damping when a permanent magnet is placed in a conductive tube. In his experiment, the eddy current damping appears as the result of a magnet in a copper tube which is developed from electromagnetics. However, their investigation, while meaningful, failed to produce a detailed eddy current damping model. It is easy to understand the eddy current effects if the analytical models are available. In [8], an analytical model is presented for a thin conductive plate exposed to a time-varying magnetic field. Using this, the system can be modelled for magnetic fields in the direction perpendicular to the plate. This can be a limitation in most problems.

1.2   Overview of Maglev System

Magnetic levitation or Magnetic suspension is a method by which an object is suspended with no support other than magnetic fields. Magnetic force is used to counteract the effects of the gravitational acceleration and any other accelerations. Maglev system,

using the electromagnetic force to float, can effectively reduce the mechanical vibration friction and wearing loss caused by contact operation. However, the parameters in the mathematical model are related to the permanent magnet geometry, distance and the total mass. Maglev is used in order to reduce the maintenance cost, increase the efficiency and thereby the useful life of the system is increased [9].

Earnshaw's theorem [10] proves that using only paramagnetic materials (such as ferromagnetic iron) it is impossible for a static system to stably levitate against gravity. Static stability means that any small displacement away from a stable equilibrium causes a net force to push it back to the equilibrium point. Dynamic stability occurs when the levitation system is able to damp out any vibration-like motion that may occur.

Magnetic fields are conservative forces and therefore in principle have no built-in damping and in practice many of the levitation schemes are under damped and in some cases negatively damped [11]. This can permit vibration modes to exist that can cause the item to leave the stable region.

Damping of motion is done in a number of ways:
- external mechanical damping (in the support), such as dashpots, air drag etc.
- eddy current damping (conductive metal influenced by field)
- tuned mass dampers in the levitated object

➢ electromagnets controlled by electronics

1.2.1 Eddy current based force

Eddy currents are used in Maglev system to stabilize the position of the levitated object.

In the Maglev system, the levitated object can be moved in z direction as well as in x and y directions. By varying the field of electromagnet [12], object will be moved in z direction and by moving the electromagnet, object will be moved in x and y directions. Eddy currents are produced in the plate by the variations of levitated object, these eddy currents produces magnetic field which opposes the motion of the levitated object (according to Lenz's Law). The eddy current in the plate is linearly proportional to the velocity of the object and the rate of change of electromagnet current.

1.2.2 Application of Maglev system

In order to appropriately serve the public, a new-generation transportation system must meet certain requirements such as rapidity, reliability and safety. In addition, it should be convenient, environment-friendly, low maintenance, compact, light-weight, unattained and suited to mass transportation. The Maglev train is one of the best example to satisfy these requirements [13].

There are three essential parts to achieve Maglev functionality; levitation, propulsion and guidance in a Maglev. Levitation is a method by which an object is suspended in air with no support other

than magnetic fields. There are three important types of levitation technology: electromagnetic suspension (EMS), electrodynamic suspension (EDS) and hybrid electromagnetic suspension (HEMS).

In electromagnetic suspension, levitation is accomplished based on the magnetic attraction force between a guideway and electromagnets. This methodology is inherently unstable due to the characteristics of the magnetic circuit [14]. Electrodynamic suspension uses repulsive force for the levitation [15]-[17]. When the magnets attached on board move forward on the inducing coils or conducting sheets located on the guideway, the induced currents flow through the coils or sheets and generate the magnetic field. The repulsive force between this magnetic field and the magnets levitates the vehicle. In order to reduce the electric power consumption in EMS, permanent magnets are partly used with electromagnets in the case of hybrid electromagnetic suspension [18].

Propulsion is the force that drives the train forward. Maglev uses a Linear Induction Motor (LIM) to achieve propulsion. A normal electric rotary motor uses magnetism to create torque and spin an axle. It has a stationary piece, the stator, which surrounds a rotating piece, the rotor. The stator is used to generate a rotating magnetic field. This field induces a rotational force on the rotor, which causes it to spin. A linear motor is simply an unrolled version of this.

1.2.3 Linear Induction Motor (LIM)

In transportation, LIMs have been implemented as propulsion systems for transit vehicles in a number of countries [19]. In steel power plants, for high quality and high productivity, linear induction motor has been researched and practically used for transporting thin steel plates during reheating and galvanization process [20].There are different types of LIMs, among them, single-sided linear induction motors (sLIMs) are widely used in transportation systems [21]–[24]

Design of single-sided Linear Induction Motors (sLIMs) demands preparation of data sheet for stator and rotor dimensions. Number of stator and rotor slots, inner and outer dimensions, tooth and slot dimensions and conductor size requirement are some of the design parameters require to manufacture a sLIM [25]. These parameters affect the performance of the machine in different manners. Increasing a certain parameter may increase an output, at the same time, it may decrease another one.

1.3   Literature Survey

R J Wai, et al. [26] implemented a backstepping fuzzy-neural-network control (BFNNC) for the real time levitated balancing and propulsive positioning of a hybrid magnetic levitation transportation system. Due to the use of hybrid electromagnets, suspension power loss is minimized.

Dan Cho, et al. [27] discussed about sliding mode controller and classical controller for stabilizing and commanding a single axis magnetic levitation system and also mentioned that classical controller does not provide as much damping as sliding mode controller.

Sirsendu S. M, et al. [28] designed a Coefficient Diagram Method based PID controller for Maglev system with time delay. The parameters of the CDM-PID controller are tuned by using algebraic based methodologies. Due to the proposed controller, there is an improvement in the transient performance and error indices.

Bhawna T, et al. [29] discussed the stability analysis of Maglev system based on a nonlinear controller using Sum of Squares (SoS) technique. Nonlinear controller must be required to apply SoS technique to Maglev System.

Rosalia H Subrata et al. [30] designed a PID controller to stabilize floating objects in Maglev systems. Maglev system has unstable nonlinear dynamics which should be taken into account. It is a great extent of controller to stabilize the system by considering nonlinear dynamics.

A. S. C. Roong et al. [31] designed a model based feed forward PI-PD controller for position tracking of Maglev system. But this controller requires a sensor and a model for each disturbance.

R. E. Precup, et al. [32] proposed an evolving Takagi-Sugeno (T-S) fuzzy models that characterize the nonlinear dynamics phenomena occurring in the position of Maglev systems. A state feedback control structure has to design first to stabilize the nonlinear process by a linearization technique at certain operating points.

B. Singh, et al. [33] proposed an adaptive control algorithm for the position tracking of real time Maglev system using MRAC technique. An important problem associated with the MRAC system is to determine the adjustment mechanism so that a stable system brings the error to zero. The parameters of PID controller are adjusted automatically in MRAC technique.

K. H. Su et al. [34] proposed fuzzy and supervisory fuzzy models based on gradient descent algorithm for the Maglev system. In the proposed method, mathematical model of Maglev system is replaced with fuzzy model to achieve the good tracking performance, reduce the chattering phenomenon and good transient response.

Ahmed El Hajjaji et al. [35] developed a non-linear model for magnetic levitation system after validation with experimental results and a non-linear control law based on differential geometry was synthesized and then implemented in real time.

R J Wai et al. [36] designed a PID controller based on particle swarm optimization for the Maglev transportation system. The main objective

is to tune the gains of PID controller by implementing particle swarm optimization technique.

Kim K et al. [37] proposed an indirect method for self-tuning PID controller gains for a digital excitation system. The proposed method uses Recursive Least Square (RLS) estimation method to tune the parameters of PID controller. The loop gain is estimated at a steady-state condition of the closed loop with a PI controller. Time constants of the exciter and generator are identified with RLS.

M Shafiq et al. [38] developed a controller based on adaptive finite impulse response (FIR) filter for the tracking of a ferric ball under the influence of magnetic force. To improve the stability, an adaptive FIR filter is added along side the PID controller. The adaptive FIR filters are inherently stable so the controller remains stable.

Chang. Wu et al. [39] developed a simple implicit generalized predictive self-tuning control based on Controlled Auto-Regressive Integrated Moving-Average (CARIMA) model for an active magnetic bearing system. The proposed control strategy is a new method of remote predictive control, which combines the advantages of various algorithms as a whole and guarantees the stability of the open loop unstable system.

S. Sgaverdea et al. [40] developed a state feedback controller as well as model predictive controllers (MPCs) for the position control of a sphere in a magnetic levitation system. A state feedback control structure is

first designed to stabilize the system. In order to ensure the zero steady-state control errors, the second controller designed based on MPC in the outer control loop.

M. Ahsan et al. [41] designed different non-linear controllers for position tracking under the presence of parametric uncertainties and external disturbances in a magnetic suspension system.

A. Rawat et al. [42] designed adaptive linear and nerocontroller for Maglev System using feedback linearization and Lyapunov's stability analysis. The combination of feedback linearizing control law and adaptive laws ensures that the closed loop system is stable.

I. Mizumoto et al. [43] designed Almost Strict Positive Real (ASPR) based adaptive PID controller for magnetic levitation system with a Parallel Feedforward Compensator (PFC). The static PFC shows a windup phenomenon at transient state and the control performance deteriorates when the input is saturated.

C. S. Chin et al. [44] designed the prototype microprocessor controlled hybrid magnetic levitation and propulsion system (MCLEVS) for conveyance purposes, consisting of a linear synchronous motor and a hybrid electromagnetic levitation.

C. S. Teodorescu et al. [45] discussed the analytical solutions and treat systematically feasibility, stability and optimality issues in a Maglev system. It is very important to understand dynamic behavior of system.

J. H. Yang et al. [46] proposed a modeling equipment for Maglev system and an automatic algorithm for making the 2D lookup table from the experimentally measured data. Modeling equipment measures the magnetic force exerted on the levitation object, the coil current of electromagnet and the distance between the levitation object and the electromagnet.

Feng Li, K et al. [47] designed a novel PTC method using multi-rate feedforward control which can be used in non-minimum phase systems of the discrete time systems. The proposed technique is applicable to non-minimum phase discrete time systems and the oscillations between the sampling points are restrained well.

A. Kumar et al. [48] proposed a nonlinear fractional order PID controller for 5- DOF redundant robot manipulator for joint trajectory tracking task. To find the parameters of the fractional order PID controller is a challenging task. The optimal FOPID controller parameters are tuned using recent Artificial Bee Colony (ABC) optimization technique.

T. George et al. [49] proposed a hybrid technique for tuning time delay system with proportional-integral-derivative (PID) controller. Due to the proposed technique performance and the robustness for a class of time delay system are improved. The proposed hybrid technique is the combination of the iterative algorithm and curve fitting technique.

N. Kanagara et al. [50] proposed an intelligent fuzzy fractional order PID Controller for pressure regulating system model. The conventional control schemes are limited to simple processes with a specified operating range and not satisfactory for load disturbances and changes in set-point. The proposed controller overcomes the problem with conventional controller.

Q. Chen et al. [51] designed a decentralized PID controller for Maglev system based on using Extremum Seeking (ES) method of optimization. The proposed controller utilizes the extremum seeking method to tune the parameters on-line to improve steady state performance with few oscillations. The ES is implemented in a decentralized way and the initial value of PID parameters came from trial-and-error methods.

Xiaojia Li et al. [52] developed a novel superconducting magnetic levitation method to support the laser fusion capsule by using permanent magnets. This method can keep the perfect symmetry of the octahedral spherical hohlraum and has the characteristics in stability, tunability and simplicity.

J. J. Hernandez Casanas et al. [53] designed a adaptive fuzzy model reference control for Maglev system. The control law chosen is a mamdani PD with two microcontrollers, to get a smooth control signal. Fuzzy controller cannot follow the reference when it is close to zero.

T.T Salim et al. [54] designed a fuzzy logic controller for the stabilization of Maglev system. Magnetic levitation is a nonlinear unstable system and the fuzzy logic controller brings the Maglev system to a stable region by keeping a magnetic ball suspended in the air and also made a comparison between the application of a fuzzy control and a linear quadratic regulator for magnetic levitation.

A. Senba et al. [55] discussed about characteristics of an Electromagnetic Levitation System using a bulk superconductor. A hybrid magnet with pinning flux has a simple structure and the capability of generating large attractive forces so that it is efficient to use it for transportation system. The magnetic circuit analysis indicates that an increase of pinning flux and a decrease of air-gap in a magnet was important factor to improve levitation capability.

Y. Jin, et al. [56] designed a Maglev device composed of field coil, iron core and aluminium ring. When the coil current is changed, the alternating magnetic field generated by the current makes the flux of the aluminium ring which is placed above the coil is continuously changing. So the induced eddy current is generated in the aluminium ring when the current in the coil changes. The negative feedback is added to the control system, which makes the control of the aluminium ring height more accurate.

Liwei Jin et al. [57] discussed about the dynamic effect of Eddy Current Damping (ECD) on the vibration amplitude and frequency of the High-Temperature Superconducting (HTS) Maglev system by

introducing different thicknesses copper damper underneath the HTS bulks with different velocities by measuring the displacement and acceleration signals of an HTS levitator. But it has a weakness of low damping, which is not beneficial to the systemic stability and security when the Maglev vehicle is disturbed by external environment such as crosswind and track irregularity.

Y. Fu et al. [58] developed a Bearing less Motors (BelMs), which can realize Maglev rotation with no mechanical contact. In general, in high speed and high output BelMs, distributed winding structure is adopted in order to suppress iron loss and neodymium sintered permanent magnet (Nd sintered PM) is employed to achieve a high power density. However, output power fall is caused due to long coil end of the distributed winding structure because a shaft length is limited by primary bending mode under high speed rotation. Eddy current loss easily occurs in the Nd sintered PM because of its high conductivity. It is difficult to achieve continuous high-speed and high-output operation due to the temperature raising in a rotor.

B. Reutzsch et al. [59] discussed about innovative Maglev system for linear direct drives. It is exclusively based on Lorentz forces and is designed in dimensions for application in precision engineering systems. Permanent magnets are arranged similar to a Halbach array within the guideway and thereby establish a magnetic field for the levitation and guidance coils. The comparatively low weight of the moving part and its lack of eddy currents allow for highest dynamics.

Moreover, easy and efficient closed loop algorithms can be implemented because of the linear correlation of Lorentz force and current.

C. Elbuken, [60] discussed about damped vibrations in a magnetic levitation of micro objects. Eddy current damping is proposed to suppress vibrations and increase the precision of magnetic levitation of tiny objects. Non-contact nature and the ease of the employed damping mechanism make eddy current damping an optimum solution for precise control of magnetically levitated miniaturized objects.

John J. Stickler [61] predicted the reaction forces developed by single-sided linear induction motors (sLIM's) with solid iron secondaries. The model predictions are compared with test results obtained from three separate sLIM investigations covering a wide range of operating conditions and sLIM design parameters. The results demonstrate the basic validity of the model and its applicability for Maglev optimization and analysis.

L. Zheng et al. [62] designed a long-primary sLIM integrated with HTS levitation system. Long-primary single-sided linear induction motors (sLIMs) have unique advantages in some applications such as an electromagnetic launcher with higher force density and acceleration due to its lightweight secondary conductive sheet compared with other types of sLIM having different structures. Furthermore, long-primary sLIM will have superiorities without any friction loss and guidance

control system when it is combined with high temperature superconducting (HTS) Maglev system.

Yong-Joo Kim et al. [63] developed an electromagnetically levitated vehicle, KOMAG-01 with 8 axial flux type electromagnets for levitation and 2 linear induction motors (LIMs) for propulsion. The levitation magnets are controlled by 1-4 quadrant PWM choppers using a state feedback control system and LIMs are controlled by an inverter using an open-loop control system. The author has designed the magnet using an analytical method and analysed using the finite-element method (FEM) to find an optimum configuration. The sLIM is analysed using a 2D FEM with current and magnetic vector potential to investigate end/edge effects in three different analysing planes. The operating characteristics of the machine are in reasonably good agreement with the analysed data.

K. Wang et al. [64] discussed the relations of the normal and thrust forces to primary flux and slip frequency in sLIM. The normal and thrust forces are applied independently to levitate and propel a sLIM maglev vehicle without additional levitation magnets. Then, experiments have been carried out on the combined levitation-and-propulsion sLIM Maglev vehicle with different operation conditions, during the whole running period, the gap length and speed of the vehicle follow well with the command ones, the stability and accuracy are well proved.

From the Literature, the inferences are drawn and the main problem in the Maglev system is, relative stability and to control the position of the levitated object with minimum error. Different types of controllers have been studied with their merits, demerits and their reliability. Controller has to adjust the strength of the magnetic field to hold the suspended object in the desired position.

1.4 Problem Formation

Literature shows many authors have proposed different control algorithms for position tracking of Maglev system. The main drawback is that the eddy current based force for position tracking of Maglev system is neglected. In this work, an analytical relationship is developed for eddy current based force as a function of the plate thickness and its distance to the levitated object. The Maglev system has unstable nonlinear dynamics which should be taken into account. It is a great extent of controller to stabilize the system by considering nonlinear dynamics. Controller will adjust the strength of the magnetic field to hold the suspended object in the desired position. In the present thesis, three controllers are proposed to stabilize the levitated object in the desired position and these are implemented in MATLAB/Simulink environment.

Another application of Maglev system is Maglev trains, in which propulsion is provided by Linear Induction motor. In the present thesis, controller has been implemented for speed tracking of Linear

Induction Motor and simulations are developed in LabVIEW environment.

1.5 Different types of Controllers

Conventional controllers may not provide satisfactory performance for nonlinear systems because of these are designed for linear systems. It attempts to correct the error between a measured process variable and a desired set point by calculating and then implementing a corrective action.

Generalized PID controller, which can be called the PI$^\lambda$D$^\mu$ controller because of involving an integrator of order λ and differentiator of order μ, is used. The transfer function of such a controller has the form

$$G_c(s) = \frac{U(s)}{E(s)} = K_P + K_I s^{-\lambda} + K_D s^\mu, \qquad (\lambda, \mu > 0)$$

The equation of the $PI^\lambda D^\mu$-controller's output in the time domain is

$$u(t) = K_P e(t) + K_I D^{-\lambda} e(t) + K_D D^\mu e(t)$$

Classic PID controller can be obtain by taking $\lambda = 1$ and $\mu = 1$. $\lambda = 1$ and $\mu = 0$, give a PI-controller. $\lambda = 0$ and $\mu = 1$, give a PD-controller. $\lambda = 0$ and $\mu = 0$, give a proportional controller.

1.5.1 Conventional controller

The main objective is to control the position tracking of the Maglev system with minimum error. For this purpose many controllers such as LQG, H_∞ and input shaping as well as singular

perturbation, manifolds and output redefinition techniques [65] have been used. All of the model-based classic or modern controllers suffer from the lack of an exact simple-enough models of the system. However, it is nearly always desired to produce a stable state in the presence of variations in the parameter uncertainty and nonlinear system, which will be ignored in these approaches.

1.5.2 Fractional order model reference adaptive controller

The Model Reference Adaptive System (MRAS) is one of the main approaches to adaptive control, in which the desired performance is expressed in terms of a reference model (a model that describes the desired input-output properties of the closed-loop system) and the parameters of the controller are adjusted based on the error between the reference model output and the system output.

It has been shown in many papers from Yang Quan Chen et al, [66] that the use of FOPID could make the entire control system perform better. The FOPID controller is more flexible and provides improved performance than conventional PID controller due to the presence of five parameters to be tuned.

1.5.3 Backstepping Fuzzy Sliding Mode Controller

Non-linear systems use specific theories and methods to ensure stability without regard to the inner dynamics of the system. Backstepping and Integrator backstepping control are few of the methods [67]. Backstepping is a technique developed circa 1990 by

Petar V. Kokotovic and others for designing stabilizing controls for a special class of nonlinear dynamical systems. These systems are built from subsystems that radiate out from an irreducible subsystem that can be stabilized using some other method. Because of this recursive structure, the designer can start the design process at the known-stable system and "back out" new controllers that progressively stabilize each outer subsystem. The process terminates when the final external control is reached. Hence, this process is known as Backstepping [68].

A back-stepping integral sliding mode controller whose sliding surface considers the integrals of the angle error and the tracking error is designed for the bounded, unmodeled system. The switching gain should be relatively large to ensure system stability [69]. This will induce severe chattering, which hinders the precision of the deflection angle. A fuzzy algorithm whose inputs include the sliding value and deflection angle is designed to adaptively tune the switching gain of the sliding mode method.

1.5.4 PID Controller based on Cuckoo Search algorithm

Pallav et al. [70] developed a PID controller with a derivative filter coefficient for the MLS. Hypiusova and Kozakova [71] proposed a robust PID controller to stabilize the nonlinear magnetic levitation system using frequency domain approach. In this approach, the designed controller does not guarantee the robust stability condition; if it fails then the controller design has to be repeated. Witchupong

and Sarawut [72] proposed state PI controller to achieve the control over the states of the MLS. Kim [73] proposed a robust air-gap controller considering disturbance force produced by magnetic suspension for Maglev system. Optimization has gained superior power and influence in many applications like industrial design and engineering. The main objective of optimization is to minimize or maximize the objective function. After an optimization problem is formulated correctly, the main task is to find the optimal solutions by some solution procedure using the right mathematical procedure.

Cuckoo search (CS) is one of the latest nature-inspired metaheuristic algorithms, developed in 2009 by Xin-She Yang [74] of Cambridge University and Suash Deb of C.V. Raman College of Engineering. CS is based on the brood parasitism of some cuckoo species. In addition, this algorithm is enhanced by the so-called Levy flights rather than by simple isotropic random walks. Recent studies show that CS is potentially far more efficient than PSO, genetic algorithm and other algorithms.

1.6 Scope and Objectives of the Thesis

The main objectives of the thesis are as follows:

➢ To study the dynamic behavior of the magnetic levitation system.

- To derive the analytical relation for the eddy current based force as a function of the plate thickness and its distance to the permagnet.

- To design a fractional order model reference adaptive controller to reduce the vibrations in the object as well as position tracking.

- To derive a linear model to represent the nonlinear dynamics of Maglev system by using feedback linearization technique.

- To design Backstepping fuzzy sliding mode controller based on the Lyapunov approach for the nonlinear Maglev system.

- To design PID controller based on Cuckoo search algorithm and to test on real time application of magnetic levitation system.

- Another application of Maglev system is single sided high speed LIM is designed based on the rotary induction motor.

- Simulations of sLIM are implemented in LabVIEW.

- Based on the design parameters of SLIM, prototype SLIM is implemented.

- PID controller based on Cuckoo search algorithm is designed for speed tracking of LIM.

1.7 Organization of the Thesis

The content of the thesis is organized in eight chapters:

- Chapter I -   Introduction

- Chapter II - Analytical model of eddy current based force in Maglev System

➢ Chapter III - Fractional order model reference adaptive controller for maglev system

➢ Chapter IV - Feedback linearization technique to Maglev system

➢ Chapter V - Backstepping fuzzy sliding mode controller to Maglev System

➢ Chapter VI - PID controller for real time maglev system based on Cuckoo search algorithm

➢ Chapter VII - Design of single sided Linear Induction Motor

➢ Chapter VIII - Conclusions and Future Scope.

Chapter I – Includes the introduction to Maglev system and issues related to it. A detailed literature survey is carried out, and also presented different controllers for position tracking of Maglev system, objectives and scope of the thesis.

Chapter II – explains brief and basic concepts involved in Maglev system and followed by analytical relationship of eddy current based force as a function of plate thickness and distance to the permagnet.

Chapter III – proposes and implements a Fractional order model reference adaptive PID controller for position tracking of Maglev system and results are compared with conventional controller.

Chapter IV – presents the linear model to represent the nonlinear dynamics of Maglev system using feedback linearization technique.

Chapter V – proposes and implements a backstepping fuzzy sliding mode controller for position tracking of Maglev system based on Lyapunov approach.

Chapter VI – proposes and implements a PID Controller based on cuckoo search algorithm for position tracking of real time magnetic levitation system and simulation results are compared with conventional controller.

Chapter VII – explains the design of single sided Linear Induction Motor and speed tracking of sLIM using PID controller based on cuckoo search algorithm.

Finally, **Chapter VIII** of the thesis presents the overall conclusions and future scope of the work, at the end of the thesis, references and publications from the research work are presented

Chapter - II

ANALYTICAL MODEL OF EDDY CURRENT BASED FORCE

IN MAGLEV SYSTEM

2.1   Introduction

In recent years there has been a growing interest in the design and development of manipulator systems to meet the requirements in various fields. One such system is Maglev system. It has numerous practical applications in research and industry where friction must be reduced or eliminated. Some of the more promising applications are transportation (Low and High Speed Maglev), low friction bearings for gyroscopes and fly wheel energy storage [75]. Other applications have been proposed, such as levitation melting of conductive metals. Applications such as eddy current braking and induction heating that involve similar physical processes as magnetic levitation can be analyzed using similar or slightly modified solution techniques.

For high precision applications, system behavior is undesirable. In [76] a precise magnetic levitation, for eddy current damping is more important. In [77] H. A. Sodano and J. S. Bae discussed various uses of eddy current damping in many areas. The eddy currents generate heat which is utilized in various applications like brazing hardening and induction furnaces etc. and also used in non-destructive testing of

25

conductive materials [78]. Gautam Sinha et.al., [79] proposed a model to understand the behavior of Maglev on rectangular plate and the consequences of it. In 1991 Hong song et.al., developed simple formulation for eddy currents based on constrained eddy currents and which are applicable to all low frequency applications [82].

Eddy currents are used in Maglev system to stabilize the position of the levitated object. [81] stated that eddy current damping significantly improves the levitation performance without changing the controller algorithm or increasing the cost or complexity of the system enabling the set-up a potential tool for micro-manipulation and micro positioning purposes. In [75] Sodano stated that the eddy current damper have an advantage over other damping systems, due to the noncontact nature of the damper, it does not change the dynamics of the structure. This chapter deals with the analytical and explicit structure for eddy current damping forces on permagnet in steady state, levitated in a field of electromagnet above the cylindrical plate.

In Maglev system, by placing a conductive plate underneath of the levitated object, eddy current damping was introduced to suppress vibrations and to ensure stability of magnetic levitation for high amplitude step inputs. In previous literatures, most controllers were designed for Maglev system with permagnet to stabilize positioning of the

object in the air by neglecting the effect of eddy current based force due to the motion of levitated permagnet.

2.2 Damping force in Magnetic Levitation System

Magnetic levitation is a method by which an object is suspended in the air with no support other than magnetic fields, the fields are used to reverse or counter act the gravitational pull and any other counter acceleration, and Maglev can create frictionless, efficient, far-out sounding technologies.

Electromagnet

radius: 'r'

it has radius of 'a', width of 'l' and permagnet

h

width 'w'   plate
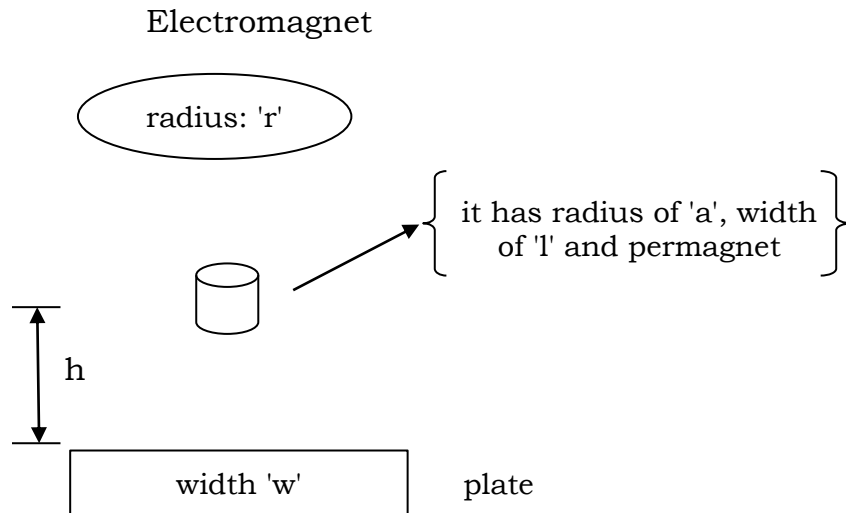
Figure 2.1 Schematic of the levitated object above the plate

In Fig 2.1, the schematic Maglev system is shown. An electromagnet, a levitated object which is a permagnet and a conductive plate are parts of this levitation system. The levitated object can be moved in z direction by exerting the magnetic field of electromagnet and in x and y directions by moving the electromagnet.

The eddy current based force may be generated by the variation of the position of the levitated object which creates eddy currents in the conductive plate. This eddy currents generates a magnetic field, opposes the motion of the permagnet (Lenz's law). Also, the variation of the electromagnet current generates eddy currents in the plate which subsequently generates eddy force on the object. The eddy current in the plate is linearly proportional to the velocity of the object and the rate of change of current in electromagnet.

Since the object is a permagnet, the eddy force is proportional to eddy current in the plate. Hence, the eddy force is a linear combination of object's velocity and rate of electromagnet's current change. So that, the obtained eddy current based force is generated by each effect separately and the resultant total eddy force is the sum of these two eddy forces coming from different sources. Also, to compute eddy forces the permagnet is considered as a magnetic dipole. If the size of the permagnet is small with respect to its distance from the plate, the analytical solution obtained in this work can be used approximately by assuming the levitated object as a magnetic dipole placed right at its center. Generally, the levitated object as the sum of magnetic dipoles at different coordinates and obtain the eddy forces by integrating over these small magnetic dipole elements. But this increases the complexities. By calculating these integrals, it is seen that when h, the distance between the center of the object and conductive plate, is such that $d/h < 1$ and

$\Delta/h < 1$, the magnetic dipole approximation is valid with 5% relative error. In these equations d is the object's diameter and Δ is its height. In most situations h is in the above ranges, so we can avoid these complexities in our calculations.

2.3 Eddy-Current Based Force due to the motion of the levitated permagnet

If μ_r, the relative permeability of the plate, is larger than 1, the plate will pull-in the levitated object toward itself, which is undesirable. Also, it is shown that using a plate with high conductivity produces a bigger eddy-current-based force. Hence, it is better to use a high conductive plate (i.e., many of Aluminum alloys) with a relative permeability of $\mu_r = 1$.

2.3.1 System Model

In magnetic levitation, permagnet material is under the influence of two opposing forces, namely, the downward gravitational force and the upward pull of the electromagnet, as shown in Fig. 2.1 Perfect levitation is achieved once these two forces exactly balance each other.

Dynamic behaviour of Maglev system can be modelled by the study of electromagnetic and mechanical sub systems.

$$M\ddot{x} = Mg - c\left(\frac{i}{x}\right)^2 - F_{PM} \qquad \qquad \dots (2.1)$$

where M is mass of the permagnet

c is magnetic force constant

g is gravitational constant

x is the displacement

F_{PM} is eddy current force induced in the permagnet.

2.3.2 Force due to motion of the permagnet

From the quasi-static Maxwell's equations, for linear conductors we have the following equation for magnetic vector potential in the conductive plate

$$\nabla^2 A = \mu_0 \sigma \frac{\partial A}{\partial t} \qquad \text{... (2.2)}$$

where A is magnetic vector potential, σ conductivity of the plate and μ_0 permeability of the free space.

In the nonconductive places, the right side of this equation vanishes. Using this equation and boundary conditions the magnetic vector potential can be obtained in order to find the eddy forces on the object.

The motion of the permagnet in z direction is considered for analysis. According to Fig. 2.1, the position of the permagnet as h(t) = h_0 + vt, where h_0 and v are the initial position and velocity of the permagnet, respectively.

It is known that a magnetic dipole with a moment m is equivalent to a coil with a small radius r and a large current I where $= \pi a^2 I$. Hence, using this conversion the problem can be made similar to the electromagnet based eddy current problem.

The space current density J, in the cylindrical coordinates is

$$J(z, \rho, t) = I\delta(z - h(t))\delta(\rho - a)\widehat{\emptyset} \qquad \text{... (2.3)}$$

where δ is Dirac's delta function and $\widehat{\emptyset}$ is the angular unit vector in cylindrical coordinate. By the Taylor series expansion around the point h_0, the current density can be written as

$$J = I\delta(\rho - a)\left[\delta\big(z - h(t)\big) + vt\frac{d\delta(z-h_0)}{dh_0} + O\left(\left(\frac{vt}{h_0}\right)^2\right)\right]\widehat{\emptyset} \qquad \text{... (2.4)}$$

In the first order of perturbation to find non-zero eddy force, the higher order terms of the series expansion can be neglected because of the small permagnet's velocity. The first term of (2.4) which is due to a static dipole cannot generate eddy current, because it is not time dependent. Thus for analyzing the eddy-current-based force only the second term is necessary.

Since vector potentials and fields are linear functions of current sources, a virtual current density J_v, can be defined as

$$J_v = I\delta(\rho - a)vt\delta(z - h_0)\widehat{\emptyset} \qquad \text{... (2.5)}$$

Hence, the magnetic field generated by J is derivative of the virtual fields, generated by J_v, with respect to h_0. Hence, the magnetic fields must be derived first due to current density J_v. This current density is obtained from a coil with radius a positioned at a distance (in parallel to the conductive plate) carrying a current $I_v = Ivt$.

So that, this time dependent current as the sum of harmonic currents with amplitude $I_v(\omega)$ in different angular frequencies using Fourier transform below

$$I_v(\omega) = \frac{1}{2\pi} \int e^{j\omega t} I_v(t) dt \qquad \qquad \ldots (2.6)$$

it can be written as

$$I_v(\omega) = -j\delta'(\omega) vI \qquad \qquad \ldots (2.7)$$

The amplitude of vector potential in angular frequency ω can be written as

$$A_v(\omega, \rho, z) = \left[\int A_1 J_1(k\rho) e^{-kz} dk + \int A_2 J_2(k\rho) e^{kz} dk \right] \hat{\varphi} \qquad \ldots (2.8)$$

where J_1 is the first-order of the first-kind Bessel function

The second term of (2.8) is the vector potential due to the direct effect of the coil current which is independent of σ and ω. Also, the first term, which decreases by increasing z, is the vector potential due to eddy current in the plate. Hence, to obtain the eddy force of the plate on the permagnet, only the first term should be considered.

Taking inverse Fourier transform and differentiating with respect to h_0 and limiting the coil radius a to zero (in the magnet dipole limit) lead to an equation for magnetic vector potential in the following form:

$$A_{eddy}(t,\rho,z) = \lim_{a \to 0} \int e^{-j\omega t}e^{-kz}\frac{dA_1}{dh_0}J_1(k\rho)dkd\omega\hat{\varphi} \qquad \dots (2.9)$$

eddy current based force can be obtained from [83]

$$F_{eddy} = \nabla(m \cdot B_{eddy}) \qquad \dots (2.10)$$

Substituting $B_{eddy} = \nabla \times A_{eddy}$ into (2.10) and using (2.9), the eddy current force due to the permagnet's motion can be written as

$$F_{eddy\ P,M,z} = -b_{pm,z}(h)m^2v_z \qquad \dots (2.11)$$

where $b_{pm,z}(h)$ is

$$b_{pm,z}(h) = \frac{\mu_0{}^2\sigma}{64\pi h^3}\left[1 - \frac{1}{\left(1+\frac{w}{h}\right)^3}\right]m^2 \qquad \dots (2.12)$$

The above equation represents the eddy force due to the motion of the permagnet perpendicular to the plate. This idea can be used to find the eddy force due to the motion of permagnet parallel to the plate by replacing the $\partial/\partial h_0$ by $\partial/\partial x$, in (2.9)

Hence, it can be

$$F_{eddy\ P,M,\rho} = -b_{pm,\rho}(h)m^2v_\rho \qquad \dots (2.13)$$

where $b_{pm,\rho}(h)$ is

$$b_{pm,\rho}(h) = \frac{\mu_0{}^2\sigma}{128\pi h^3}\left[1 - \frac{1}{\left(1+\frac{w}{h}\right)^3}\right] \qquad \dots (2.14)$$

33

2.4 Eddy-Current Based Force due to change of Electromagnetic current

In this section, the goal is to obtain an analytical model of eddy current based force due to change of electromagnet current. An electromagnet consists of many coils and cores. If the problem is solved for one coil, can be solved the problem for a complex electromagnet by summing the effect of each coil.

The coil current is I and is a function of time. To find non-zero eddy force in the first order of perturbation, we use Taylor series expansion about the initial time value and disregard the higher order terms

$$I(t) = I(0) + I(\dot{0})t + \cdots \qquad \dots (2.15)$$

Using fourier transform, the current can be written as sum of harmonic currents with amplitude $I(\omega)$ in different angular frequencies

$$I(\omega) = -j\delta'(\omega)I(\dot{0}) + \delta(\omega)I(0) \qquad \dots (2.16)$$

$A(\omega, \rho, z),$ the amplitude of magnetic vector potential has been obtained as

$$A(\omega, \rho, z) = \left[\int_0^\infty A_1 e^{-kz} J_1(k\rho) dk + \int_0^\infty A_2 e^{kz} J_1(k\rho) dk \right] \hat{\varphi} \qquad \dots (2.17)$$

The second term of (2.17) is the vector potential due to the direct effect of the coil current. Also, the first term is the vector potential due to

the eddy current of the plate. Therefore, to obtain the eddy force, only the first term should be considered.

The eddy force on the object is obtained from (2.10) and is written in the following form in two directions of z and ρ

$$F_{eddy,coil,z}(h,r) = b_{em,z}(h,r)mI(0) \qquad \qquad \text{... (2.18)}$$

$$F_{eddy,coil,\rho}(h,r) = b_{em,\rho}(h,r)mI(0) \qquad \qquad \text{... (2.19)}$$

where $b_{em,z}$ and $b_{em,\rho}$ are

$$b_{em,z}(h,r) = \int_0^\infty \frac{\mu_0{}^2\sigma}{4(1+\coth kw)} e^{-k(D+h)} aJ_1(ka)J_0(kr)dk \qquad \text{... (2.20)}$$

$$b_{em,\rho}(h,r) = \int_0^\infty \frac{\mu_0{}^2\sigma}{4(1+\coth kw)} e^{-k(D+h)} aJ_1(ka)\frac{dJ_0(kr)}{d(kr)}dk \qquad \text{... (2.21)}$$

where index "em" in b_{em} refers to electromagnet based eddy force

Since increasing the distance from the symmetry axis results in a considerable reduction of the magnetic field, for effective damping in the radial direction, r, the distance of the object from the symmetry axis, should be small compared to h and a. Therefore, replace the zero order of the first Kind Bessel function by its Taylor series to obtain the first non-zero term of eddy force in each direction as follows

$$J_0(kr) = 1 - \left(\frac{kr}{2}\right)^2 + O((kr)^4) \qquad \qquad \text{... (2.22)}$$

Hence, the integrals can be written as laplace transform of first kind Bessel function and can be solved analytically as

$$b_{em,z}(h) = \frac{\mu_0^2 \sigma}{8} [f(D + h + 2w, a) - f(D + h, a)] \qquad \text{... (2.23)}$$

where $f(x, a) = (x)/\sqrt{x^2 + a^2}$ and

$$b_{em,\rho}(h, r) = \frac{r}{2} \frac{\partial b_{em,z}}{\partial h} \qquad \text{... (2.24)}$$

Also, at small distances r, the second term of (2.17) which leads to the direct magnetic force on the permagnet,

$$F_{coil,z}(h, r) = mI(0) \int_0^\infty \frac{k^2 \mu_0}{2} e^{-k(D-h)} a J_1(ka) dk \qquad \text{... (2.25)}$$

2.5   Analytical Results

Fig. 2.2 and Fig. 2.3 show $b_{pm,z}$, the damping coefficient in direction (2.12), as a function of h and w. In all of these figures, the plate conductivity is set to be $30 \, \mu m \cdot \Omega^{-1}$.
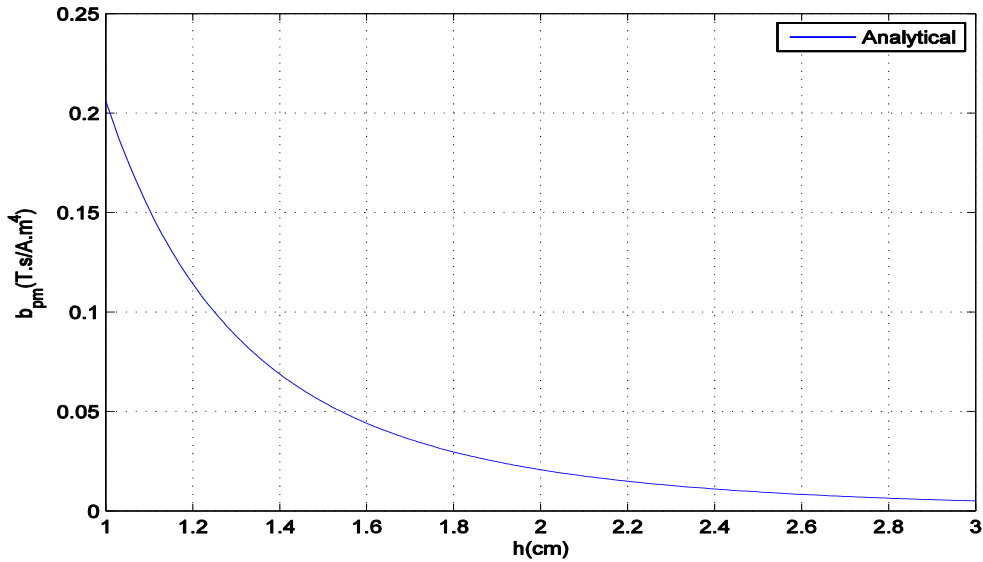
Figure 2.2 Damping coefficient as a function of the permagnet height from

the plate of 1cm thickness
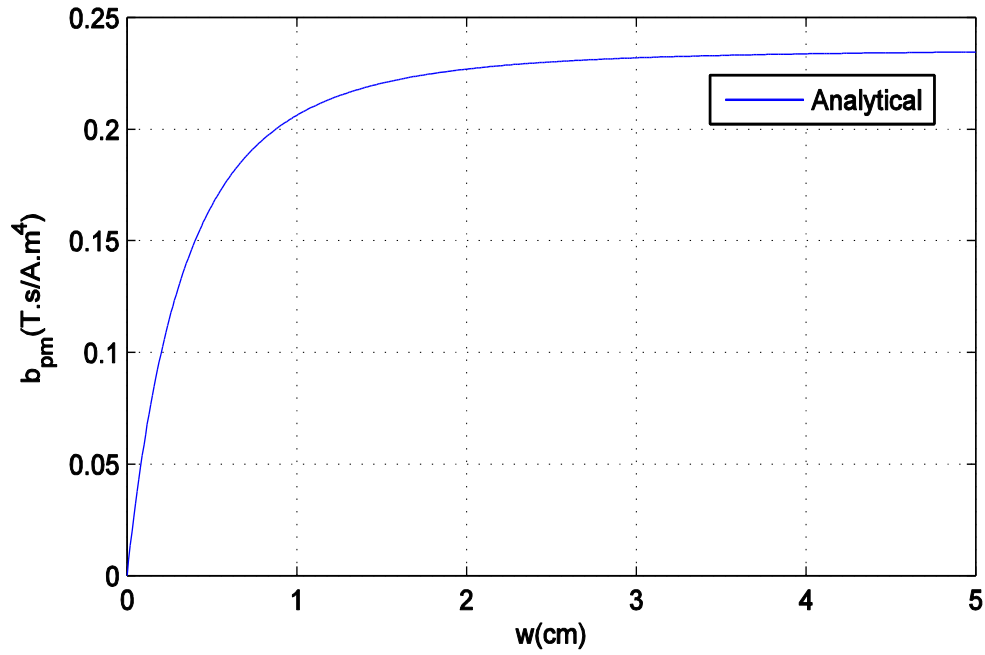
Figure 2.3 Damping coefficient as a function of the plate thickness with a

height of 1cm between the permagnet and plate
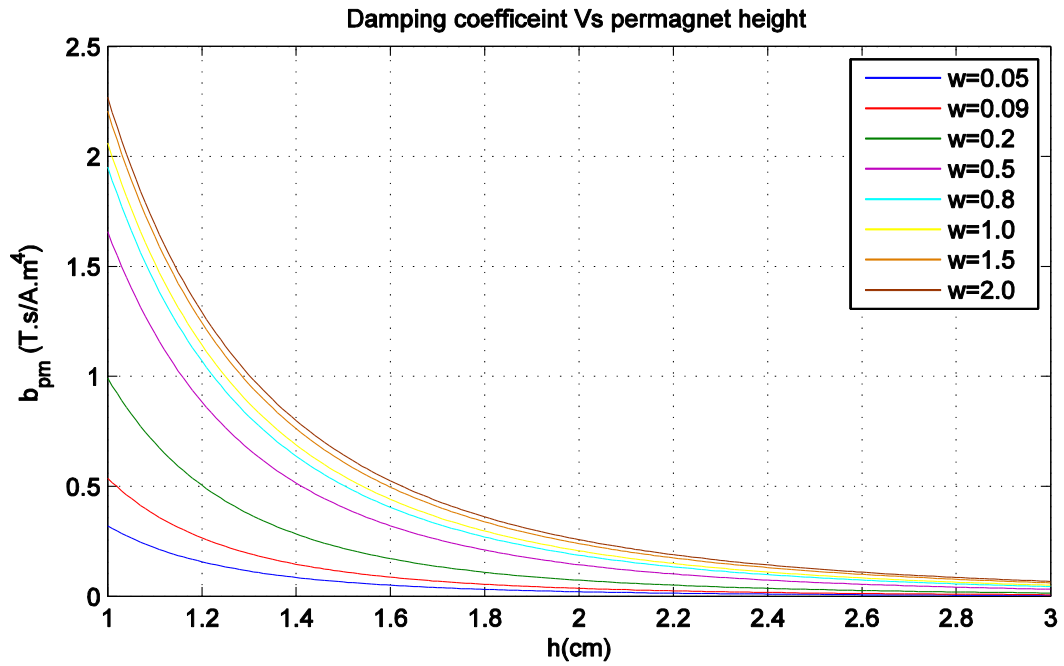
Figure 2.4 Damping coefficient as a function of the permagnet height from the

plate for different plate thicknesses
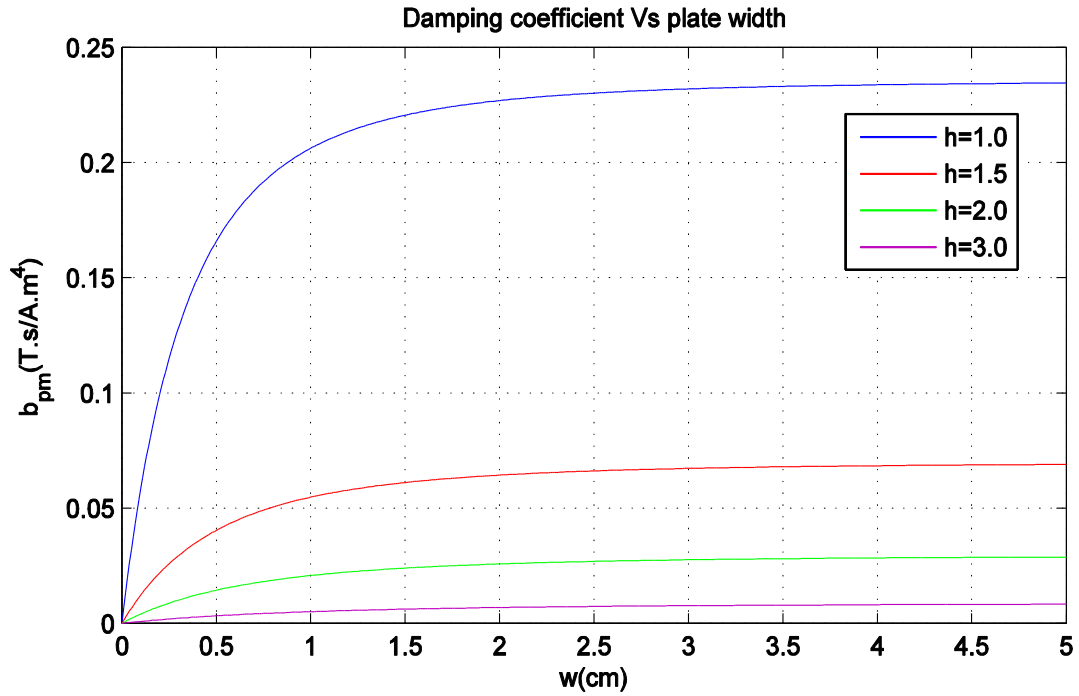
Figure 2.5 Damping coefficient as a function of the plate thickness with

distance varies from 1cm to 3cm

It is seen that by increasing w/h, $b_{pm,z}$ increases until it reaches to a maximum value which is proportional to h^{-3}; this effect can be seen in Fig. 2.3 and Fig. 2.5. Equation (2.12) indicates that the damping coefficient for $w > h$ is greater than 85% of its value for semi-infinite plate $(w/h \to \infty)$. So a plate with a thickness of the order of the permagnet distance can be a good choice for practical considerations.
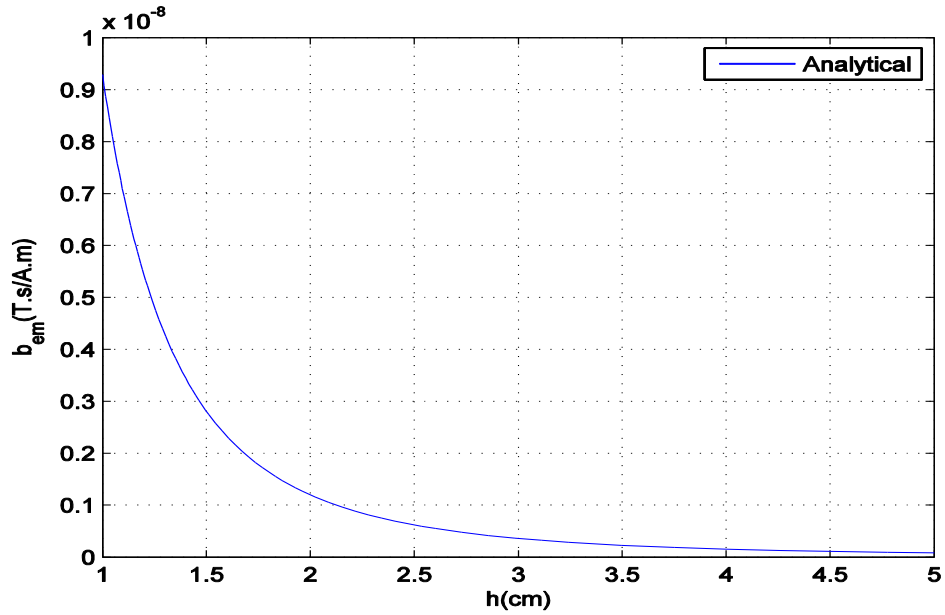
Figure 2.6 Damping coefficient as a function of the permagnet height from

the plate with coil radius 2.5 cm and the plate thickness of 1 cm
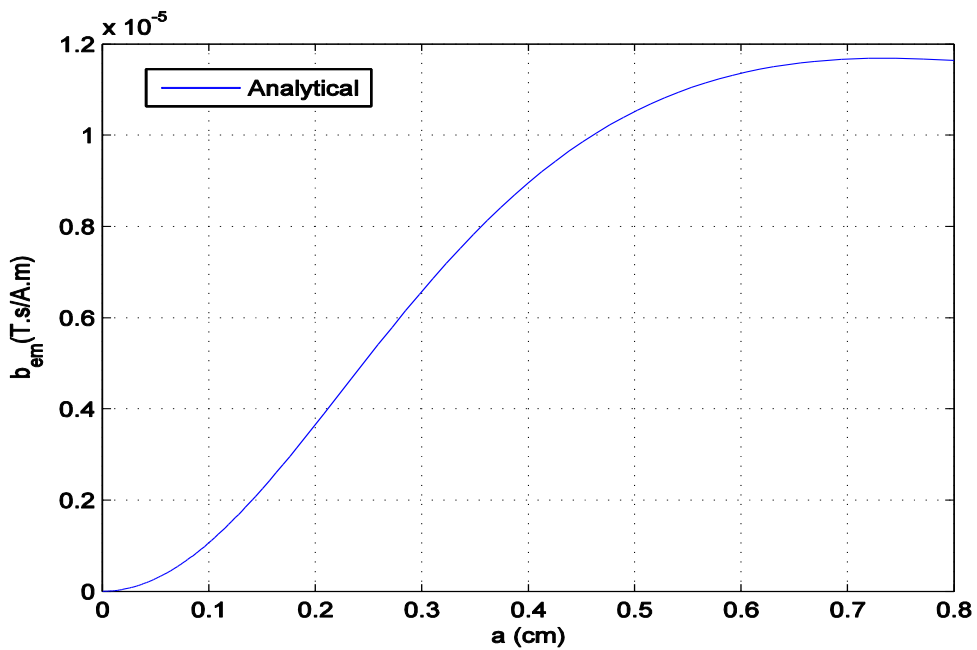
Figure 2.7 Damping coefficient as a function of coil radius with height of

5 cm and the plate thickness of 1 cm
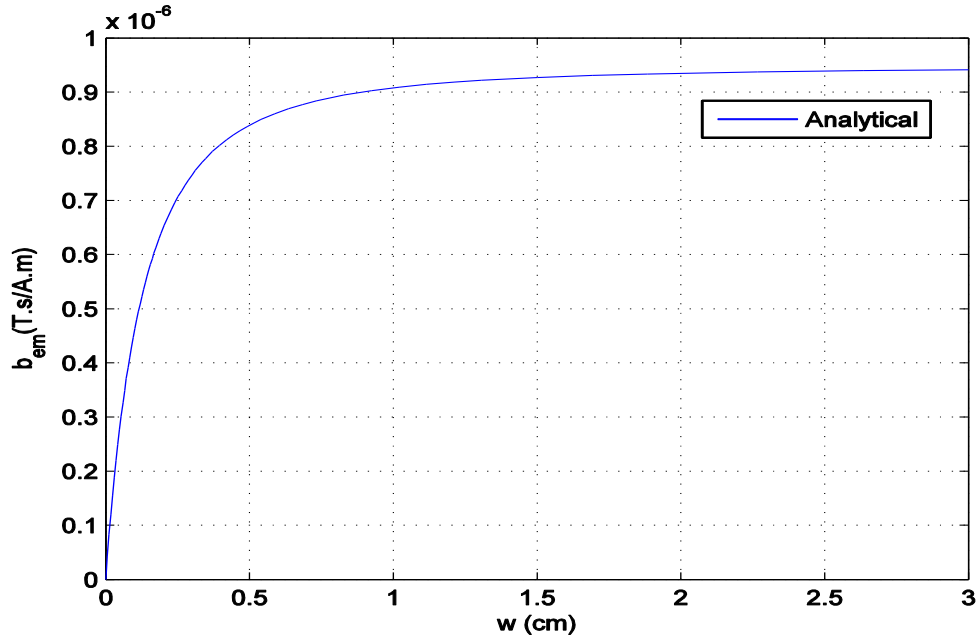
Figure 2.8 Damping coefficient as a function of plate thickness with height of 5 cm and coil radius of 2.5 cm

Fig. 2.6, Fig. 2.7, and Fig. 2.8 show $b_{em,z}$, the damping coefficient in the direction in (2.23), as a function of h, a and w. In all of Fig.2.2 to Fig. 2.8, the plate conductivity is set to be $40\ \mu m \cdot \Omega^{-1}$ and the distance between the plate and the coil is set to be 10 cm.

If considered the effect of one coil, $b_{em,z}$ has an insignificant value (about 10^{-6}). But for an electromagnet with a large number of coils and iron cores, the amount of $F_{eddy,em}$ is in the order of milli-Newton. This amount is in the order of $F_{eddy,pm}$ for a dipole with velocity 1 cm/s in z direction.

2.6   Conclusions

In Maglev system eddy current based force will be generated by the variation in position of the levitated object (permagnet) and current in the electromagnet. In this work, an explicit analytical solution has been presented to calculate eddy current based force as a function of the plate thickness and its distance to the magnet. The effect of dimensions of the levitated permagnet on eddy current based force is observed in MATLAB environment. The simulation results shows variation in the force by varying the plate thickness and its distance to the magnet.

Chapter - III

FRACTIONAL ORDER MODEL REFERENCE ADAPTIVE CONTROLLER FOR MAGLEV SYSTEM

3.1 Introduction

The Model Reference Adaptive System (MRAS) is one of the main approaches to adaptive control, in which the desired performance is expressed in terms of a reference model (a model that describes the desired input-output properties of the closed-loop system) and the parameters of the controller are adjusted based on the error between the reference model output and the system output. These basic principles are illustrated in Fig. 3.1. It is clear from Fig. 3.1 that, there are two loops: an inner loop which provides the ordinary control feedback, and an outer loop which adjusts the parameters in the inner loop.
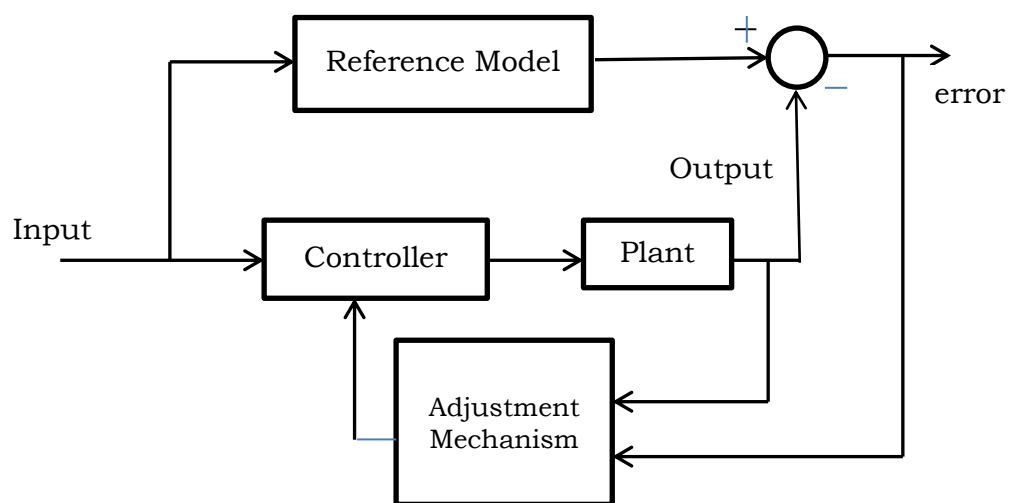
Figure 3.1 Basic model reference adaptive system

3.2   The Gradient Approach

The gradient approach to model reference adaptive control is based on the assumption that the parameters change more slowly than the other variables in the system. This assumption, which admits a quasi-stationary treatment, is essential for the computation of the sensitivity derivatives that are needed in the adaptation.

Let e denote the error between the system output y and the reference output, y_m. Let θ denote the parameters to update. By using the criterion

$$J(\theta) = \frac{1}{2}\theta^2 \qquad\qquad \dots (3.1)$$

the adjustment rule for changing the parameters in the direction of the negative gradient of J is that

$$\frac{d\theta}{dt} = -\gamma\frac{\partial J}{\partial \theta} = -\gamma e\frac{\partial e}{\partial \theta} \qquad\qquad \dots (3.2)$$

If it is assumed that the parameters change much more slowly than the other variables in the system, the derivative $\frac{\partial e}{\partial \theta}$, i.e., the sensitivity derivative of the system, can be evaluated under the assumption that θ is constant.

There are many variants about the Massachusetts Institute of Technology (MIT) rules for the parameters adjustment. For example, the sign-sign algorithm is widely used in communication systems [98]; the PI- adjustment rule is used in [99]. In this work, a new variant of the MIT rule for the parameter adjustment is introduced by using the fractional order calculus. In addition, the reference model is extended

to the fractional order. This chapter deals with fractional order calculus and the related notion about the fractional order dynamic systems, which will be very briefly in the next section.

3.3 Fractional Order Operators

Fractional Calculus is a generalization of integration and differentiation to non-integer (fractional) order fundamental operator $_aD_t^\propto$, where a and t are the limits and $\propto$ ($\propto\in \mathbb{R}$) the order of the operation. The two definitions used for the general fractional integro-differential are the Grunwald-Letnikov (GL) definition and Riemann-Liouville (RL) definition [100, 101]. The GL definition is that

$$_aD_t^\propto f(t) = \lim_{h\to 0} h^{-\alpha} \sum_{j=0}^{\left[t-\frac{a}{h}\right]} (-1)^j \binom{\alpha}{j} f(t-jh) \qquad \dots (3.3)$$

Where [·] means the integer part while the RL definition

$$_aD_t^\propto f(t) = \frac{1}{\Gamma(n-\alpha)} \frac{d^n}{dt^n} \int_a^t \frac{f(\tau)}{(t-\tau)^{\alpha-n+1}} \qquad \dots (3.4)$$

for ($n-1 < r < n$) and $\Gamma(\cdot)$ is the Euler's gamma function.

For convenience, Laplace domain notion is generally used to describe the differential operation [101]. The Laplace transform of the RL fractional derivative/integral (3.4) under zero initial conditions for order $\propto$, 0 $<\propto<$ 1 is given by [100]

$$\mathcal{L}\{ _aD_t^{\pm\propto} f(t); s\} = s^{\pm\propto} F(s) \qquad \dots (3.5)$$

3.4 Fractional Order Control Systems

In theory, the control systems can include both the fractional order dynamic system to be controlled and the fractional order controller. A fractional order plant to be controlled can be described by a typical n-term linear Fractional Order differential Equation (FODE) in time domain

$$a_n D_t^{\beta_n} y(t) + \cdots + a_1 D_t^{\beta_1} y(t) + a_0 D_t^{\beta_0} y(t) = 0 \qquad \ldots (3.6)$$

where $a_k (k = 0,1,\ldots,n)$ are constant coefficients of the FODE; $\beta_k (k = 0,1,\ldots,n)$ are real numbers. Without loss of generality, assume that $\beta_n > \beta_{n-1} > \cdots > \beta_1 > \beta_0 \geq 0$.

Consider a control function which acts on the FODE system (3.6) as follows:

$$a_n D_t^{\beta_n} y(t) + \cdots + a_1 D_t^{\beta_1} y(t) + a_0 D_t^{\beta_0} y(t) = u(t) \qquad \ldots (3.7)$$
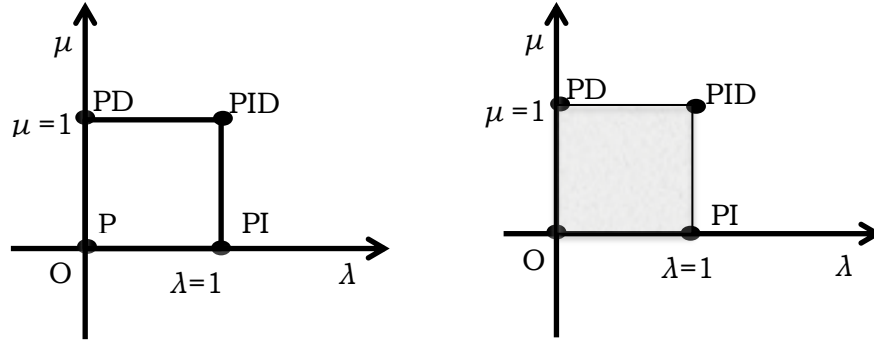
Figure 3.2 PID controller: from points to plane

By Laplace transform, a fractional transfer function can be obtained as

$$G_p(s) = \frac{Y(s)}{U(s)} = \frac{1}{a_n s^{\beta_n} + \cdots + a_1 s^{\beta_1} + a_0 s^{\beta_0}} \qquad \ldots (3.8)$$

In general, a fractional order dynamic system can be represented by a transfer function of the form

$$G_p(s) = \frac{Y(s)}{U(s)} = \frac{b_m s^{\alpha_m} + \cdots + b_1 s^{\alpha_1} + b_0 s^{\alpha_0}}{a_n s^{\beta_n} + \cdots + a_1 s^{\beta_1} + a_0 s^{\beta_0}} \qquad \text{... (3.9)}$$

However, in control practice, it is common to consider the fractional order controller. This is due to the fact that the plant model may have already been obtained as an integer order model in classical sense. In most cases, the objective is to apply the fractional order control to enhance the system control performance. Taking the conventional PID controller as an example, its fractional order version, $PI^\lambda D^\mu$ controller, was studied in time domain in [103] and in frequency domain in [102]. The time domain formula is that

$$u(t) = K_p e(t) + T_i D_t^{-\lambda} e(t) + T_d D_t^\mu e(t) \qquad \text{... (3.10)}$$

It can be expected that $PI^\lambda D^\mu$ controller may enhance the systems control performance due to more tuning knobs introduced, which is illustrated by figure 3.2.

Consider an example, a simple fractional order controller for a double integrator plant $H(s) = A/s^2$ where A is the open loop plant gain. Suppose a fractional order controller of the form $D(s) = s^\alpha$, $0 < \alpha < 1$ is to be used. The open loop transfer function of the overall controlled system will be of the form

$$F_o(s) = D(s)H(s) = \frac{A}{s^{2-\alpha}}$$

Which is in fact the form of the bode's ideal transfer function [104]. It has the following characteristics

46

Open loop:

➢ The bode amplitude plot has constant slope of $-(2-\alpha)$

➢ The crossover frequency depends only on A

➢ The phase curve is a horizontal line at $-(2-\alpha)(\pi/2)$

➢ The Nyquist curve is a straight line through the origin with argument $-(2-\alpha)(\pi/2)$.

Closed loop with unity feedback:

➢ The transfer function of the form $F_c(s) = \dfrac{A}{s^{2-\alpha}+A}$

➢ The gain margin is infinity

➢ The phase margin is constant $\emptyset_m = \pi\left(1 - \dfrac{2-\alpha}{2}\right)$

➢ The step response has the expression

$$y(t) = At^{2-\alpha}E_{2-\alpha,\ 2-\alpha+1}(-At^{2-\alpha})$$

Where $E_{2-\alpha,\ 2-\alpha+1}(-At^{2-\alpha})$ is the Mittag-Leffler function in two parameters. Assuming $A \in \mathbb{R}^+$, such a step response exhibits an overshoot independent of parameter A and dependent on the parameter α.

Clearly, from the above discussion, it is a very desirable property that the overshoot is independent of parameter A and dependent only on the fractional order α. This has been explored by Oustaloup in terms of iso-damping [106].

3.5 Fractional Order Calculus in MRAC Scheme

In this section, the fractional order calculus is introduced into MRAC scheme in two ways. One is the use of fractional derivatives for the MIT adjustment rules and the other one is the use of fractional order reference models. The modified MRAC schemes are explained with some simulation illustrations.

3.5.1 The Fractional order Adjustment Rule

As can be observed in (3.2), the rate of change of the parameters depends solely on the adaptation gain γ. Taking into account the properties of the fractional differential operator, it is possible to make the rate of change depending on both the adaptation gain γ, and the derivative order α, by using the adjustment rule

$$\frac{d\theta}{dt} = -\gamma \frac{\partial J}{\partial \theta} = -\gamma e \frac{\partial e}{\partial \theta} \qquad \text{... (3.11)}$$

where α is a real number denoting the fractional order derivative. In other words, the above parameter updating rule can be expressed as follows:

$$\theta = -\gamma I^\propto \left[\frac{\partial J}{\partial \theta}\right] = -- \gamma I^\propto \left[e \frac{\partial e}{\partial \theta}\right]; I^\propto = D^{-\propto} \qquad \text{... (3.12)}$$

3.6 Magnetic levitation system

Magnetic levitation system considered in the current analysis is consisting of a ferromagnetic ball suspended in a voltage-controlled magnetic field. Fig. 2.1 shows the schematic diagram of magnetic levitation system.

Coil acts as electromagnetic actuator, while an optoelectronic sensor determines the position of the ferromagnetic ball. By regulating the electric current in the circuit through a controller, the electromagnetic force can be adjusted to be equal to the weight of the steel ball, thus the ball will levitate in an equilibrium state. But it is a nonlinear, open loop and unstable system that demands a good dynamic model and a stabilized controller.

The electromagnetic force produced by current is given by the KVL

$$u(t) = iR + \frac{dL(x)i}{dt}$$

where u is the applied voltage, i is the current in the coil of electromagnetic, R is the coil's resistance and L is the coil's inductance.

Net force acting on the ball is given by newton's third law of motion, while neglecting the friction and drag force of the air etc.

$$m\ddot{x} = mg - C\left(\frac{i}{x}\right)^2 - F_{PM}$$

where m is the mass of the ball, g is the gravitational constant, x is the position of the ball, C is the magnetic force constant and F_{PM} is the eddy current force induced in the permagnet.

Nonlinear model of magnetic levitation system can be described in terms of following set of differential equations

$$V = \frac{dx}{dt} \qquad\qquad\qquad \text{... (3.13)}$$

$$u(t) = iR + \frac{dL(x)i}{dt} \qquad\qquad\qquad \text{... (3.14)}$$

$$m\ddot{x} = mg - C\left(\frac{i}{x}\right)^2 - F_{PM} \qquad\qquad\qquad \text{... (3.15)}$$

(3.14) indicates that $L(x)$ is nonlinear function of ball position x [107], [108]. Various approximations have been used for determination of inductance for a magnetic levitation system. If we take the approximation that inductance varies with the inverse of permagnet's position, that is

$$L(x) = L + \frac{L_0 x_0}{x} \qquad \dots (3.16)$$

where L is the constant inductance of the coil in the absence of ball, L_0 is the additional inductance contributed by the presence of the ball, x_0 is the equilibrium position.

Substituting $L_0 x_0 = 2C$ then get

$$u(t) = iR + L\frac{di}{dt} + C\left(\frac{i}{x^2}\right)\frac{dx}{dt} \qquad \dots (3.17)$$

The system is linearized around a point $x_1 = x_{01}$

$$X_0 = [x_{01} \quad x_{02} \quad x_{03}]^T$$

At equilibrium, time rate derivative of x must be equal to zero i.e, $x_{02} = 0$. Also equilibrium current can be evaluated from (3.15) and it must satisfy the following condition

$$x_{03} = x_{01}\sqrt{\frac{gm}{C}} \qquad \dots (3.18)$$

Parameters taken for the analysis of Maglev system are given in table 3.1.

Parameter	unit	value
m	Kg	0.05
g	m/s^2	9.81
R	Ohm Ω	1
L	H	0.01
C	--	0.0001
x_{01}	m	0.012
x_{02}	m/s	0
x_{03}	A	0.84

Table 3.1 Physical parameters of Maglev system

3.7 Fractional order MRAC PID Controller Design

As indicated in preliminary study, we realize that the system is with typical nonlinear characteristics. Then, a more advanced controller should be adopted. Although in the model reference adaptive controller (MRAC), the desired index of performance is given by the reference model, and the controller can establish robustness with respect to unmodeled dynamics. It is hard to adjust the parameters to obtain a good performance, even worse it is very difficult to make the system stable. From previous study, [109] the PID controller can be used to control the designed micro-positioning stage in different working range with different PID parameters. That is to say, the parameters of the PID controller need to be adjusted online. Many ways can be used to tune the PID parameters, aiming for

51

combining the advantages of the MRAC and PID controller, the MRAC PID controller is adopted in this research.

The basic structure of a model reference adaptive control system is shown in the block diagram in Fig.3.1. The reference model is chosen to generate the desired trajectory for the plant output to follow. The tracking error represents the deviation of the plant output from the desired trajectory. According to the tracking error, output of the controller and the output of the plant, the adjustment mechanism automatically adjusts controller parameters so that the behavior of the closed-loop control plant output closely follows that of reference model. Structures of the reference model and the adaptive gains are chosen, which are based on the requirements of control performance.

The adjustment mechanism of MRAC system constructs by a MIT rule for computing the approximated sensitivity function. The algorithms for MIT rules can be derived by tracking error:

$$e = y_p - y_m \qquad \qquad \text{... (3.19)}$$

Cost function: $\quad J(\theta) = \frac{1}{2}e(\theta)^2$

From the MIT rule, the change rate of θ is proportional to negative gradient of J as follows:

$$\frac{d\theta}{dt} = -\gamma\frac{\partial J}{\partial \theta} = -\gamma e\frac{\partial e}{\partial \theta}$$

where e denotes the model error and θ is the controller parameter vector. The components of $\frac{\partial e}{\partial \theta}$ are sensitivity derivatives of

the error with respect to θ. The parameter γ is known as the adaption gain. The MIT rule is a gradient scheme that aims to minimize the squared model cost function.

Large force is required for immediate position tracking of maglev system. From Fig. 3.3, FOMRAC provides a large force in a transient period. Fig. 3.4 shows the position tracking of level height with FOMRAC and conventional controllers. Fig. 3.4 shows improvement in the response of Maglev system when compared with conventional controller for the parameters $K_p = 8.41464, K_i = 15.82332, K_d = 0.07195$ and fractional integrator =fractional derivative=0.9. Table 3.2 shows the performance specifications of the Maglev system with FOMRAC and conventional controller.

Controller	Rise time (Sec)	Peak time (Sec)	Settling time (Sec)	Max. Peak overshoot (%)
FOMRAC	0.370	0.56	0.79	7.43
Conventional	0.94	1.5	2.32	15.84

Table 3.2 time response specifications of the maglev system
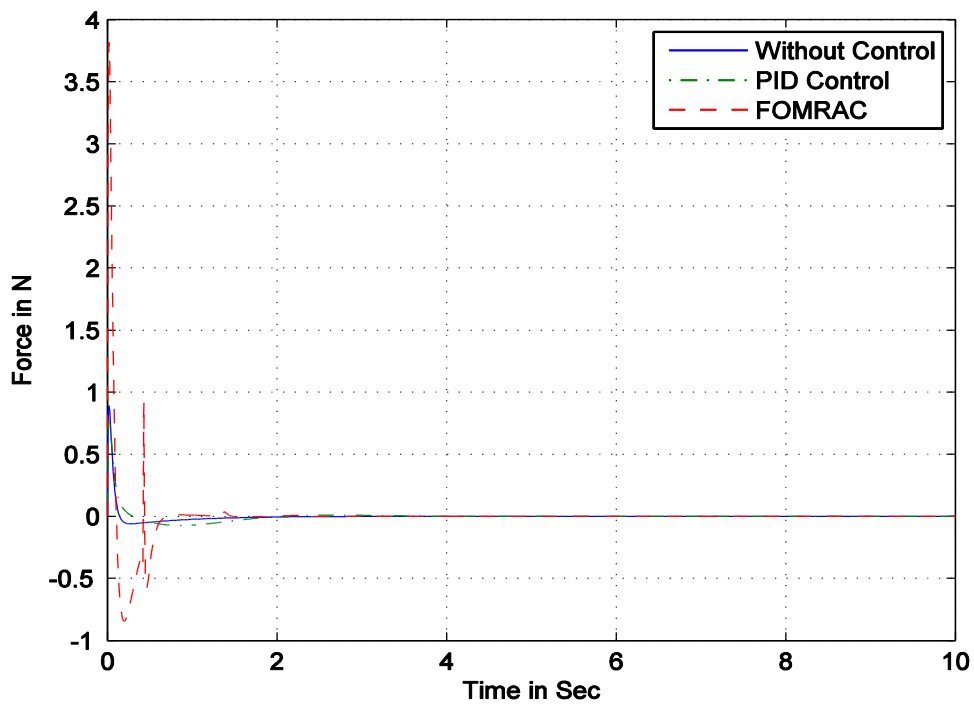
Figure 3.3 Comparison of forces in maglev, with conventional
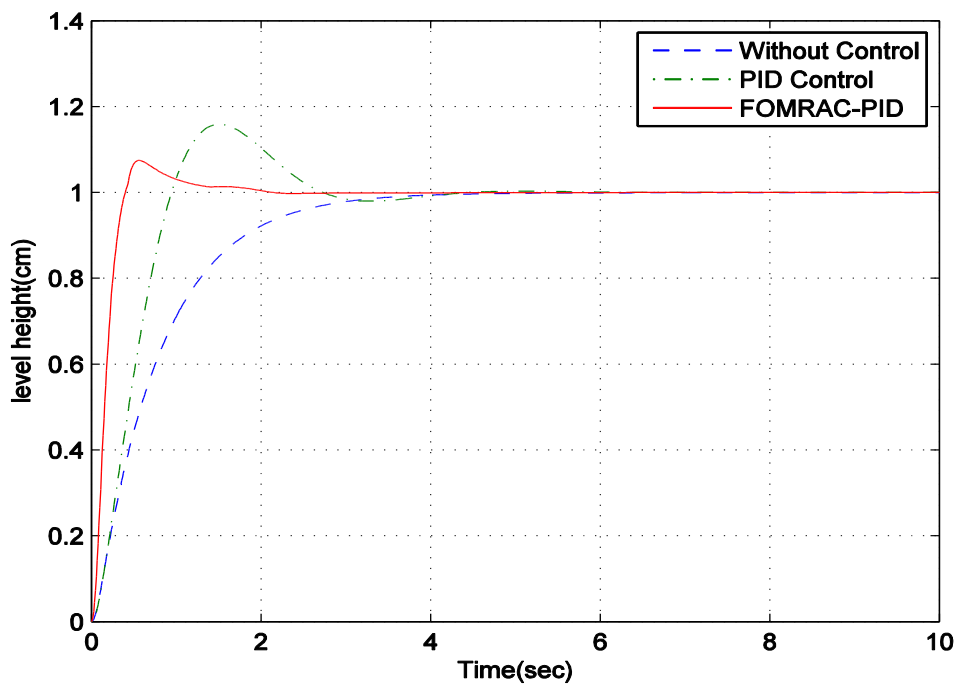
and FOMRAC-PID

Figure 3.4 Comparison of maglev with conventional and FOMRAC-PID

3.8 Conclusions

In this chapter, Fractional order PID controller is combined with the model reference adaptive system is designed for position tracking of Maglev system. Fractional order model reference adaptive PID controller for Maglev system with permagnet not only reduces the vibration in the object (permagnet) to achieve the stable positioning and also reduce the effect of eddy current-based force due to the motion of the levitated object. To show effectiveness of the proposed controller, the responses are compared with conventional controller. Simulation results indicate the superiority of the proposed controller over the conventional controller.

Chapter - IV

FEEDBACK LINEARIZATION TO MAGLEV SYSTEM

4.1 Introduction

The basic task of synthesis of a nonlinear system is to propose control algorithm, which ensures that the nonlinear system will behave according to desired goals of control, wither stabilization of system or system trajectory. Many nonlinear systems can be controlled by classical PID controllers, which ensure desired quality of regulation. However, there are systems with large range or with nonlinearities, which can not be linearized and PID control algorithm is not sufficient for such dynamic systems. In such a case, nonlinear synthesis methods, like gain scheduling method, control design by Lyapunov function, exact linearization method, etc., are used. The analysis and synthesis of the nonlinear systems require knowledge of mathematical disciplines such as differential geometry and also these methods have limited use in practice, with development of computer technology.

In this chapter, the basic theory of feedback linearization is presented and issues of particular relevance to process control applications are discussed. Two fundamental nonlinear controller design techniques, input output linearization and state space linearization are discussed in detail. The theory also presented for linear systems to facilitate understanding of the nonlinear results. A

survey of process control strategies and applications show that a variety of nonlinear control design techniques are based on input output linearization have been presented.

This chapter differs from existing reviews of feedback linearization by providing a balanced discussion of theoretical issues of interest to process control engineers.

4.2 Nonlinear Process Model

There are several types of finite dimensional, nonlinear process models available in literature [110] & [111]. This work focuses on continuous time, state space models of the form

$$\dot{x} = f(x) + g(x)u \qquad \qquad \dots (4.1)$$

$$y = h(x)$$

where x is an n-dimensional vector of state variables, u is an m-dimensional vector of manipulated input variables, y is an m-dimensional vector of controlled output variables, $f(x)$ is an n-dimensional vector of nonlinear functions, $g(x)$ is an (n × m)-dimensional matrix of nonlinear functions and $h(x)$ is an m-dimensional vector of nonlinear functions. The single input, single output (SISO) case where m = 1 will be emphasized to facilitate understanding of the basic concepts. The model (4.1) will be modified as necessary to describe more complex nonlinear processes, such as those with measured disturbances or time delays.

Consider the Jacobian linearization of the nonlinear model (4.1) about an equilibrium point (u_0, x_0, y_0)

$$\dot{x} = \left[\frac{\partial f(x_0)}{\partial x} + \frac{\partial g(x_0)}{\partial x} u_0\right](x - x_0) + g(x_0)(u - u_0) \qquad \dots (4.2)$$

$$y - y_0 = \frac{\partial h(x_0)}{\partial x}(x - x_0)$$

Using deviation variables, the Jacobian model can be written as a linear state space system, with obvious definitions for the matrices A, B and C.

$$\dot{x} = Ax + Bu \qquad \dots (4.3)$$

$$y = Cx$$

It is important to note that the Jacobian model is an exact representation of the nonlinear model only at the point (x_0, u_0). As a result, a control strategy based on a linearized model may yield unsatisfactory performance and robustness at other operating points.

In this chapter, a class of nonlinear control technique that can produce a linear model which is an exact representation of the original nonlinear model over a large set of operating conditions is presented. Here, local feedback linearization is considered (i.e. the coordinate transformation and control law may be only locally defined) to avoid complications associated with the global problem.

The feedback linearization method basically consists of two operations. Nonlinear change of co-ordinates and nonlinear state feedback.

After feedback linearization, the input-output model is linear, which is given by

$$\dot{\xi} = A\xi + Bv \qquad\qquad \text{... (4.4)}$$

$$w = C\xi$$

where ξ is an r- dimensional vector of transformed state variables, v is an m- dimensional vector of transformed output variables and the matrices A, B and C have a very simple canonical structure. If $r < n$, an additional $n - r$ state variables must be introduced to complete the coordinate transformation. The integer r is called the relative degree and is a fundamental characteristic of a nonlinear system.

Most feedback linearization approaches are based on input-output linearization or state space linearization. In the input-output linearization approach, the objective is to linearize the map between the transformed inputs (v) and the actual outputs (y). A linear controller is then designed for the linearized input-output model, which can be represented by (4.4) with $r \leq n$ and $w = y$. However, there is a subsystem that typically is not linearized,

$$\dot{\eta} = q(\eta, \xi) \qquad\qquad \text{... (4.5)}$$

where η is an $(n - r)$-dimensional vector of transformed state variables and q is a $(n - r)$- dimensional vector of nonlinear functions. Input-output linearization techniques are restricted to systems in which zero dynamics are stable.

In the state space linearization approach, the goal is to linearize the map between the transformed inputs and the entire vector of transformed state variables. This objective is achieved by deriving artificial outputs (w) that yield a feedback linearized model with sate dimension $r = n$. A linear controller is then synthesized for the linear input state model. However, this approach may fail to simplify the controller design task because the map between the transformed inputs and the original outputs (y) generally is nonlinear. As a result, input-output linearization is preferable to state space linearization for most process control applications. For some processes, it is possible to simultaneously linearize the input state and input-output maps because the original outputs yield a linear model with dimension $r = n$.

4.3 Input-output Linearization

An input output linearizing controller is designed for SISO version of the linear system (4.3). This illustrates the basic controller design procedure employed in the nonlinear case. That the system can be transformed into the following normal form via a linear change of coordinates $[\xi^T, \eta^T]^T = \mathrm{T}x$,

$$\dot{\xi}_1 = \xi_2$$

$$\dot{\xi}_2 = \xi_3$$

$$.$$
$$. \qquad\qquad\qquad\qquad ... (4.6)$$
$$.$$

$$\dot{\xi}_r = R\xi + S\eta + ku$$

$$\dot{\eta} = P\xi + Q\eta$$

$$y = \xi_1$$

where r is the relative degree. The static state feedback control law,

$$u = \frac{v - R\xi - S\eta}{k} \qquad \ldots (4.7)$$

changes the r-th equation in (4.6) to $\dot{\xi}_r = v$. The transformed input v is the designed to stabilize the ξ subsystem, as

$$v = -\alpha_r \xi_r - \alpha_{r-1} \xi_{r-1} - \cdots - \alpha_1 \xi_1 \qquad \ldots (4.8)$$

In the original coordinates, the complete control law has the form,

$$u = \frac{-CA^r x - \alpha_r CA^{r-1} x - \cdots - \alpha_1 Cx}{CA^{r-1}b} \qquad \ldots (4.9)$$

The proposed control law yields the following characteristic equation for the ξ subsystem, is as follows

$$s^r + \alpha_r s^{r-1} + \cdots + \alpha_1 s + \alpha_0 = 0 \qquad \ldots (4.10)$$

Nominal stability of the ξ subsystem, and therefore boundedness of the output, is ensured if the controller tuning parameters α_i are chosen such that (4.10) is hurwitz polynomial. The closed loop system is internally stable if and only if the eigen values of the matrix Q are in the open left half plane. Hence, the proposed controller design technique is restricted to linear systems which are minimum phase.

4.3.1 Controller Design

In order to illustrate the basic concepts, consider the following two dimensional nonlinear system,

$$\dot{x}_1 = f_1(x_1, x_2) + g_1(x_1, x_2)u$$

$$\dot{x}_2 = f_2(x_1, x_2) \qquad \qquad \text{... (4.11)}$$

$$y = x_1$$

If the nonlinear function g_1 is non-zero in the operating region of interest, the static feedback control law,

$$u = \frac{v - f_1(x_1, x_2)}{g_1(x_1, x_2)} \qquad \qquad \text{... (4.12)}$$

changes the first equation (4.11) to $\dot{x}_1 = v$. Thus, the control law exactly linearizes the map between the transformed input v and the output y. Consequently, a linear controller can be designed to satisfy control objectives such as setpoint tracking. It is important to note that the x_2 dynamics remain nonlinear. Asymptotic stability of these zero dynamics is a necessary condition for nominal closed loop stability.

4.3.2 General design Procedure

Now consider the design of an input output linearizing controller for the n-th order nonlinear system (4.1). The systems (4.1) can be transformed into normal form via a diffeomorphism

$$[\xi^T, \eta^T]^T = \Phi(x)$$

if the relative degree r is well defined. The ξ coordinates are defined as,

$$\xi_k = \Phi_k(x) = L_f^{k-1} h(x), \qquad 1 \le k \le r \qquad \qquad \text{... (4.13)}$$

and $\eta_k = \Phi_{r+k}(x), \ \ 1 \le k \le n - r$, where $L_g \Phi_k(x) = 0$. The normal form can be written as,

$$\dot{\xi}_1 = \xi_2$$

$$\dot{\xi}_2 = \xi_3$$

$$\cdot$$
$$\cdot \qquad \qquad \dots (4.14)$$
$$\cdot$$

$$\dot{\xi}_r = b(\xi, \eta) + a(\xi, \eta)u$$

$$\dot{\eta} = q(\xi, \eta)$$

$$y = \xi_1$$

The static feedback control law

$$u = \frac{v - b(\xi, \eta)}{a(\xi, \eta)} \qquad \qquad \dots (4.15)$$

changes the r-the equation of (4.14) to $\dot{\xi}_r = v$. As a result, the map between the transformed input v and the output y is exactly linear. Thus, a linear state feedback controller can be synthesized to stabilize the ξ subsystem. For instance, the pole placement design (4.17) yields the characteristic polynomial for the linear sub system. When expressed in the original coordinates, the two control laws have the following form,

$$u = \frac{v - L_f^r h(x)}{L_g L_f^{r-1} h(x)} \qquad \qquad \dots (4.16)$$

$$v = -\alpha_r L_f^{r-1} h(x) - \alpha_{r-1} L_f^{r-2} h(x) - \cdots - \alpha_1 h(x) \qquad \dots (4.17)$$

Hence, the complete state feedback control law can be written as

$$u = \frac{-L_f^r h(x) - \alpha_r L_f^{r-1} h(x) - \alpha_{r-1} L_f^{r-2} h(x) - \cdots - \alpha_1 h(x)}{L_g L_f^{r-1} h(x)} \qquad \dots (4.18)$$

63

4.3.3 Integral Control

In most process control applications, the objective is to maintain the output at a non-zero setpoint despite unmeasured disturbances and plant/model mismatch. It can be achieved by using the integral control and the state feedback control law with integral control is given as

$$u = \frac{-L_f^r h(x) - \alpha_r L_f^{r-1} h(x) - \alpha_{r-1} L_f^{r-2} h(x) - \cdots - \alpha_1 h(x) + \alpha_0 \int_0^t \left[y_{sp} - h(x) \right] d\tau}{L_g L_f^{r-1} h(x)}$$

$$\dots (4.19)$$

where α_0 is an additional controller tuning parameter associated with the integral term. The integral control law (4.19) yields the following characteristic equation for the ξ subsystem

$$s^{r+1} + \alpha_r s^r + \cdots + \alpha_1 s + \alpha_0 = 0 \qquad \dots (4.20)$$

By choosing the controller parameters α_i in terms of single tuning parameter ϵ, the following closed loop transfer function is obtained for setpoint changes if $y(0) = y_{sp}(0)$

$$\frac{y(s)}{y_{sp}(s)} = \frac{\frac{r+1}{\epsilon \tau} s + 1}{(\epsilon s + 1)^{r+1}} \qquad \dots (4.21)$$

The objective is to find conditions which ensure that the origin is a locally or globally asymptotically stable equilibrium point of input-output linearized system

Consider the closed loop system comprised of the nonlinear system (4.1) and the input-output linearizing controller (4.19). The

closed loop system has the transformed coordinates. If the controller tuning parameters α_i are chosen such that the characteristic polynomial (4.10) is hurwitz, then the linear state variable ξ converge exponentially to the origin for any initial state $\xi(0)$ for which the control law (4.15) remains well defined.

4.4 Application to Maglev system

In this section, proposed approach is applied to a non-linear Maglev system. The Maglev system consists of a ferromagnetic ball suspended in a voltage controlled magnetic field.

A free body diagram of the levitated object being suspended vertically by balancing the force generated by the electromagnet $f(p, i)$ and the gravity force mg. The force experienced by the levitated object $f(p, i)$ is a function of the air-gap or distance below the electromagnet p and the current supplied to the magnet is found by direct application of both ampere's law and faraday's laws

$$f(p, i) = -\frac{i^2}{2}\frac{dL(p)}{dp} \qquad \text{... (4.22)}$$

The total inductance, $L(p)$ is a nonlinear function of the position in the electromagnetic field. A typical approximation is to assume that inductance varies in an inverse relationship with respect to the position as

$$L(p) = L_c + \frac{L_0 p_0}{p} \qquad \text{... (4.23)}$$

where L_c is the constant inductance of the electromagnet in the absence of the levitated object, L_0 is the additional inductance

65

contributed by the presence of the object and p_0 is the equilibrium position.

$$f(p,i) = -\frac{i^2}{2} \frac{d\left(L_c + \frac{L_0 p_0}{p}\right)}{dp} = \frac{L_0 p_0}{2} \frac{i^2}{p^2}$$

$$f(p,i) = c\left(\frac{i}{p}\right)^2 \text{ where } c = \frac{L_0 p_0}{2} \qquad \ldots (4.24)$$

Application of newton's third law of motion for this suspended object yields

$$m\ddot{p} = mg - c\left(\frac{i}{p}\right)^2 \qquad \ldots (4.25)$$

The dynamic model of the system can be written as

$$\begin{cases} \frac{dp}{dt} = v \\ Ri + \frac{d}{dt}\left(L(p,i)\right) = e \\ m\frac{dv}{dt} = mg - C\left(\frac{i}{p}\right)^2 \end{cases} \qquad \ldots (4.26)$$

where p denotes ball position, v is the ball's velocity, i is the current in the coil of the electromagnet, e is the applied voltage, R is the coil's resistance, L is the coil's inductance, g is the gravitational constant, C is the magnetic force constant and m is the mass of the levitated ball.

Let the states and control input are chosen as $x_1 = p$, $x_2 = v$, $x_3 = i$, $u = e$ and $x = (x_1\ x_2\ x_3)^T$ is the state vector. Thus the state-space model of the Maglev system can be written as

$$\begin{cases} \dot{x}_1 = x_2 \\ \dot{x}_2 = g - \frac{C}{m}\left(\frac{x_3}{x_1}\right)^2 \\ \dot{x}_3 = -\frac{R}{L}x_2 + \frac{2C}{L}\left(\frac{x_2 x_3}{x_1}\right) + \frac{1}{L}u \end{cases} \qquad \ldots (4.27)$$

66

Let the measurable output of Maglev system be given as

$$y = x_1 = [1 \quad 0 \quad 0][x_1 \quad x_2 \quad x_3]^T \qquad \ldots (4.28)$$

The assumption for use of the input-output feedback linearization method is nonlinear system written in state space representation

$$\begin{cases} \dot{x}(t) = f(x,t) + g(x,t) * u(t) \\ \qquad y(t) = h(x,t) \end{cases} \qquad \ldots (4.29)$$

where $x \in R^n$ is state vector, $u(t)$ is control input, $y(t)$ is system output, $f(x,t), g(x,t)$ and $h(x,t)$ are smooth nonlinear functions.

The stepwise procedure followed for linearization of nonlinear system (4.25) using input-output feedback linearization method in given below:

➤ Calculation of first derivation:

$$\dot{y} = \frac{\partial h}{\partial x} f + \frac{\partial h}{\partial x} gu = L_f h(x) + L_g h(x) u \qquad \ldots (4.30)$$

➤ If valid $L_g h(x) \neq 0$ then substitution $\dot{y} = v$ to determine the resulting input transformation

$$u = \frac{1}{L_g h(x)} (-L_f h(x) + v) \qquad \ldots (4.31)$$

➤ But if valid $L_g h(x) = 0$ then continue derivative of the output y

$$\ddot{y} = L_f{}^2 h(x) + L_g L_f h(x) u \qquad \ldots (4.32)$$

➤ If valid $L_g L_f h(x) = 0$, then continue derivative of the output y

➤ Derivative of the output continues until $L_g L_f{}^{r-1} h(x) u \neq 0$ is valid.

67

➤ If $L_g L_f^{r-1} h(x) u = 0$, then substitute $y^r = v$ to determine the resulting input transformation,

$$u = \frac{1}{L_g L_f^{r-1} h(x)} \left(-L_f^{\,r} h(x) + v\right) \qquad \text{... (4.33)}$$

➤ To determine state transformation $z = T(x)$

$$z = T(x) = \left[h(x), L_f h(x), \ldots, L_f^{\,r-1} h(x)\right] \qquad \text{... (4.34)}$$

➤ Nonlinear system (4.27)can be transformed into linear form

$$\dot{z} = \begin{bmatrix} 0 & 1 & \cdots & 0 \\ 0 & 0 & 1 & 0 \\ \cdots & \cdots & \cdots & \cdots \\ 0 & 0 & \cdots & 0 \end{bmatrix} z + \begin{bmatrix} 0 \\ 0 \\ \cdots \\ 1 \end{bmatrix} v \qquad \text{... (4.35)}$$

➤ For the above systems (4.28), it is necessary to propose feedback control law by linear method of synthesis, to ensure the desired behavior of the system in case of change of the reference trajectory or to compensate disturbance.

When input-output feedback linearization method is used with relative order of nonlinear system $r < n$, the state variables are divided into two vectors $\xi = [z_1, z_2, \ldots, z_r]^T$ and $\eta = [z_1, z_1, \ldots, z_1]^T$. For state variables of the vector ξ proceed as in case when $r = n$. Variables from η are chosen so as to be mutually independent. Thereafter, control is proposed, that linear dynamic is dictated only output and first r state variables. The other state variables do not contain input of the system u, so they are not controlled, but require that they are limited and do not exceed specified limits.

To transform the above system coordinates into new coordinates by using feedback linearization, let the choice of variables be made as

$$\begin{cases} z_1 = x_1 \\ z_2 = x_2 \\ z_3 = g - \frac{C}{m}\left(\frac{x_3}{x_1}\right)^2 \end{cases} \qquad \dots (4.36)$$

The dynamic model of the Maglev system in the new co-ordinate system can be written as

$$\begin{cases} \dot{z}_1 = z_2 \\ \dot{z}_2 = z_3 \\ \dot{z}_3 = f(z) + g(z)u \end{cases} \qquad \dots (4.37)$$

where $f(z) = 2(g - z_3)\left(\left(1 - \frac{2C}{Lz_1}\right)\frac{z_2}{z_1} + \frac{R}{L}\right)$

$$g(z) = \frac{-2}{Lz_1}\sqrt{\frac{C}{m}}(g - z_3)$$

It should be noted that the function $f(z)$ and $g(z)$ with $z \in R^3$ corresponds to original co-ordinates, to the following functions respectively

$$f_1(x) = \frac{2C}{m}\left(\left(1 - \frac{2C}{Lx_1}\right)\frac{x_2 x_3^2}{x_1^2} + \frac{R}{L}\frac{x_3^2}{x_1^2}\right)$$

$$g_1(x) = -\frac{2Cx_3}{mx_1^2}$$

Let the output of the system be

$$y = z_1 = x_1 \qquad \dots (4.38)$$

Using (4.27) - (4.34), the relationship between the input and output of the system can be found as

69

$$\ddot{y} = f(x) + g(x)u \qquad \qquad \dots (4.39)$$

After substitution of $\ddot{y} = w$, the resulting input transformation has the following form

$$u = \frac{1}{g_1(x)}(-f_1(x) + w) \qquad \qquad \dots (4.40)$$

And corresponding state transmission $z = T(x)$ can be determined as

$$z = \begin{bmatrix} z_1 \\ z_2 \\ z_3 \end{bmatrix} = \begin{bmatrix} y \\ \dot{y} \\ \ddot{y} \end{bmatrix} \qquad \qquad \dots (4.41)$$

After the application of the input transformation u and state transformation z, it is possible to transform the nonlinear system to the following form

$$\dot{z} = \begin{bmatrix} 0 & 1 & 0 \\ 0 & 0 & 1 \\ 0 & 0 & 0 \end{bmatrix} z + \begin{bmatrix} 0 \\ 0 \\ 1 \end{bmatrix} w \qquad \qquad \dots (4.42)$$

Based on the matrix of the state space, suitable chosen roots $p = [p_1, p_2, p_3]$, the state feedback control law in the form

$$w = -Kz + Ny_r \qquad \qquad \dots (4.43)$$

where K is the vector gains and N is the feedforward gain.

The resulting input transformation and state transformation together with control law are implemented for control of Maglev system.

4.5 Simulation Results

Since the magnetic levitation system is unstable in open loop, physical analysis of the simulation model was carried in a feedback control structure with defined reference signal y_r.
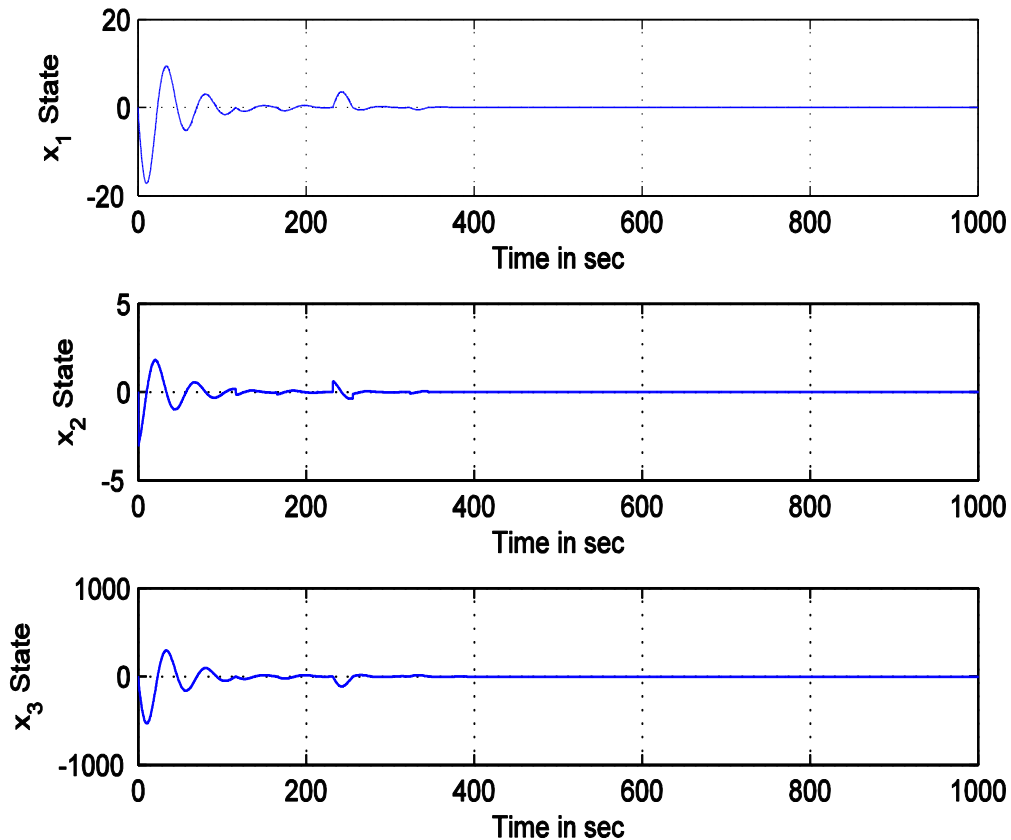
Figure 4.1 All the states of the Maglev system

Fig. 4.1 shows the stabilization of all the states by using feedback linearization techniques. Fig. 4.2 shows the error signal, corresponding to controlled input as well as transformed states of the magnetic levitation system.
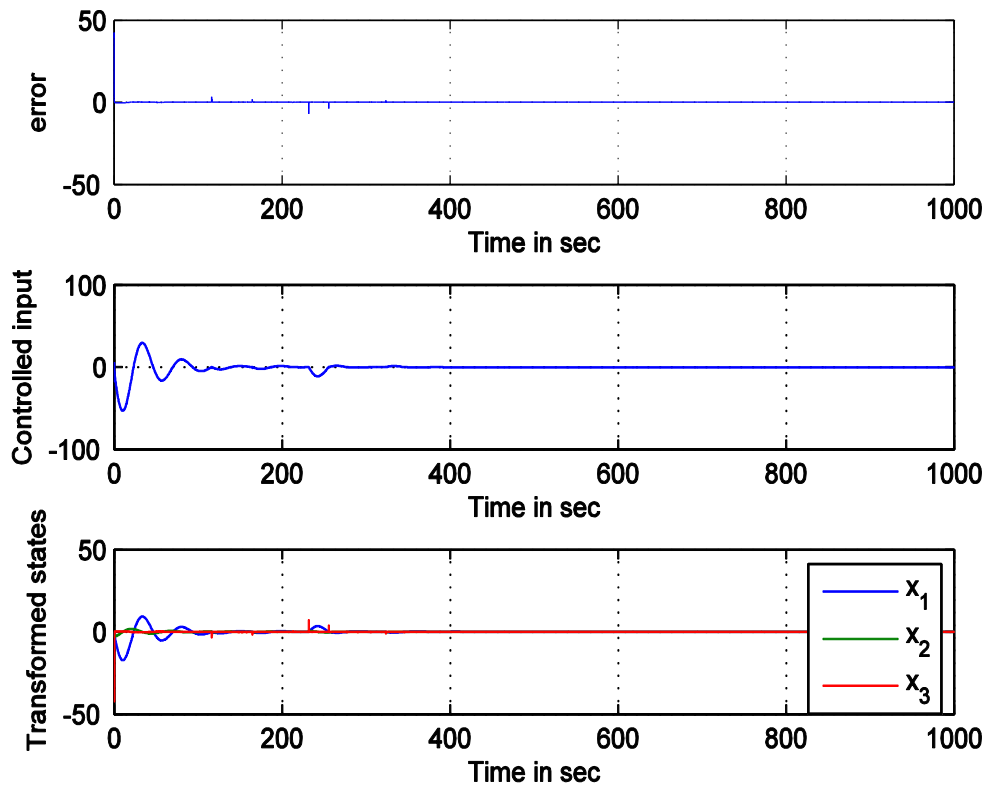
Figure 4.2 Error signal, controlled input and new states
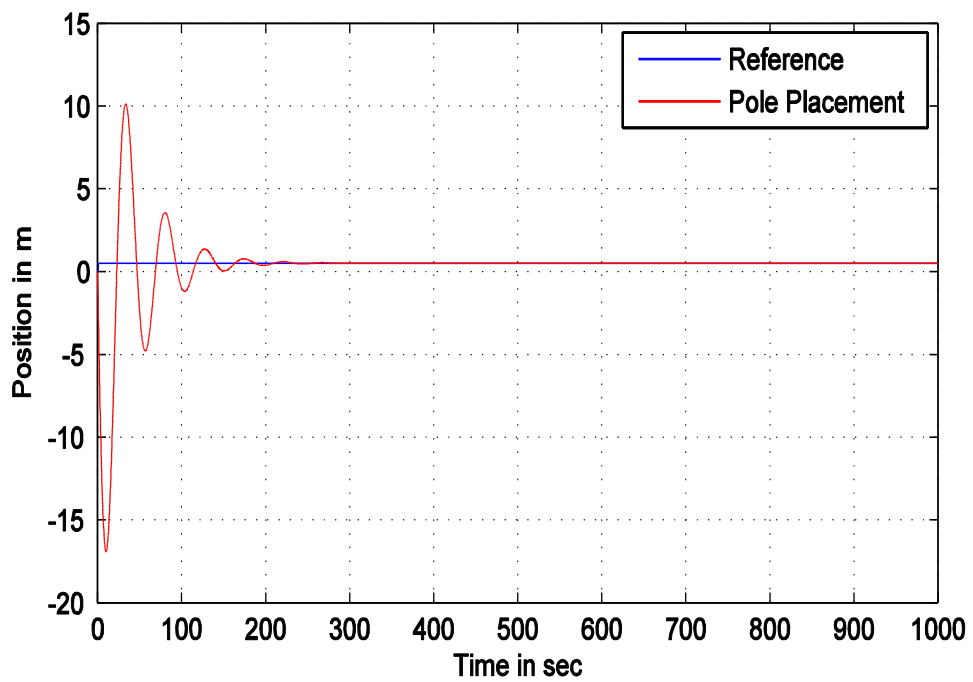
Figure 4.3 Position tracking of maglev system using pole placement

4.6 Conclusions

In this chapter, input-output linearization method is successfully applied to Maglev system with the relative degree of nonlinear system $r < n$. A linear model is developed to represent the nonlinear dynamics of Maglev system. Control Law has been derived for the Maglev system. By using the control law, pole placement technique has been implemented for the position tracking of Maglev system. Simulation results indicate large transient variations in the levitated object with pole placement technique. These variations may lead to the levitated object attract towards electromagnet or fall down.

Chapter – V

BACKSTEPPING FUZZY SLIDING MODE CONTROLLER TO MAGLEV SYSTEM

5.1 Introduction

The control of complex nonlinear systems appears generally difficult, particularly in the case of ill-defined models and when these systems are subject to unidentified noise or disturbance for which the only available information is the amplitudes of the uncertainties resulting in the definition of the model.

In the past few years, researchers have paid attention to control and have proposed different kinds of control methods such as linear and adaptive PID control, dynamic inversion control, feedback linearization control, model predictive control, backstepping control, sliding mode control, LMI based linear control, observer based control, adaptive control and nonlinear control, just to numerate a few. Recently, with the development of intelligence control theory, some advanced or modified controllers, which combine the aforementioned basic methods with intelligent control methods, such as fuzzy control and switching topology, have been presented for a few complicated tasks.

Feedback linearization is one of the important approaches for nonlinear control [118], [119]; the reason is that whenever a nonlinear system is linearizable, nonlinearities can be exactly cancelled so that

the control techniques are now feasible to linear systems as well as nonlinear systems. The conditions for feedback linearization of nonlinear systems are restrictive and it is of practical interest to investigate situations where these conditions fail but do so only slightly [120]. In 2010, Ting-Li Chien, et al., [121] developed the feedback linearization design for the control of a MIMO cancer model system to improve the cancer load. Jing Lei et al., [122] proposed the output feedback predictive control to solve the realization issues of future states; a high gain observer is constructed as a predictor. L Yan et al., [123] and T. R. Oliveira, et al., [124] introduced tracking sliding mode control designs for single-input single-output (SISO) uncertain linear and nonlinear plants with unknown control direction and arbitrary relative degree. John Hauser, et al., [120] presented an approach for the approximate input–output linearization of nonlinear systems, particularly those for which relative degree is not well defined.

Shaocheng Tong, et al., [125] proposed observer based adaptive fuzzy output feedback control approach for a class of uncertain stochastic nonlinear systems with unmeasured states. It has been designed based on the principle of the adaptive backstepping technique, although it can solve the problem of the unmeasured states and guarantee the stability of the close-loop system. Backstepping is a recursive procedure for systematically selecting the

control Lyapunov functions that allows the design of adaptive controllers for a class of nonlinear processes.

This chapter is organized as follows: Sections 5.2 describes the problem formulation, Section 5.3 describes the application to nonlinear Maglev system and simulation results are presented in Section 5.4.

5.2   Problem Formulation

Let us consider a general n^{th} order dynamical system with following description:

$$\dot{x}_1 = F_1(x_1) + G_1(x_1)x_2$$

$$\dot{x}_2 = F_2(x_1, x_2) + G_2(x_1, x_2)x_3 \qquad \dots (5.1)$$

$$\vdots$$

$$\dot{x}_2 = F_n\big(x_1, x_{2,} \dots x_n\big) + G_n(x_1, x_{2,} \dots x_n)u$$

where $x_1, x_{2,} \dots x_n$ represents the states of the nth order system, u is the scalar input and $F_i(x_i)$, $G_i(x_i)$ for $i = 1,2, \dots n-1$, are linear functions of the system states where as $F_n(x_n)$, $G_n(x_n)$ are non-linear functions. x is the vector representing states [126], [127].

The objective of the controller is to make x_1 track a desired trajectory x_{1d}. The first tracking error is defined as

$$e_1 = x_1 - x_{1d} \qquad \dots (5.2)$$

The dynamics of e_1 can be described by

$$\dot{e}_1 = F_1(x_1) + G_1(x_1)x_2 - \dot{x}_{1d} \qquad \text{... (5.3)}$$

Then x_{2d} is chosen as virtual control input to drive e_1 to zero so that x_1 can track x_{1d}

$$x_{2d} = G_1^{-1}(-F_1 - K_1 e_1 + \dot{x}_{1d}) \qquad \text{... (5.4)}$$

The above control results in the following error dynamics

$$\dot{e}_1 = -K_1 e_1 \qquad \text{... (5.5)}$$

Now the next step is to make x_2 track x_{2d}, which ensures existence of convergence dynamics (5.5). So defining the second tracking error as

$$e_2 = x_2 - x_{2d} \qquad \text{... (5.6)}$$

The dynamics of e_2 can be described by

$$\dot{e}_2 = F_2(x_1, x_2) + G_2(x_1, x_2)x_3 - \dot{x}_{2d} \qquad \text{... (5.7)}$$

To stabilize dynamics in (5.7), x_{3d} is chosen as virtual control to drive e_2 to zero so that x_2 can track x_{2d}

$$x_{3d} = G_2^{-1}(-F_2 - K_2 e_2 + \dot{x}_{2d}) \qquad \text{... (5.8)}$$

The above control results in following error dynamics:

$$\dot{e}_2 = -K_2 e_2 \qquad \text{... (5.9)}$$

Proceeding similarly, define $(n-1)^{th}$ tracking error as

$$e_{n-1} = x_{n-1} - x_{(n-1)d} \qquad \text{... (5.10)}$$

The corresponding dynamics of the $(n-1)^{th}$ tracking error can be described by

$$\dot{e}_{n-1} = F_{n-1}(x_1, x_2, \dots x_{n-1}) + G_{n-1}(x_1, x_2, \dots x_{n-1})x_n - \dot{x}_{(n-1)d} \qquad \dots (5.11)$$

where x_{nd} is chosen to drive e_{n-1} to zero and is given by

$$x_{nd} = G_{n-1}{}^{-1}(-F_{n-1} - K_{n-1}e_{n-1} + \dot{x}_{(n-1)d}) \qquad \dots (5.12)$$

The above control results in the following error dynamics:

$$\dot{e}_{n-1} = -K_{n-1}e_{n-1} \qquad \dots (5.13)$$

Let the sliding surface is chosen as

$$s = x_n - x_{nd} \qquad \dots (5.14)$$

The control input u is computed using SMC design to bring s to zero in finite time. The dynamics of s can be described by

$$\dot{s} = F_n(x_1, x_2, \dots x_n) + G_n(x_1, x_2, \dots x_n)u - \dot{x}_{nd} \qquad \dots (5.15)$$

The equivalent control is chosen as

$$u_e = G_n(x)^{-1}(-F_n(x) + \dot{x}_{nd}) \qquad \dots (5.16)$$

In the procedure presented through above equations, $K_1, K_2, \dots K_n$ are controller parameters and their values are constant to be selected appropriately. In order to satisfy sliding mode condition given as

$$\frac{1}{2}\frac{d}{dt}(s^2) \leq -\eta|s| \qquad \dots (5.17)$$

the following discontinuous switching term is added to equivalent control u_e

$$u_s = -k\,sgn(s) \qquad \text{... (5.18)}$$

where $sgn(.)$ is a standard sign function and k is the switching gain.

The control action then becomes

$$u = u_e + u_s \qquad \text{... (5.19)}$$

If all the tracking errors $e_1, e_2, e_3, \dots e_{n-1}$ are driven to zero as $t \to \infty$, then x_1 will converge to x_{1d}, x_2 will converge to x_{2d} and so on and hence asymptotic regulation of system states to desired states can be achieved.

5.3   Application to Non-Linear Magnetic Levitation System

In this section, proposed approach is applied to a non-linear Maglev system. The Maglev system consists of a ferromagnetic ball suspended in a voltage controlled magnetic field. The dynamic model of the system can be written as

$$\begin{cases} \dfrac{dp}{dt} = v \\[2mm] Ri + \dfrac{d}{dt}\big(L(p,i)\big) = e \\[2mm] m\dfrac{dv}{dt} = mg - C\left(\dfrac{i}{p}\right)^2 \end{cases} \qquad \text{... (5.20)}$$

where p denotes ball position, v is the ball's velocity, i is the current in the coil of the electromagnet, e is the applied voltage, R is the coil's resistance, L is the coil's inductance, g is the gravitational

constant, C is the magnetic force constant and m is the mass of the levitated ball [128]. Let the states and control input are chosen as $x_1 = p$, $x_2 = v$, $x_3 = i$, $u = e$ and $x = (x_1\ x_2\ x_3)^T$ is the state vector. Thus the state-space model of the Maglev system can be written as

$$\begin{cases} \dot{x}_1 = x_2 \\ \dot{x}_2 = g - \dfrac{C}{m}\left(\dfrac{x_3}{x_1}\right)^2 \\ \dot{x}_3 = -\dfrac{R}{L}x_2 + \dfrac{2C}{L}\left(\dfrac{x_2 x_3}{x_1}\right) + \dfrac{1}{L}u \end{cases} \qquad \dots (5.21)$$

Let the measurable output of Maglev system be given as

$$y = x_1 = [1\quad 0\quad 0][x_1\quad x_2\quad x_3]^T \qquad \dots (5.22)$$

To transform the above system coordinates into new coordinates by using feedback linearization, let the choice of variables be made as

$$\begin{cases} z_1 = x_1 \\ z_2 = x_2 \\ z_3 = g - \dfrac{C}{m}\left(\dfrac{x_3}{x_1}\right)^2 \end{cases} \qquad \dots (5.23)$$

The dynamic model of the Maglev system in the new co-ordinate system can be written as

$$\begin{cases} \dot{z}_1 = z_2 \\ \dot{z}_2 = z_3 \\ \dot{z}_3 = f(z) + g(z)u \end{cases} \qquad \dots (5.24)$$

where $f(z) = 2(g - z_3)\left(\left(1 - \dfrac{2C}{Lz_1}\right)\dfrac{z_2}{z_1} + \dfrac{R}{L}\right)$

$$g(z) = \dfrac{-2}{Lz_1}\sqrt{\dfrac{C}{m}}(g - z_3)$$

It should be noted that the function f(z) and g(z) with $z \in R^3$ corresponds to original co-ordinates, to the following functions respectively

$$f_1(x) = \frac{2C}{m}\left(\left(1 - \frac{2C}{Lx_1}\right)\frac{x_2 x_3^2}{x_1^2} + \frac{R}{L}\frac{x_3^2}{x_1^2}\right)$$

$$g_1(x) = -\frac{2Cx_3}{mx_1^2}$$

Let the output of the system be

$$y = z_1 = x_1 \qquad \qquad \text{... (5.25)}$$

Using (5.13) - (5.17), the relationship between the input and output of the system can be found as

$$\ddot{y} = f(x) + g(x)u \qquad \qquad \text{... (5.25a)}$$

5.3.1 Design of sliding mode control with backstepping

The control objective is to design a controller u so that the output y converges to its desired trajectory y_r. The tracking error is given by

$$e_1 = y - y_r \qquad \qquad \text{... (5.26)}$$

The time derivative of e_1 is given by

$$\dot{e}_1 = x_2 - \dot{y}_r \qquad \qquad \text{... (5.27)}$$

Let $\qquad x_{2d} = -K_1 e_1 + \dot{y}_r \qquad \qquad \text{... (5.28)}$

where x_{2d} is the desired signal of state variable x_2

The time derivative of e_2 is given by

$$\dot{e}_2 = \dot{x}_2 - \dot{x}_{2d} \qquad \qquad \text{... (5.29)}$$

81

Let x_{3d} be the desired signal of state variable x_3 and is given as

$$x_{3d} = -K_2 e_2 + \dot{x}_{2d} \qquad \qquad \text{... (5.30)}$$

where $\dot{x}_{2d} = -K_1 e_1 + \ddot{y}_r \qquad \qquad \text{... (5.31)}$

For designing a SMC for the system, switching surface is required to be designed.

Let the switching surface s be

$$s = z_3 - x_{3d} \qquad \qquad \text{... (5.32)}$$

The choice of switching surface guarantees that $z_3 - x_{3d}$ converges to zero as $t \to \infty$ when sliding surface $s = 0$.

$$u_e = g_1(x)^{-1}(-f_1(x) + x_{3d}) \qquad \qquad \text{... (5.34)}$$

A switching term discontinuous across the surface $u_s = -K_3 sgn(s)$ is added to equivalent control u_e as per (5.19) to get control action

The control action becomes

$$u = u_e + u_s = g_1(x)^{-1}(-f_1(x) + x_{3d}) - K_3 sgn(s) \qquad \qquad \text{... (5.35)}$$

Differentiating (5.32) with respect to time

$$\dot{s} = \dot{z}_3 - \dot{x}_{3d} \qquad \qquad \text{... (5.36)}$$

Substituting (5.24) and (5.35) in (5.36)

$$\dot{s} = f_1(x) + g_1(x)[g_1(x)^{-1}(-f_1(x) + x_{3d}) - K_3 sgn(s)] - \dot{x}_{3d} \qquad \qquad \text{... (5.37)}$$

$$\dot{s} = -K_3 sgn(s) \qquad \qquad \text{... (5.38)}$$

The dynamics in (5.37) guarantees the finite time reachability of s to zero from any given initial condition $s(0)$ provided that the constant K_3 is chosen to be strictly positive. The dynamics in (5.37) guarantees that $s\dot{s} < 0$ (the condition needed to guarantee switching. Since s is driven to zero in finite time, the output $y = z_1$ is governed after such finite amount of time by $s = 0$. Thus the output will

82

converge asymptotically to zero as $t \to \infty$ because K_1 and K_2 are positive scalars. Since z_1 converges to zero, then z_2 and z_3 will converge to zero as $t \to \infty$ thus x_1, x_2 and x_3 will also converge to their desired values as $t \to \infty$.

When the control action applied to the magnetic levitation system, asymptotically stabilizes x_1, x_2 and x_3 to their desired values as $t \to \infty$.

5.3.2 Design of Fuzzy sliding mode control law

Fuzzy sliding mode system, in which a fuzzy logic inference mechanism is used to mimic the hitting control laws is developed in this section.

Mamdani type fuzzy reaching control term is proposed to have the following form

$$u_s(t) = -K_f u_f(t) \qquad \text{... (5.39)}$$

Where K_f is the normalizing factor. The output fuzzy variable u_f, is continuously adjusted using fuzzy if-then rule base with respect to s.

The membership functions corresponding to the normalized input and output fuzzy sets of s and u_f are presented in Fig.5.1 where PB, PM, PS, NB, NM, NS and Z stands for positive big, positive medium, positive small, negative big, negative medium, negative small and zero respectively.
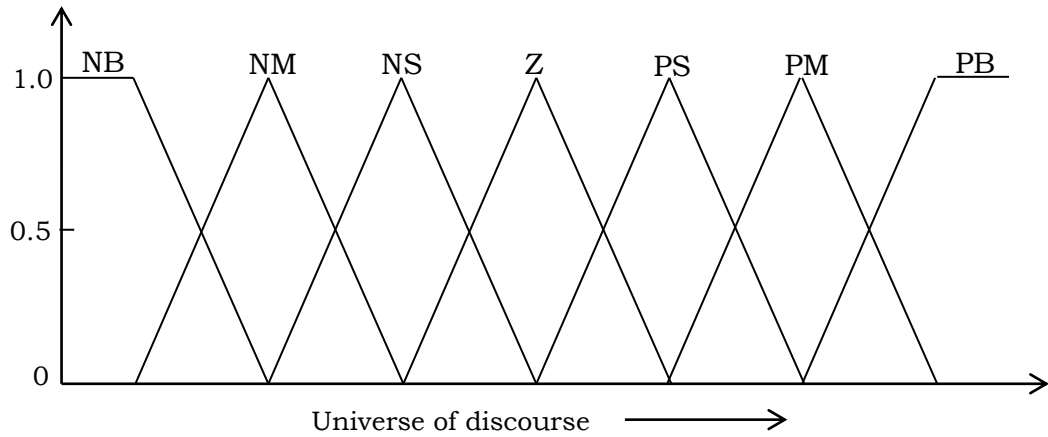
Figure 5.1 Fuzzy membership functions

Corresponding to the seven membership functions for each input variable, 7 if-then rules are tabulated.

Input	NB	NM	NS	Z	PS	PM	PB
Output	PB	PM	PS	Z	NS	NM	NB

Table 5.1 Fuzzy Rules

5.4 Simulation Results

Numerical simulations are performed for the fuzzy sliding mode controller with backstepping, desired trajectory of the output of the system and tracking error between output of the system and desired value of the output.
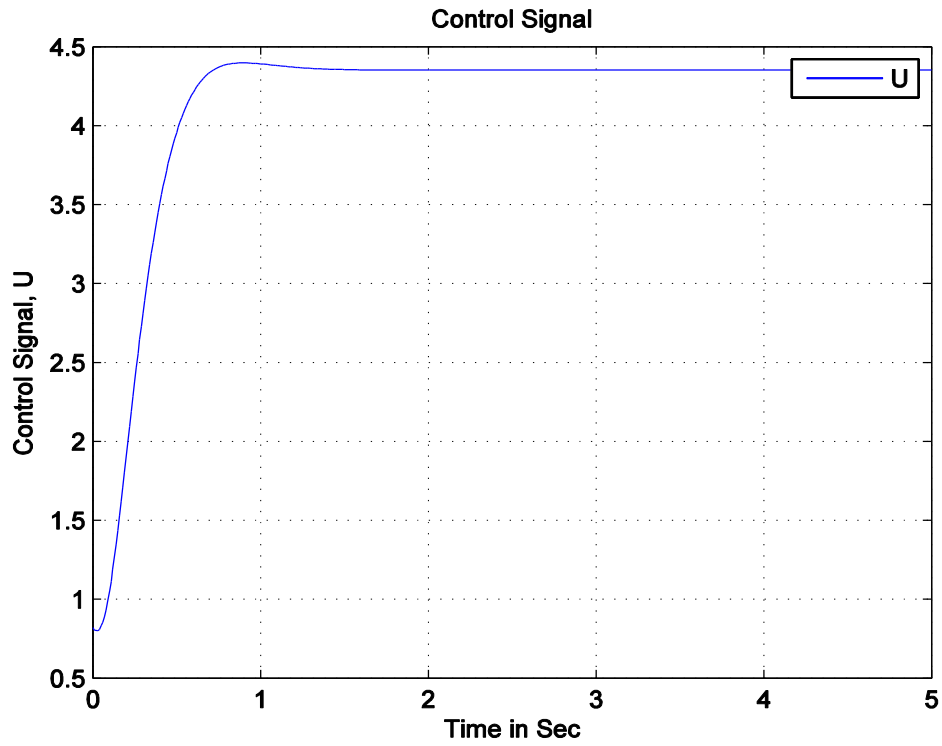
Figure 5.2 Controlled signal
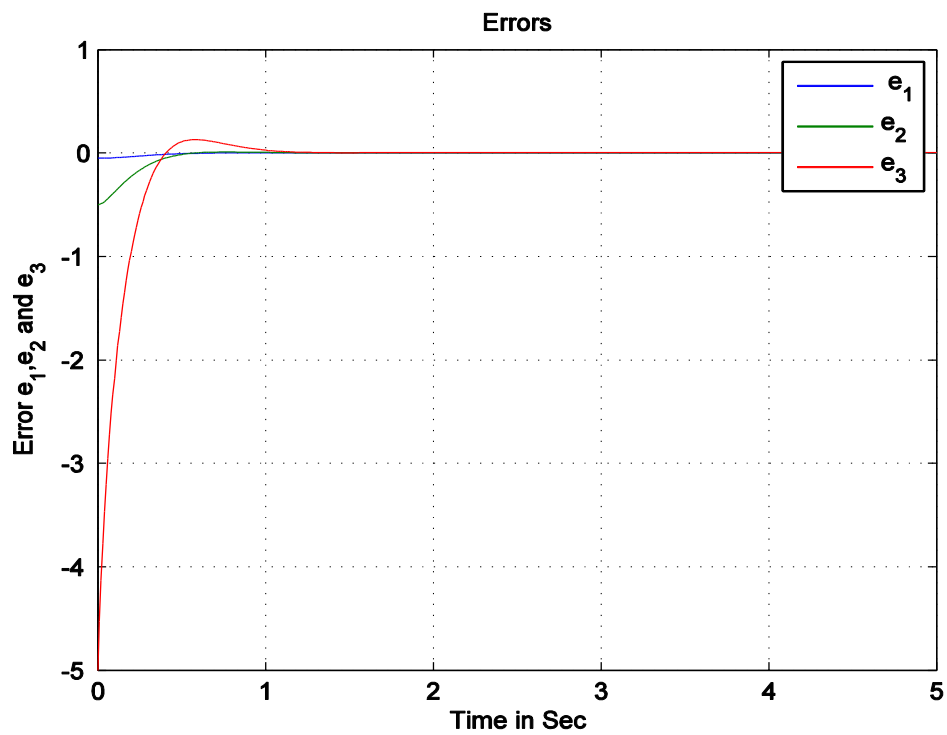
Figure 5.3 Tracking of error signals e_1, e_2 and e_3
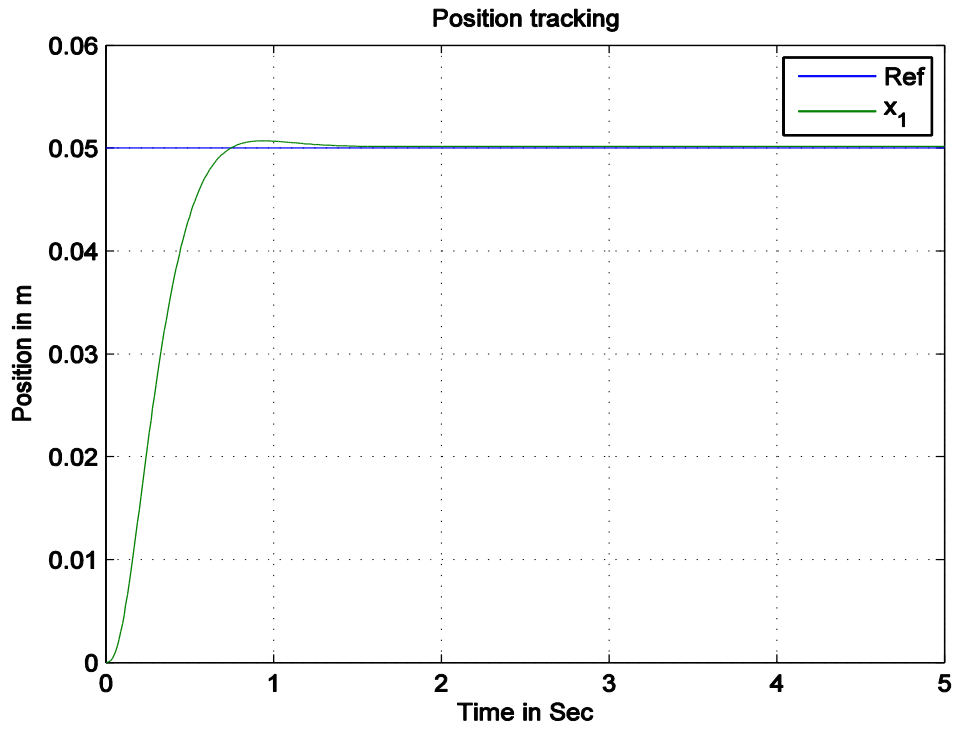
Figure 5.4 Tracking of reference position
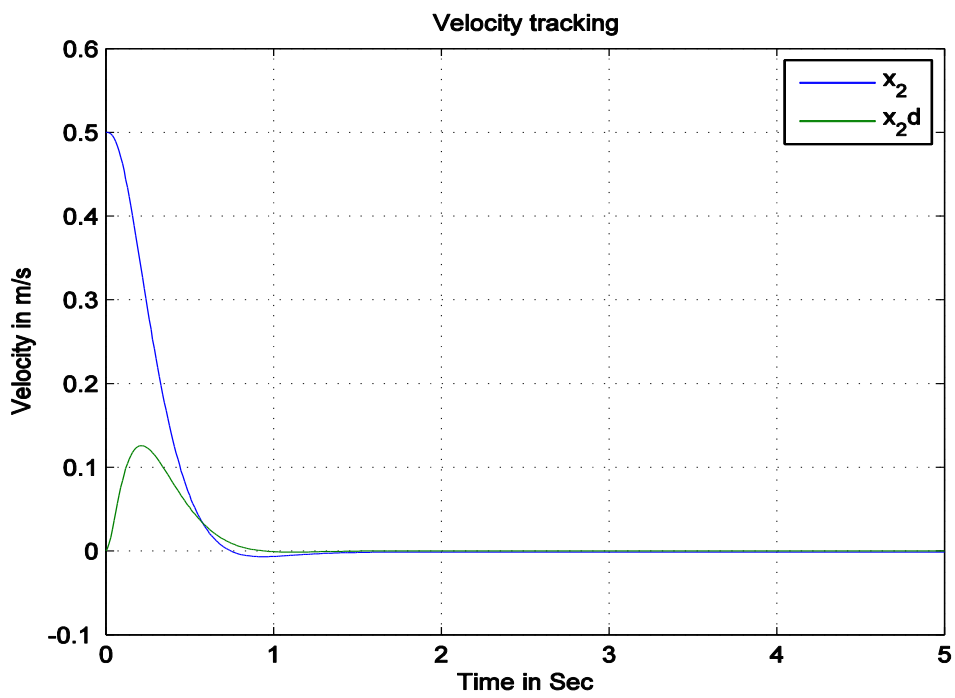
Figure 5.5 Tracking of velocity of the system

Fig 5.2 shows that control signal produced in backstepping fuzzy sliding mode control of Maglev system, Fig. 5.3 shows the tracking of error signals of all the statets, Fig.5.4 shows that position tracking of Maglev system with Backstepping fuzzy sliding mode control and Fig. 5.5 shows that tracking of second state of the Maglev system.

5.5 Conclusions

In this chapter, a fuzzy sliding mode controller for position tracking problem of a Maglev system is proposed in a backstepping manner, based on the nonlinear system model. In this method, Maglev system is described based on dynamic model and the nonlinear system is translated into local linear model by input–output feedback linearization method, not only make the system stable and avoid the chattering effect of sliding mode control. Simulation results indicate that the proposed control schemes works well when applied to the Maglev system.

Chapter - VI

PID CONTROLLER OF MAGLEV SYSTEM BASED ON CUCKOO SEARCH ALGORITHM

6.1 Introduction

Magnetic levitation is the process by which an object is suspended in air against the direction of the gravitational force with the help of a magnetic field [129] [130]. Controlling the position of the levitated object is not an easy task. Conventional controllers fail in producing perfect performance when the systems are nonlinear and uncertain. Zhenyu Yang et al, [131] designed an automatic PID controller using Non dominated Sorting Genetic Algorithm (NSGA-II) for one dimensional Nonlinear Magnetic Levitation System (NMLS). Pallav S K et al, [132] developed a PID controller with a derivative filter coefficient for the MLS. Marria Hypiusova et al, [133] proposed a robust PID controller to stabilize the NMLS using frequency domain approach. In this approach, the designed controller does not guarantee the robust stability condition; if it fails then the controller design has to be repeated. Witchupong W et al, [134] proposed state PI controller to achieve the control over the states of the MLS. Chang-Hyun Kim [135] proposed a robust air-gap controller considering disturbance force produced by magnetic suspension for MLS.

Optimization has gained superior power and influence in many applications like industrial design and engineering. The main objective

of optimization is to minimize or maximize the objective function. Hongpo Wang et al, [136] designed a controller using optimizing the control algorithms for the MLS based on the state observer. R. J. Wai et al, [137] proposed PSO PID controller to control the Maglev transportation system. I. Ahmad et al, [138] designed PID controller for MLS based on method of tuning control parameters using Genetic Algorithm (GA). Literature shows that cuckoo search algorithm satisfies the global convergence requirements when compared with other optimization techniques, so it can guarantee the global convergence properties [139]. Civiciglu, P et al, [140] and Dhivya, M et al, [141] have shown cuckoo Search algorithm is very efficient for the applications of data fusion and wireless sensor networks and also proved that the cuckoo search algorithm produces more robust results when compared with other algorithm, PSO, ABC etc.

Cuckoo search is one of many nature-inspired algorithms used extensively to solve optimization problems in different fields of engineering. It is a very effective in solving global optimization because it is able to maintain balance between local and global random walks using switching parameter. The switching parameter for the original cuckoo search algorithm is fixed at 25% and not enough studies have been done to assess the impact of dynamic switching parameter on the performance of cuckoo search algorithm [145]. This chapter mainly concentrates on position tracking of the MLS, by using cuckoo search based PID controller. Section 6.2 describes the real time

Maglev system. Section 6.3 describes the design of PID controller based on cuckoo search algorithm. Section 6.4 describes the effectiveness of cuckoo search based PID controller for position tracking of Maglev system.

6.2   Real Time Magnetic Levitation Model

The Magnetic Levitation System mainly consists of suspended steel ball, position Infra-Red sensors, controller and actuator. The steel ball is mainly controlled through current in the electrical circuit. The force acting on the steel ball is due to the current flowing in the coil and distance y between coil and centre of the steel ball [130]. Fig. 6.1 shows the experimental setup of MLS.

Figure 6.1 Real time setup of Maglev system

The non-linear model of Maglev system, which relates to the current 'i ' flowing in the coil and the position y of the steel ball is expressed as

$$m\ddot{y} = mg - K\frac{i^2}{y^2} \qquad \qquad \dots (6.1)$$

where K is constant which depends on parameters of coil, m is mass of the ball, g is gravitational constant.

The Maglev system expressed in (6.1) is nonlinear in nature, it is linearized for the analysis and design of controller is about the equilibrium point $i_0 = 0.8\, A$ and $y_0 = 0.009$ meters.

$$f(i, y) = K \frac{i^2}{y^2} \qquad \dots (6.2)$$

The linearized model of maglev system is

$$\Delta \ddot{y} = \left(\frac{\partial f(i,y)}{\partial i} \Big|_{i_0, y_0} \Delta i + \frac{\partial f(i,y)}{\partial i} \Big|_{i_0, y_0} \Delta h \right) \qquad \dots (6.3)$$

obtained by calculating the partial derivative and taking Laplace transform on both sides of (6.3),

$$\frac{\Delta y}{\Delta i} = \frac{-k_i}{s^2 - k_y} \qquad \dots (6.4)$$

where k_i and k_y are the constant values for the MLS and are expressed as

$$k_i = \frac{2g}{i_0}, \; k_y = \frac{2g}{y_0} \qquad \dots (6.5)$$

In the electrical circuit of Maglev system, the current flowing in the circuit is proportional to the control voltage V

$$i = k_1 V \qquad \dots (6.6)$$

where k_1 is proportionality constant. Now the transfer function would be

$$\frac{\Delta y}{\Delta V} = \frac{-k_1 k_i}{s^2 - k_y} \qquad \dots (6.7)$$

where ΔV is small change in control voltage around its mean value.

By considering the sensor gain, the overall transfer function of the Maglev system is

$$\frac{\Delta y_{so}}{\Delta V} = \frac{-k_1 k_2 k_i}{s^2 - k_y} \qquad \dots (6.8)$$

where, Δy_{so} is the sensor output voltage

The open loop transfer function of the Maglev system is a second order system. The closed loop response of the Maglev system is oscillatory in nature i.e., either the metal ball attracted towards the electromagnetic coil or it may be fallen down. Therefore, there is a requirement of a controller which can effectively achieve the desired setpoint.

6.3   PID Controller Design based on Cuckoo Search Algorithm

In general, the parameters of PID controller are searched in a certain space. If those parameters satisfy the system performance indices, then they are optimal parameters of PID controller. These parameters searching space can extend on the base of results obtained by Z-N method.

In order to get optimal parameters of PID Controller, nature inspired metaheuristic algorithm is required i.e. Cuckoo search algorithm. Cuckoo search uses levy flights rather than standard random walks for its global search, so that it can explore the search space more efficiently. The steps involved in finding the optimal parameters of PID controller are as follows.

Cuckoos are a family of birds with unique reproductive strategy more aggressive compared to other bird's species. Some of cuckoo bird's species like Ani and Guira lay eggs in communal nests; however, they may remove others' eggs to increase the hatching probability of their own eggs. Other species use brood parasitism method of laying their eggs in the nests of other birds or host nests.

6.3.1 Cuckoo Search Algorithm

Step 1: Confirm the objective function $f(x), x = (x_1, x_2, \ldots, x_{nd})^T$, where nd is the number variables.

Generate the set of values for each variable in the objective function, i.e., $x_i (i = 1,2, \ldots, m)$ randomly, and set the related parameters associated with the algorithm - population size, dimension nd, maximum detection probability P_k and maximum number of iterations a;

Step 2: According to objective function, confirm the fitness function p(x), $x = (x_1, x_2, \ldots, x_{nd})^T$, calculate the fitness value for each value of the variable, and record it.

$$Fitness\ function = Sum(b * ISE + a * System\ overshoot)$$

where ISE is Integral square error and System overshoot is Maximum(y)-y_{ref}; y is the position of the levitated object;

Step 3: Keep the best fitness value of each parameter value in each generation, using objective function in Step 1 to update the other suboptimal values.

93

Step 4: Compare the most recent best parameter value with the best one of last generation, keep the better one to be the optimal value.

Step 5: Set the number of consecutive iterations a = 5, if the fitness value did not change or it changes less than a value 0.05 in five consecutive iterations, then execute step 6, Otherwise, execute step 7.

Step 6: The cuckoos could search the best parameter value and the worst parameter value during iteration, then use an optimal parameter value generated during the previous iteration replace the worst one, form an intermediate group. Mutate the optimal parameter value by fitness value obtained in step 2, regard the parameter values except the optimal one as suboptimal parameter values and mutate the suboptimal parameter values by step 3.

Compare the current fitness value and historical optimal value. If the current one is better, then indicate the mutation is successful, set num = 0, update the optimal solution, execute step 8, otherwise, mutate again. If within the prescribed maximum number of times the variation is still not successful, then choose the optimal variation, execute step 8;

Step 7: After the update, compare maximum detection probability P_k with a random number $r \in (0,1)$: if $r > P_k$, change $x_i^{(a+1)}$ randomly. If there is no change, then keep the best group parameter values.

Step 8: To judge terminate condition: meet the maximum number a of iterations or reach the minimum error ε. If do not attained, then return to step 2. Otherwise output the global optimal value.

6.4 Simulation Results

In this chapter, a PID controller is designed for Maglev system to levitate the metal ball in the air-space. The Maglev system consists of electromagnetic coil, mounted on top of the box. The IR sensor is fixed on opposite sides of the box, so that it may easily sense the position of the metal ball. The metal ball gets attracted when it is near to the electromagnetic coil and otherwise fallen down due to the gravitational force.

The purpose of the PID controller is to maintain an equivalent electromagnetic force, so that the metal ball is levitated. The response of the MLS is undamped and therefore, to control such an oscillatory system, the controller should be fast and capable of improving the design requirements. The parameters of the PID controller $k_p = 4.0$, $k_i = 0.05$ and $k_d = 0.2$ are obtained using Ziegler-Nichols method. The other parameters used in simulations as well as in real time application are given in table 6.1

Parameter	Value	observation
m	0.02 kg	Mass of the levitated ball
y_0	0.009 m	Equilibrium Position
i_0	0.8 A	Equilibrium current
k_i	24.5250 N/A	Current amplification gain
k_1	0.1 A/V	Control voltage gain
k_2	Aprox. 3333 V/m	Sensor gain

Table 6.1 Maglev system parameters

The cuckoo search algorithm optimizes the parameters of the PID controller while minimizing the performance indices like ISE, IAE, ITAE and ITSE. In this work integral square error (ISE) performance index is chosen to optimize the parameters of PID controller. The search space for the cuckoo search algorithm is selected on the basis of the parameters tuned using Z-N rule and it will act as a leader for the first iteration. The other wolves are selected randomly around alpha by a suitable guess. The search space should be defined properly to obtain a global optimum solution.

The optimized parameters of PID controller are obtained by searching for the global optimum solution for around 30 iterations. The comparison of response of the Maglev system with PID controller tuned using cuckoo search algorithm and Z-N Method are shown in Fig. 6.2. For the same parameters of the PID controllers has been implemented for real time Maglev system shown in Fig. 6.3.

Table 6.2 shows the performance characteristics of Classical and Cuckoo search based PID controllers for position tracking maglev system.

	Rise time in Sec	Settling time in Sec	Steady state error
Classical	0.335	0.397	11%
Cuckoo Search	0.164	0.274	8%

Table 6.2 comparison of classical and cuckoo search based PID controllers

Fig. 6.4 shows the settling time variation of MLS for different values of mass of the ball. Conventional controller produces large variation in settling time as increasing the mass of the ball from minimum to maximum. As compared with conventional controller, cuckoo search based PID controller produces small variation in settling time as increasing the mass of the ball from minimum to maximum. Conventional controller needs to change the design parameters, if there is any variation in the system parameters. Cuckoo search based PID controller do not need any variation in the design parameters. The parameters obtained with cuckoo search algorithm are as follows $K_p = 2.276367$, $K_i = 0.054108$, and $K_d = 0.1173$.
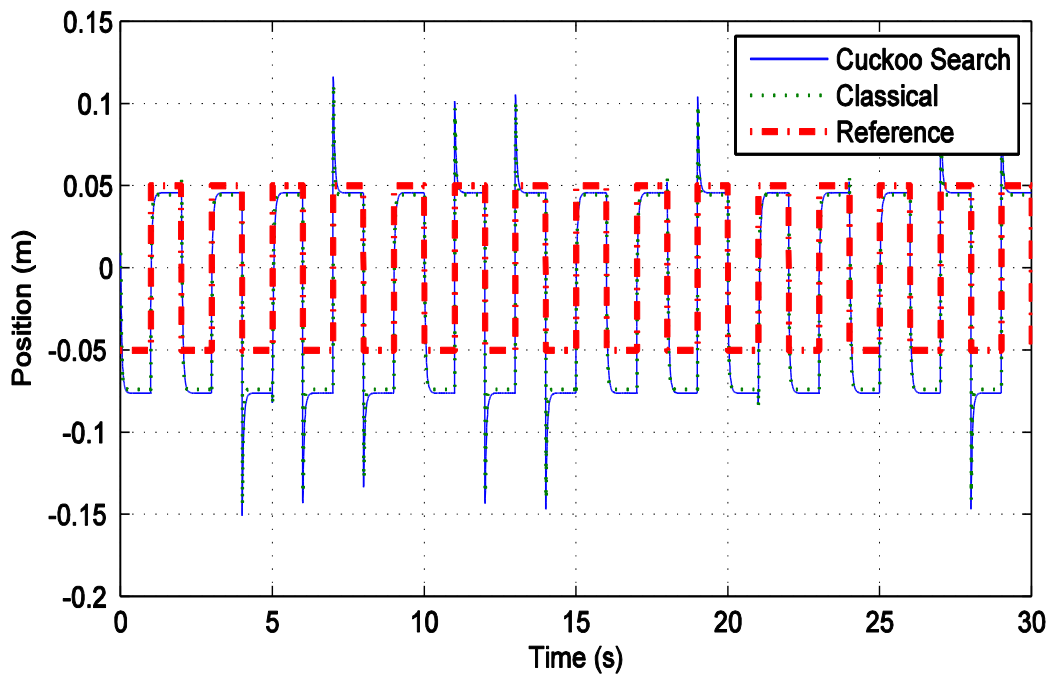
Figure 6.2 Comparison of position tracking of Maglev system in

simulation
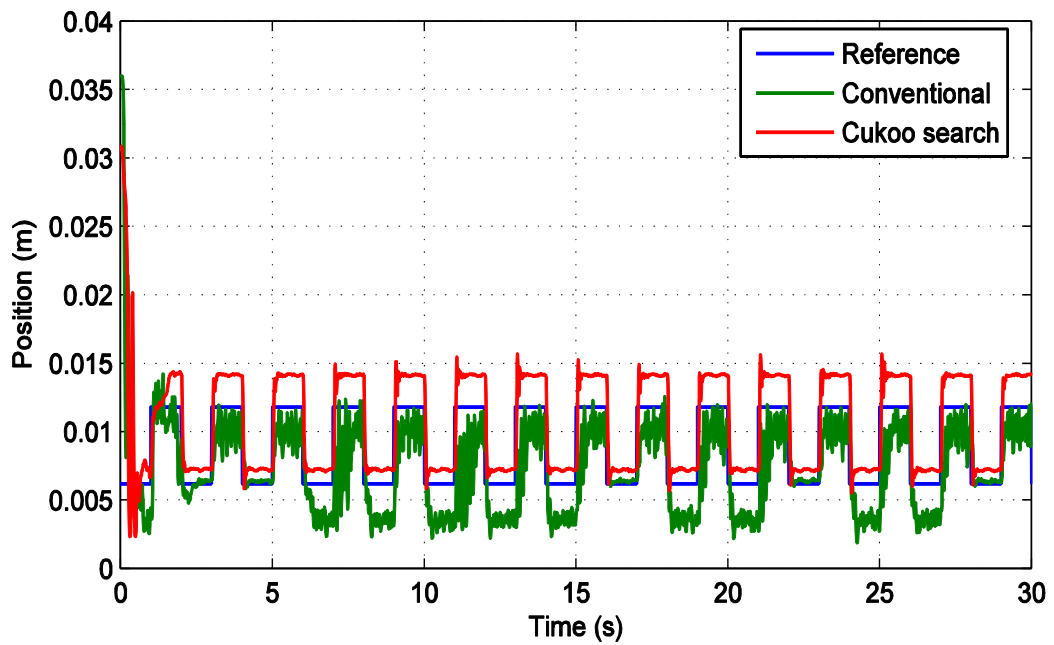
Figure 6.3 Comparison of real time position tracking of Maglev

system

98
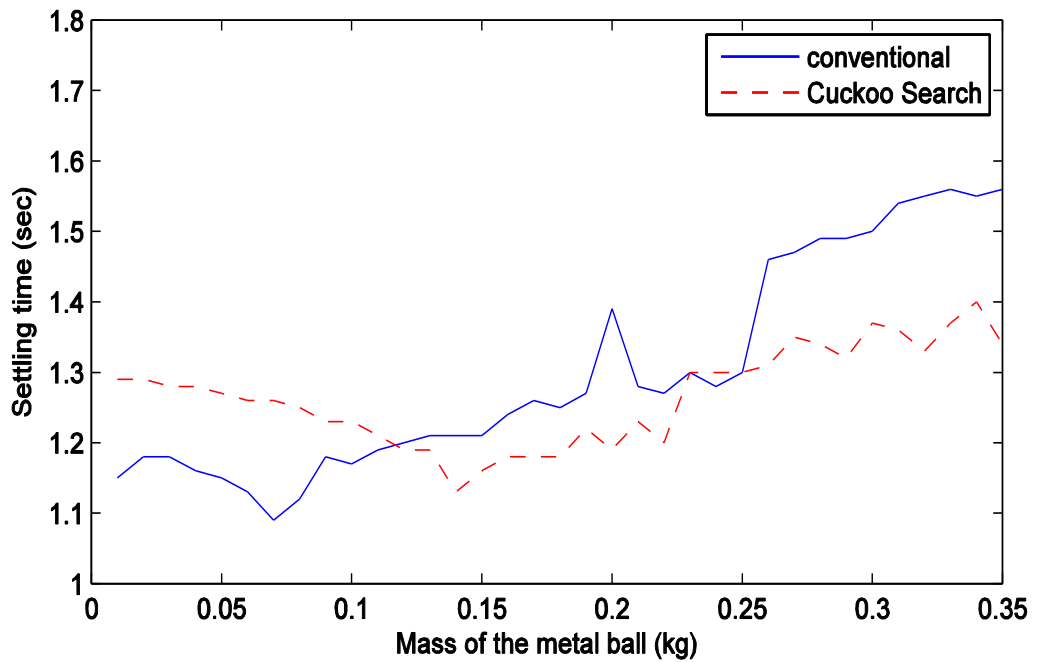
Figure 6.4 Comparison of settling time of response of real time

Maglev system

6.5   Conclusions

An optimized PID controller is designed to levitate the metal ball of the Maglev system. The parameters of the PID controller are optimized by using a cuckoo search algorithm. The cuckoo search optimization technique ensures the improvement of the time domain specifications by minimising the performance indices of the system. The effectiveness of the proposed techniques is validated by comparing the results with the classical design technique.

Chapter - VII

DESIGN OF SINGLE SIDED LINEAR INDUCTION MOTOR

7.1 Introduction

The principle of operation of a LIM is the same as that of a rotary induction motor. A linear Induction motor is basically obtained by opening the rotating squirrel cage induction motor and laying it flat. This flat structure produces a linear force instead of producing rotary torque from a cylindrical machine. LIMs can be designed to produce thrust up to several thousands of Newtons. The winding design and supply frequency determine the speed of a LIM.

The basic principle of LIM operation is similar to that of a conventional rotating squirrel-cage induction motor. Stator and rotor are the two main parts of the conventional three phase rotary induction motor. The stator consists of a balanced poly-phase winding which is uniformly placed in the stator slots along its periphery. The stator produces a sinusoidally distributed magnetic field in the air-gap rotating at the uniform speed $2\omega/p$, with ω representing the network pulsation (related to the frequency f by $\omega = 2\pi f$) and p the number of poles. The relative motion between the rotor conductors and the magnetic field induces a voltage in the rotor. This induced voltage will cause a current to flow in the rotor and will generate a magnetic field. The interaction of these two magnetic fields will produce a torque that drags the rotor in the direction of the field. This principle would not be

modified if the squirrel cage were replaced by a continuous sheet of conducting material.

7.2 Concept and equations

From the induction motor principle explained above, a linear motor is obtained if imagine cutting and unrolling the motor, causing the motor to have a linear motion.

Instead of rotating flux, the primary windings now create flux in a linear fashion. The primary field interacts with the secondary conductors and hence exerts a force on the secondary. Generally, the secondary is made longer than the primary to make maximum use of the primary magnetic field [159].

As stated earlier, there should be relative motion between the conductor and the magnetic lines of flux, in order for a voltage to be induced in the conductor. That is why induction motors, normally operate at a speed V_r that is slightly less than the synchronous velocity V_s. Slip is the difference between the stator magnetic field speed and the rotor speed. Slip is the relative motion needed in the induction motor to induce a voltage in the rotor, and it is given by

$$s = \frac{V_s - V_r}{V_s} \qquad \qquad \dots (7.1)$$

The sLIM synchronous velocity V_s is the same as that of the rotary induction motor, given by

$$V_s = \frac{2\omega R}{p} = 2f\tau \qquad \qquad \dots (7.2)$$

101

where, R is the stator radius of the rotary induction motor. It is important to note that the linear speed does not depend upon the number of poles but only on the pole pitch.

The parameter τ is the distance between two neighboring poles on the circumference of the stator, called pole pitch, defined as [160]

$$\tau = \frac{2\pi R}{p} \qquad \qquad \ldots (7.3)$$

The stator circumference of the rotary induction motor, $2\pi R$, in (7.3) is equal to the length of the SLIM stator core, L_s. Therefore, the pole pitch of a SLIM is

$$\tau = \frac{2\pi R}{p} = \frac{L_s}{p} \qquad \qquad \ldots (7.4)$$

If the velocity of the rotor is V_r then the slip of sLIM can be defined as

$$s = \frac{V_s - V_r}{V_s} \qquad \qquad \ldots (7.5)$$

The air-gap is the clearance between the rotor wall and the sLIM of stator.

7.2.1 Concept of Current sheet

As mentioned earlier, the stator of an induction machine consists of several coils, each having many turns of wires – the windings – embedded in slots of laminated iron. The current carried by the windings can be replaced by a fictitious and infinitely thin layer of current distributed over the surface of the stator facing the air gap. This current is called the "current sheet". The current sheet produces

the same sinusoidal magneto motive force (mmf) in the air gap as that produced by the conductors.

The current sheet strength, i.e., the amount of current per unit stator length (L_s) in a current sheet of a sLIM, can be calculated as in [161] as follows:

$$J_m = \frac{2\sqrt{2}mk_w N_c I_1}{L_s} \qquad \text{... (7.6)}$$

In (7.6), J_m is the current sheet strength ($amp/meter$); m is the number of phases of the motor; k_w is the winding factor, defined below; N_c is the number of turns per slot; I_1 is the RMS value of the input current; L_s is the length of one section of the stator of the LIM, which is equivalent to the circumference of a rotary motor, namely, $L_s = 2\pi R = p\tau$.

The winding factor, k_w, is defined as the product of pitch factor k_p and the distribution factor k_d

$$k_w = k_p\, k_d \qquad \text{... (7.7)}$$

where k_p is the pitch factor of the coil, which is given by

$$k_p = \sin\left(\frac{\theta_p}{2}\right) \qquad \text{... (7.8)}$$

where θ_p is the coil span in electrical degrees. In (7.7), k_d is the breadth or distribution factor given by

$$k_d = \frac{\sin\left(\frac{q_1 \alpha}{2}\right)}{q_1 \sin\left(\frac{\alpha}{2}\right)} \qquad \dots (7.9)$$

where α is the slot angle in electrical degrees given as

$$\alpha = \frac{\pi}{mq_1} \qquad \dots (7.10)$$

One pole pitch is equal to 180 electrical degrees. So, in a full pitch coil where the coil span is equal to one pole pitch, the pitch factor becomes one. Therefore, the winding factor for the fundamental harmonic of a full pitch coil can be obtained by substituting (7.10) in (7.9) resulting in (7.11) [162].

$$k_d = \frac{\sin\left(\frac{\pi}{2m}\right)}{q_1 \sin\left(\frac{\pi}{2mq_1}\right)} \qquad \dots (7.11)$$

In (7.11), q_1 is the number of slots-per-pole-per-phase in the stator iron core.

7.2.2 Power and input phase current

The electrical power input to the stator windings is converted into useful mechanical power by the principle of electrical induction, as explained before and the expressions relating to the power balance are derived as follows.

The power input to the stator windings is given by

$$P_i = m\, V_1 I_1 \cos\emptyset \qquad \dots (7.12)$$

104

where m is the number of electrical phases, V_1 and I_1 are the RMS input phase voltage and current, respectively, and $\emptyset$ is the power factor angle, which is the phase angle between V_1 and I_1. Included in this input power is a component for the copper losses in the stator windings and a component for the iron losses in the stator core and teeth. The remaining input power is transferred to the rotor through the magnetic field of the air-gap. Neglecting the rotor conductor losses and friction and windage losses, the power transferred to the rotor can be equated to the mechanical power developed by the rotor. The total mechanical power developed by the rotor of the sLIM is given by

$$P_0 = F_s V_r \qquad\qquad \dots (7.13)$$

where F_s is the electromagnetic thrust generated on the rotor by the stator, and, as stated before, V_r is the speed of the rotor. The sLIM efficiency η is calculated from

$$\eta = \frac{P_0}{P_i} = \frac{F_s V_r}{m\, V_1 I_1 \cos \emptyset} \qquad\qquad \dots (7.14)$$

From (7.14), assume initially a suitable operating value for $\eta \cos \emptyset$ and then the rated input phase current can be estimated from

$$I_1 = \frac{F_s V_r}{m\, V_1 \eta \cos \emptyset} \qquad\qquad \dots (7.15)$$

7.2.3 Flux Linkage and Induced Voltage:

Consider a coil of N turns carrying a current of I amperes and let ϕ be the resulting flux linking the coil. Assuming that the flux

density ϕ in the air-gap is purely sinusoidal, then it can be expressed as

$$\phi = \phi_p \sin \omega t \qquad \qquad \text{... (7.16)}$$

where ϕ_p is the amplitude of the flux linkage per pole. By flux linkage, it mean the product of flux in webers and the number of turns with which the flux is linked. The induced voltage per turn in the above coil due to a change of flux is given by the first derivative of the above equation, (7.16) and is represented as

$$e = \frac{d\phi}{dt} = \omega \phi_p \cos \omega t \qquad \qquad \text{... (7.17)}$$

The RMS value of e is

$$E_1 = \frac{2\pi}{\sqrt{2}} f \emptyset_p = \sqrt{2} \pi f \emptyset_p \qquad \qquad \text{... (7.18)}$$

If the coil has N_1 turns per phase and a winding factor k_w, (7.18) becomes

$$E_1 = \sqrt{2} \pi f \emptyset_p k_w N_1 \qquad \qquad \text{... (7.19)}$$

Magnetic flux density is found by dividing the flux by the cross sectional area. Hence, the average air-gap magnetic flux density, B_{gavg} can be determined as

$$B_{gavg} = \frac{\emptyset_p p}{L_s W_s} \qquad \qquad \text{... (7.20)}$$

where, W_s is the width of sLIM stator iron core and L_s is the length of stator and p is the number of poles. Assume that the flux produced in

the air-gap is sinusoidal, having a maximum of $B_{g\,max}$. Hence, the average value of the rectified magnetic flux density is

$$B_{gavg} = \frac{2}{\pi}\, B_{g\,max} \qquad \qquad \text{... (7.21)}$$

7.2.4 Equations for sLIM slot Geometry
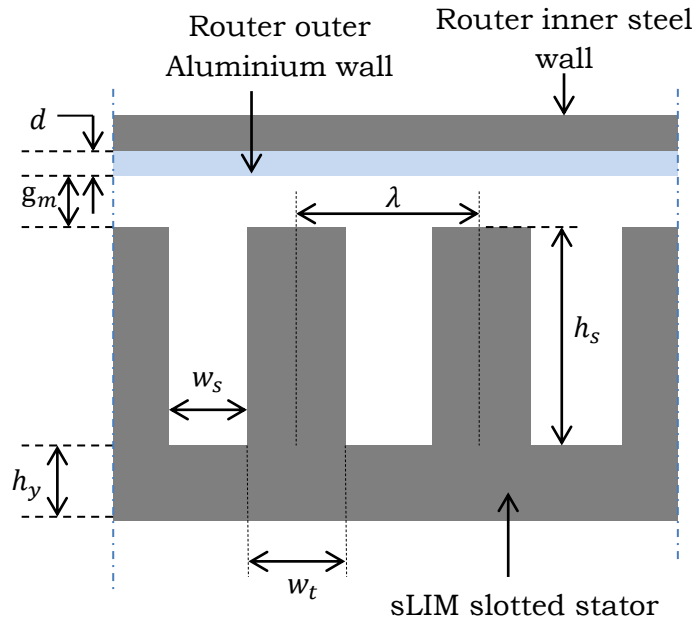
Figure 7.1 Single sided linear induction motor geometry

The air-gap is a very important parameter in a machine. The effective air-gap, g_e of the sLIM is different from the physical air-gap, g_m because of the slotted structure of the stator, as shown in Fig. 7.1 According to [163]

$$g_e = k_c g_0 \qquad \qquad \text{... (7.22)}$$

where g_0 is the magnetic air-gap, given by

$$g_0 = g_m + d \qquad \qquad \text{... (7.23)}$$

where d is the thickness of the conducting layer on the surface of the rotor, and k_c is known as Carter's coefficient, given by

$$k_c = \frac{\lambda}{\lambda - \gamma g_0} \qquad \text{... (7.24)}$$

The parameter λ in (7.24) is the slot pitch, which is the distance between the centers of two consecutive teeth, given by

$$\lambda = \frac{\tau}{m q_1} \qquad \text{... (7.25)}$$

The quantity γ in (7.24) can be expressed as

$$\gamma = \frac{4}{\pi} \left[\frac{w_s}{2g_0} arctan\left(\frac{w_s}{2g_0}\right) - \ln\sqrt{1 + \left(\frac{w_s}{2g_0}\right)^2} \right] \qquad \text{... (7.26)}$$

Slot pitch is the sum of slot width and tooth width and hence the slot width can be calculated with

$$w_s = \lambda - w_t \qquad \text{... (7.27)}$$

where, w_t is the tooth width. To avoid magnetic saturation in the stator teeth, there is a minimum value of tooth width $w_{t\,min}$, which depends on the maximum allowable tooth flux density, $B_{t\,max}$. The quantity $w_{t\,min}$ can be determined from [158]

$$w_{t\,min} = \frac{\pi}{2} B_{g\,avg} \frac{\lambda}{B_{t\,max}} \qquad \text{... (7.28)}$$

The stator slot depth h_s shown in Fig. 7.1, can be calculated from

$$h_s = \frac{A_s}{w_s} \qquad \text{... (7.29)}$$

where, A_s is the cross-sectional area of a slot. Generally, 30% of the area of the slot is filled with insulation material. Therefore, A_s can be calculated from

$$A_s = \frac{10}{7} N_c A_w \qquad \qquad \text{... (7.30)}$$

where N_c is the number of turns per slot, determined from

$$N_c = \frac{N_1}{p q_1} \qquad \qquad \text{... (7.31)}$$

The variable A_w in (3.30) is the area of cross section of a conductor winding without insulation, which can be obtained with

$$A_w = \frac{I_1}{J_1} \qquad \qquad \text{... (7.32)}$$

where, I_1 is the rated input phase current defined in (7.15), and J_1 is the stator current density. The value of J_1, which depends on the machine output power and the type of cooling system, is assumed to be $6 A/m^2$ at the beginning of the program and later modified appropriately

The yoke height of the stator core h_y [31] is the portion of the core below the teeth, as shown in Fig. 7.1. If it is assumed that the flux in the yoke is one-half of the flux in the air-gap, then it can be expressed as [159]

$$h_y = \frac{\phi_p}{2 \, B_{y \, max} W_s} \qquad \qquad \text{... (7.33)}$$

7.3 Forces in Linear Induction Motor

The main forces involved with the LIM are thrust, normal force, and lateral force. The normal force is perpendicular to the stator in the z-direction. Lateral forces are undesirable forces which are developed in a sLIM because of the orientation of the stator.

Thrust:

Under normal operations, the LIM develops a thrust proportional to the square of the applied voltage and this reduces as slip is reduced similarly to that of an induction motor with a high rotor resistance. From (7.13), the amount of thrust produced by a LIM is as follows:

$$F_s = \frac{P_0}{V_c} \qquad \qquad \text{... (7.34)}$$

where P_0 is the mechanical power transmitted to the rotor or the output power and V_c is the linear speed of the rotor.

Normal Forces:

In a double-sided linear induction machine (DLIM) configuration, the reaction plate is centrally located between the two primary stators. The normal force between one stator and the reaction plate is ideally equal and opposite to that of the second stator and hence the resultant normal force is zero. Therefore, a net normal force will only occur if the reaction plate (secondary) is placed asymmetrically between the two stators. This force tends to center the reaction plate. In a sLIM configuration, there is a rather large net

normal force between the primary and secondary because of the fundamental asymmetrical topology. At synchronous speed, the force is attractive and its magnitude is reduced as the speed is reduced. At certain speeds the force will become repulsive, especially at high-frequency operation.

Lateral forces:

Lateral forces act in the y- direction, perpendicular to the movement of the rotor. Lateral forces make the system unstable. These occur due to the asymmetric positioning of the stator in a LIM. Generally, small displacements will only result in very small lateral forces. These forces are a matter of concern in high frequency operation (>>50Hz) where they increase in magnitude. A set of guided mechanical wheel tracks is sufficient to eliminate a small lateral force.

7.4 Equivalent circuit model of sLIM

For the analysis and design of a sLIM having negligible end-effects, the per phase conventional equivalent circuit shown in Fig 7.2 may be used. The circuit components are determined from the SLIM parameters. The sLIM performances to be determined are thrust and efficiency.

The approximate equivalent circuit of a LIM is presented as shown in Fig. 7.2. This circuit is on a per phase basis. The core losses are neglected because a realistic air-gap flux density leads to moderate flux densities in the core and hence, rather low core losses.

111

Skin effect is small at rated frequency for a flat linear induction motor with a thin conductive sheet on the secondary. Therefore, equivalent rotor inductance is negligible [164]. The remaining non-negligible parameters are shown in Fig 7.2 and are discussed below.
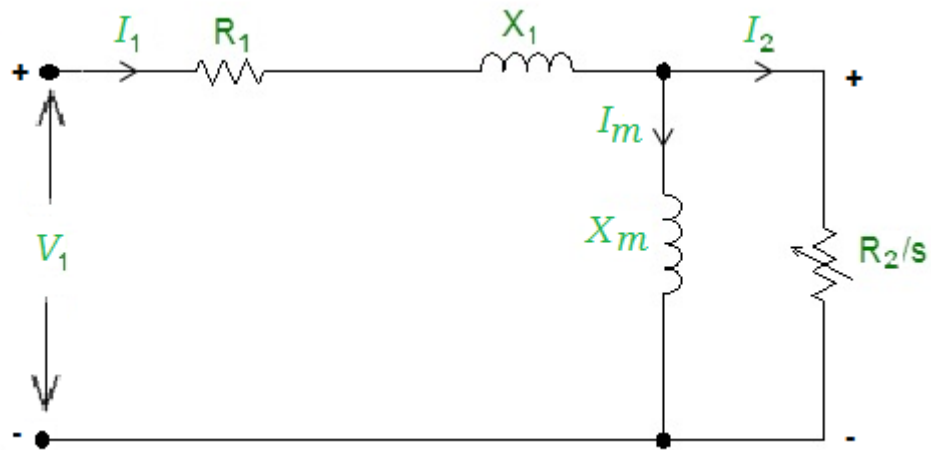
Figure 7.2 Per phase sLIM equivalent circuit

i) Per-phase stator resistance R_1:

This is the resistance of each phase of the sLIM stator windings. R1 is calculated from

$$R_1 = \rho_w \frac{l_w}{A_{wt}} \qquad \text{... (7.35)}$$

where, ρ_w is the volume resistivity of the copper wire used in the stator winding, l_w is the length of the copper wire per phase, and A_{wt} is the cross-sectional area of the wire as given in (7.32). The length of the copper wires l_w is calculated from

$$l_w = N_1 l_{w1} \qquad \text{... (7.36)}$$

112

where, l_{w1} is the mean length of one turn of the stator winding per phase and l_{ce} is the length of end connection.

$$l_{w1} = 2(W_s + l_{ce}) \qquad \text{... (7.37)}$$

$$l_{ce} = \frac{\theta_p}{180°}\tau \qquad \text{... (7.38)}$$

ii) Per-phase stator-slot leakage reactance X_1:

The flux that is produced in the stator windings is not completely linked with the rotor conductors. There will be some leakage flux in the stator slots and hence stator-slot leakage reactance X_1. This leakage flux is generated from an individual coil inside a stator slot and caused by the slot openings of the stator iron core. In a sLIM stator having open rectangular slots with a double-layer winding, X_1 can be determined from [165]

$$X_1 = \frac{2\,\mu_0 f\pi\left[\left(\lambda_s\left(1+\frac{3}{p}\right)+\lambda_d\right)\frac{W_s}{q}+\lambda_e l_{ce}\right]N^2}{p} \qquad \text{... (7.39)}$$

where,

$$\lambda_s = \frac{h_s(1+3k_p)}{12w_s} \qquad \text{... (7.40)}$$

k_p is the pitch factor given by (7.8), also

$$\lambda_e = 0.3(3k_p - 1) \qquad \text{... (7.41)}$$

$$\lambda_d = \frac{5\left(\frac{g_e}{w_s}\right)}{5+4\left(\frac{g_o}{w_s}\right)} \qquad \text{... (7.42)}$$

iii) Per-phase magnetizing reactance X_m:

The per-phase magnetizing reactance, X_m is shown in Fig 7.2 and is given by

$$X_m = \frac{24\mu_0 \pi f W_{se} k_w N_1^2 \tau}{\pi^2 p g_e} \qquad \text{... (7.43)}$$

where k_w is the winding factor defined as in (7.7), g_e is the equivalent air gap given by (7.22) and W_{se} is the equivalent stator width given as

$$W_{se} = W_s + g_0 \qquad \text{... (7.44)}$$

iv) Per-phase rotor resistance R_2:

The per-phase rotor resistance R_2 is a function of slip, as shown in Fig. 7.2. R_2 can be calculated from the goodness factor G and the per-phase magnetizing reactance X_m as

$$R_2 = \frac{X_m}{G} \qquad \text{... (7.45)}$$

where the goodness factor, G is defined as [165]

$$G = \frac{2\mu_0 f \tau^2}{\pi \left(\frac{\rho_r}{d}\right) g_e} \qquad \text{... (7.46)}$$

In (7.46), ρ_r is the volume resistivity of the rotor conductor outer layer, which is aluminium.

From the equivalent circuit shown in Fig. 7.2, the magnitude of the rotor phase current I_2 can be seen to be

$$I_2 = \frac{X_m}{\sqrt{\left(\frac{R_2}{s}\right)^2 + X_m^2}} I_1 \qquad \text{... (7.47)}$$

114

By substituting the value of R_2 from (7.45), the rotor phase current I_2 becomes

$$I_2 = \frac{X_m}{\sqrt{\frac{1}{(sG)^2}+1}} \qquad \dots (7.48)$$

Symbol	Parameter	Value (units)	Symbol	Parameter	Value (units)
p	No. of poles	4	w_s	Width of stator	12.67mm
f	Frequency	50Hz	R_s	Stator resistance per phase	0.9098 Ω
τ	Pole pitch	50 mm	X_s	Stator reactance per phase	0.0676 Ω
w_s	Sheet thickness	5mm	R_r	Rotor resistance per phase	0.0619 Ω
g_e	Airgap length	5mm	X_m	Magnetizing reactance per phase	0.8135 Ω
m	No. of slots	12	G	Goodness factor	13.1337
L_s	Length of stator	120mm			

Table 7.1 LIM parameters
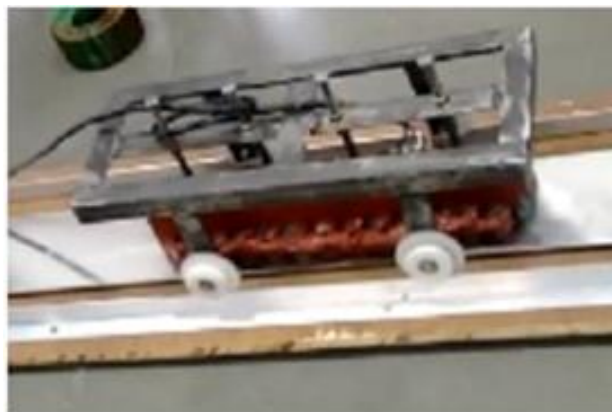
7.3 Implementation of LIM

7.5 Mathematical model of LIM

The dynamic model of the linear Induction motor can be expressed in the dq synchronously rotating frame. On the primary side, it is composed of three phase windings and laminated steel cores. Moreover, the combination of aluminum sheets (nonmagnetic conductors) and back irons (magnetic conductors) is used to form the secondary side. In addition, the dynamic model of the LIM modified from the traditional model of a three-phase, Y-connected induction motor in a synchronous rotating reference frame can be described by the following differential equations [155].

$$\frac{di_{ds}}{dt} = \frac{1}{\sigma L_s} \left(\begin{array}{l} -\left(R_s + \left(\frac{L_m}{L_r} \right)^2 R_r \right) i_{ds} + \sigma L_s \frac{\pi}{h} v_e i_{qs} \\ + \frac{L_m R_r}{L_r^2} \phi_{dr} + \frac{P L_m \pi}{L_r h} \phi_{qr} v_r + V_{ds} \end{array} \right) \qquad \ldots (7.49)$$

$$\frac{di_{qs}}{dt} = \frac{1}{\sigma L_s} \left(\begin{array}{l} -\sigma L_s \frac{\pi}{h} v_e i_{ds} - \left(R_s + \left(\frac{L_m}{L_r} \right)^2 R_r \right) i_{qs} \\ - \frac{P L_m \pi}{L_r h} \phi_{dr} v_r + \frac{L_m R_r}{L_r^2} \phi_{qr} + V_{qs} \end{array} \right) \qquad \ldots (7.50)$$

$$\frac{d\phi_{dr}}{dt} = \frac{L_m R_r}{L_r} i_{ds} - \frac{R_r}{L_r} \phi_{dr} + \left(\frac{\pi}{h} v_e - P \frac{\pi}{h} v_r \right) \phi_{qr} \qquad \ldots (7.51)$$

$$\frac{d\phi_{qr}}{dt} = \frac{L_m R_r}{L_r} i_{qs} - \left(\frac{\pi}{h} v_e - P \frac{\pi}{h} v_r \right) \phi_{dr} - \frac{R_r}{L_r} \phi_{qr} \qquad \ldots (7.52)$$

$$F_e = K_f \left(\phi_{dr} i_{qs} - \phi_{qr} i_{as} \right) = M \dot{v_r} + D v_r + F_L \qquad \ldots (7.53)$$

116

where R_s is the winding resistance per phase; R_r is the secondary resistance per phase referred primary; L_m is the magnetizing inductance per phase; L_r is the secondary inductance per phase; L_s is the primary inductance per phase; v_r is the mover linear velocity; h is the pole pitch; P is the number of pole pairs; $\emptyset_{dr}$ and $\emptyset_{qr}$ are d-axis and q-axis secondary flux; i_{ds} and i_{qs} are d-axis and q-axis primary current; V_{ds} and V_{qs} are d-axis and q-axis primary voltages;

$$\text{Secondary time constant } \tau_r = \frac{L_r}{R_r} \; ;$$

$$\text{leakage coefficient } \sigma = 1 - \left(\frac{L_m^2}{L_s L_r} \right) ;$$

$$\text{Force constant } K_f = \frac{3P\pi L_m}{2hL_r}$$

F_e is the electromagnetic force; F_L is the external force disturbance; M is the total mass of the moving element and D is the viscous friction and iron-loss coefficient.

In an ideally LIM drive, the secondary flux linkage axis is forced to align with the d-axis. It follows that

$$\emptyset_{qr} = 0, \dot{\emptyset}_{qr} = 0 \qquad\qquad \dots (7.54)$$

Using (7.52) and (7.54), the desired secondary flux linkage is

$$\emptyset_{dr} = \frac{\frac{L_m}{T_r}}{s + \frac{1}{T_r}} i_{ds} \qquad\qquad \dots (7.55)$$

where s is the Laplace operator,

by using (7.51) and (7.55) the feed forward slip is

$$v_{sl} = \frac{hL_m}{\pi T_r \emptyset_{dr}} i_{qs} \qquad \qquad \dots (7.56)$$

Since the secondary time constant T_r is sensitive to different operating conditions.

The transversal parameters of the equivalent circuit of the LIM have been computed by using required aspects. The parameters which are used for simulation as well as design are shown in table 7.1.

7.6 Results and wave forms

Simulations related to LIM are implemented in LabVIEW environment. Fig. 7.3 shows the implementation of LIM. In all the figures x-axis represents the time in Seconds and y- axis represents the correspond parameters, i.e., Current in amps and flux in webers.

Fig.7.4 & Fig. 7.5 show the d-axis and q-axis primary currents, Fig.7.5 shows the primary current of the LIM when using the speed reference and linear flux.
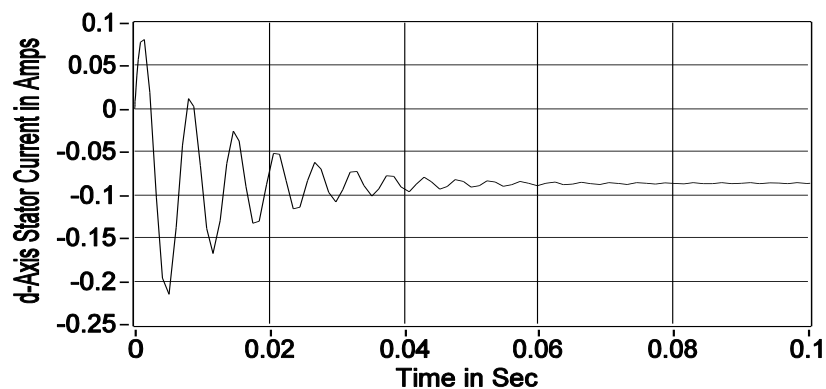
Figure 7.4 d-axis primary current

118
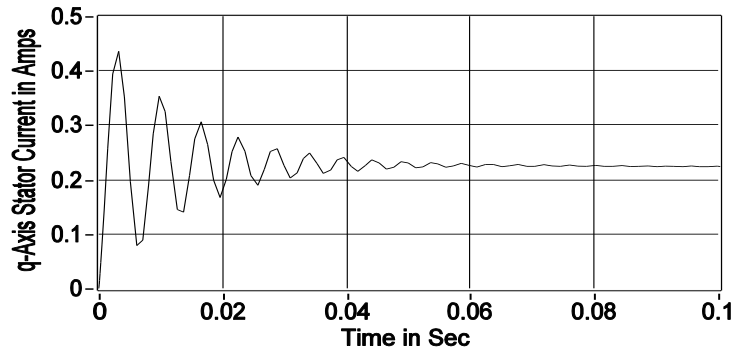
Figure 7.5 q-axis primary current

From Fig. 7.6, it can be observed that d-axis linear flux becomes less than the reference speed, due to increasing of the end effects caused by the increased speed as shown in Fig. 7.8.
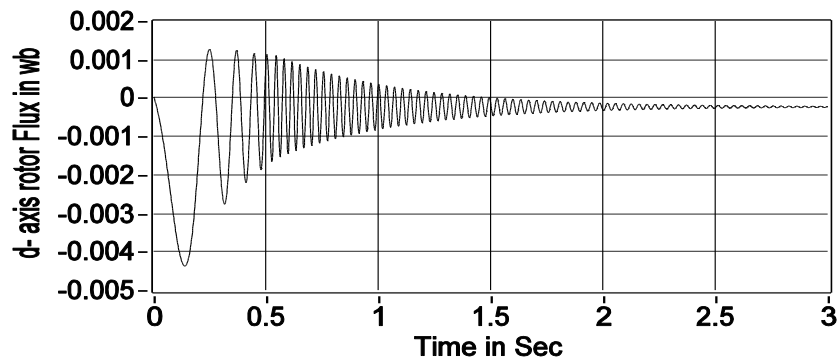
Figure 7.6 d-axis linear flux
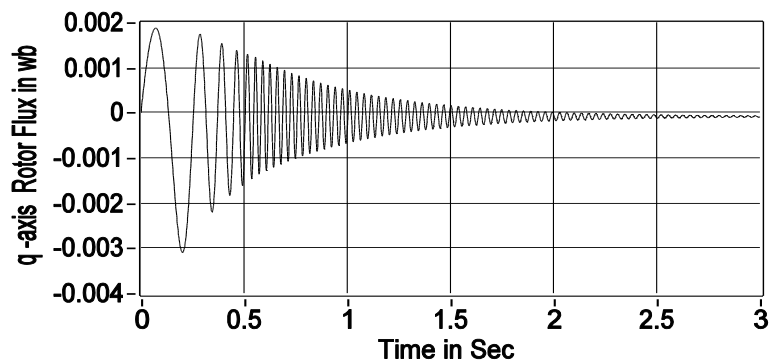
Figure 7.7 q-axis linear flux

Fig.7.6 and Fig. 7.7 show the d-axis and q-axis linear fluxes, it is observed that q-axis linear flux will be zero.

119
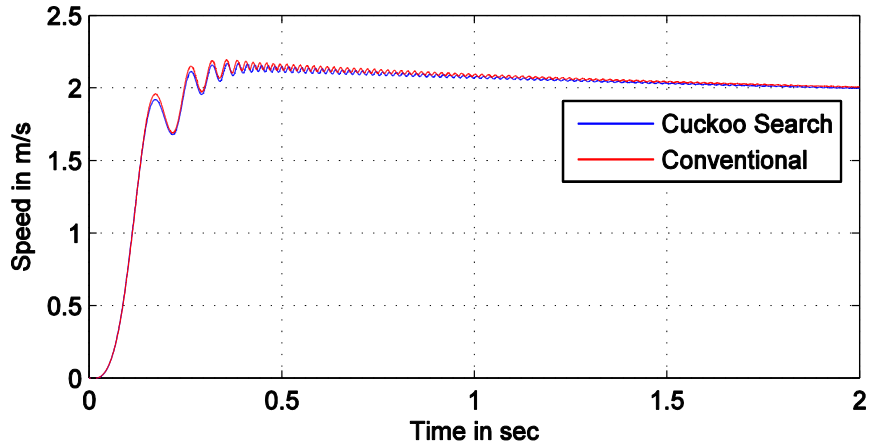
Figure 7.8 Performance of PID Controller based on Cuckoo Search algorithm for linear speed of 2m/s

Fig. 7.8 and Fig. 7.9 show the performance of the PID controller based on cuckoo search algorithm for speed tracking of LIM. Several design techniques of PID controllers were mentioned in literature. The most used are the Ziegler-Nichols method and the poles assignment method. But their disadvantage is that they require prior knowledge of the various parameters of the Linear Induction Motor. The cuckoo search algorithm has been used to tune the parameters of PID controller.
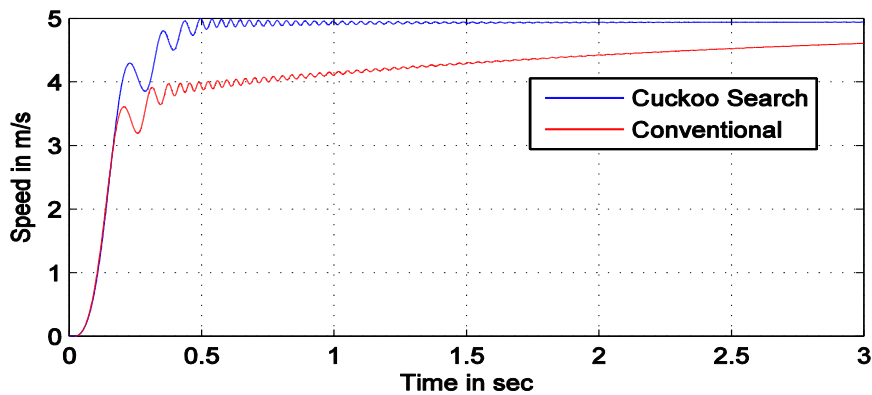
Figure 7.9 Performance of the PID controller based on CSA for linear speed of 5m/s

Table 7.2 shows the comparison of PID controller based on cuckoo search algorithm over the conventional controller for speed tracking of sLIM.

	Rise time in Sec	Peak time in Sec	Settling time in Sec	Steady state error
Conventional	0.1763	0.2063	2.916	8.12%
Cuckoo Search	0.1938	0.228	0.994	1.38%

Table 7.2 comparison of conventional and cuckoo search based PID controller for speed tracking of sLIM

The simulation result show that the introduction of PID controller based CSA led to an improvement in the speed regulation of the Linear Induction Motor.

7.7 Conclusions

The air-gap plays a very important role in the performance of the LIM. The air-gap needs to be as small as possible to have a better thrust and efficiency. Another crucial design parameter is the thickness of rotor outer layer which is aluminium. As the thickness of the aluminium sheet increases thrust also increases along with the length of magnetic air-gap which is undesirable. Small variations in the linear flux were observed as shown in Fig. 7.5 and Fig. 7.6. These variations are due to the end effects. Fig.7.7 & Fig.7.8 show the effectiveness of the cuckoo search based PID controller for speed tracking of LIM.

Chapter -VIII

CONCLUSIONS

8.1 Conclusions

In this thesis, the research work carried out broadly touches the different aspects of the Maglev system such as eddy current based force, which is used to stabilize the levitated object, forces acting on the levitated object, conventional controller, fractional order model reference adaptive controller, feedback linearization technique, backstepping fuzzy sliding mode controller and PID controller based on Cuckoo Search algorithm for position tracking of Maglev system. From the comprehensive literature review inferences the research work, objectives and methodology has been presented in detail.

Modelling and simulation of Maglev system has been developed in MATLAB environment. The characteristics of the eddy current based force are drawn for different plate widths and heights of the levitated object from plate. Eddy currents are generated in the plate placed underneath of the levitated object due to the variation in current flowing through the electromagnetic coil. The eddy currents in the plate is linearly proportional to the velocity of the levitated object and rate of change of electromagnet current.

The analytical relationship was developed for the eddy current based force as a function of the plate thickness and distance between center of the levitated object to the plate placed underneath of the

levitated object. It is shown that, magnetic levitation system utilises the eddy current based force to stabilize the levitated object.

Fractional order model reference adaptive controller was implemented for position tracking of nonlinear Maglev system. Model reference adaptive system uses with fractional order PID controller to achieve the desired performance and the parameters of the controller are adjusted based on the error between the reference model output and the actual system output. An important problem associated with the model reference adaptive control system is to determine the adjustment mechanism so that a stable system brings the error to zero. Simulation results show that the efficacy of the FOMRAC PID controller over the conventional controller.

Linear model has been developed to represent the nonlinear dynamics of Maglev system by using feedback linearization technique. Simulation results show that the dynamic errors of all the states converge to its neighbourhood of zero. So that stable system is achieved.

Backstepping fuzzy sliding mode controller has been developed for position tracking of a Maglev system. Backstepping technique is a powerful tool for adjusting the error dynamics to neighbourhood of zero. Small change in the control voltage produces large variations in position of the levitated object. Due to this object will be attracted to electromagnet or fall down. Therefore backstepping fuzzy sliding mode controller is not suitable for real time application of Maglev system.

Simulation results show the effectiveness of backstepping fuzzy sliding mode controller for the position tracking of Maglev system.

Further PID controller based on cuckoo search algorithm has been implemented for the position tracking of Maglev system. The parameters of the PID controller are tuned by using Cuckoo search algorithm. The proposed controller reduces the peak overshoot and settling time when compared with conventional controller. The proposed controller stabilizes the levitated object if there is any variation in the mass of the levitated object. Simulation results show the effectiveness of proposed controller over the conventional controller.

The proposed controller has been tested practically on Maglev system in laboratory to validate the obtained results. The results are compared with the conventional controller results. It is proved that the proposed controller gives better performance when compared with conventional controller.

Moreover the proposed controller is implemented for speed tracking of single sided linear induction motor. Simulations related to the sLIM are implemented in LabVIEW environment. Simulation results show that the proposed controller produces a satisfactory performance for speed tracking of sLIM.

In conclusion, it can be observed that the PID controller based on cuckoo search algorithm gives improved performance in the considered Maglev system in real time.

8.2 Future Scope

As a result of extensive investigation carried out in this thesis in the area of Maglev systems, the following suggestions for future research seem to be worth pursuing.

In this thesis, FOMRAC, conventional controller, backstepping fuzzy sliding mode controller and PID controller based on cuckoo search algorithm are considered for position tracking of Maglev system. With the advancements in controllers, like Backstepping neuro fuzzy controller can be used for further investigation.

In this thesis, in order to tune the parameters of the PID controller, cuckoo search algorithm has been considered. With advancements in optimization techniques, like Gravitational search algorithm, grey wolf optimization and Bacteria foraging optimization can be used for further investigation.

In this thesis, Linear Induction parameters are designed based rotary induction motor and PID controller based on cuckoo search algorithm has been considered for speed tracking of linear induction motor. Optimization algorithm can be used to design the parameters of LIM so that improved efficiency and power factor may be obtained.

125

BIBLIOGRAPHY

[1] P. Suster , A. Jadlovska, "Modeling and control design of magnetic levitation system", IEEE 10th International Symposium on Applied Machine Intelligence and Informatics, 2012, pp. 295–299, 2012

[2] Cermak, R., Barton, L., Spal, P., Bartak, J. and Vavrik, J. "Overview of magnetic levitation principles and their application in maglev systems", Advanced Engineering, Vol. 2, No. 1,pp.19–28, 2008.

[3] Ono, M., Koga, S. and Ohtsuki, H. "Japan's superconducting maglev train", IEEE Instrum. Meas. Mag., March, Vol. 5, No. 1, pp.9–15, 2002

[4] Brooks, J.S., Reavis, J.A., Medwood, R.A. and Stalcup, T.F. "New opportunities in science, materials, and biological systems in the low-gravity (magnetic levitation) environment", IEEE-Journal of Applied Physics, 18 June, Vol. 87, No. 9, pp.6194–6199, 2000

[5] Thompson, M.T. "Eddy current magnetic levitation models and experiments", IEEE Pottentials, Vol. 19, No. 1, pp.40–44, 2000

[6] M. K. Kwak, M. I. Lee and S. Heo, "Vibration Suppression Using Eddy Current Damper", K. S. N. V. E, Vol. 233, pp. 441-453, 2003

[7]   Bae, J.S., Hwang, J.H., Park, J.S. and Kwag, D.G. "Modeling and experiments on eddy current damping caused by a permanent magnet in a conductive tube", Journal of Mechanical Science and Technology, Vol. 23, No. 11, pp. 3024 – 3035, 2009

[8]   Ebrahim, M., Khodabakhsh, M. and Vossough, G. "An analytical 3-D model for calculating eddy current damping force for a magnetic levitation system with permanent magnet", IEEE Transc. on Magnetics, September, Vol. 48, No. 9, pp.2472–2478, 2012

[9]   Sinha, G. and Prabhu, S.S. "Analytical model for estimation of eddy current and power loss in conducting plate and its application", Phys. Rev. Special Topics – Accelerators and Beams, June, Vol. 14, No. 6, p.062401, 2011

[10]   W. Jones, "Earnshaw's theorem and the stability of matter", Eur. J. Phys. 1, pp.85-88,1980, Printed in Northern Ireland

[11]   Heller, A. "Maglev on the Development Track for Urban Transportation", November, Lawrence Livermore National Laboratory, University of California for the U.S. Department of Energy, 2003

[12]   Jiang, D., Yang, J-X., Ma, L-L. and Jiang, D. "Model building and simulating for hybrid magnetic levitation ball system", International Conference on Mechanic Automation and Control Engineering (MACE), 26–28 June, Wuhan, pp.6105–6110, 2010

[13] Lee, H, W., Ki-Chan Kim, and J, Lee. "Review of Maglev Train Technologies", IEEE Transactions on Magnetics, Vol.42, No.7, 2006.

[14] E. Riches, "Will Maglev lift off?", IEE Review, pp. 427–430, 1988

[15] J. Hogan and H. Fink, "Comparison and optimization of lift and drag forces on vehicles levitated by eddy current repulsion for various null and normal flux magnets with one or two tracks", IEEE Trans. Magn., vol. 11, no. 2, pp. 604–607, 1975

[16] T. Iwahana, "Study of superconducting magnetic suspension and guidance characteristics on loop tracks", IEEE Trans. Magn., vol. 11, no. 6, pp. 1704–1711, 1975

[17] O. Tsukamoto, Y. Iwata, and S. Yamamura, "Analysis of ride quality of repulsive type magnetically levitated vehicles", IEEE Trans. Magn., vol. 17, no. 2, pp. 1221–1233, 1981

[18] T. C. Wang and Y.-K. Tzeng, "A new electromagnetic levitation system for rapid transit and high speed transportation", IEEE Trans. Magn., vol. 30, no. 6, pp. 4734–4736, 1994

[19] S. Yamamura, 'Theory of Linear Induction Motors", New York: Wiley, 1972

[20] Fujisaki, K., "Application of electromagnetic force to thin steel plate", in Industry Applications Conference, 37th IAS Annual Meeting. Conference Record of the, vol.2, no., pp.864- 870 vol.2, 2002

[21] S. Nonaka and T. Higuchi, "Elements of linear induction motor design for urban transit", IEEE Trans. Magn., vol. 23, no. 5, pp. 3002–3004, 1989.

[22] S. Yoon, J. Hur, and D. Hyun, "A method of optimal design of single-sided linear induction motor for transit", IEEE Trans. Magn., vol. 33, no. 5, pp. 4215–4217, 1997

[23] W. Xu, J. Zhu, L Tan, Y. Guo, S Wang, and Y. Wang, "Optimal design of a linear induction motor applied in transportation", in Proc. IEEE Int. Conf. Ind. Tech., pp. 1–6, 2009

[24] D. Yumei and J. Nenggiang, "Research on characteristics of single-sided linear induction motors for urban transit", in Proc. IEEE Int. Con. Elect. Mach. Syst., pp. 1–4, 2009

[25] Shiri, A., Shoulaie, A., "Design Optimization and Analysis of Single-Sided Linear Induction Motor, Considering All Phenomena", IEEE Transactions on Energy Conversion, vo1.27, no.2, pp.5l6-525, 2012

[26] Rong-Jong Wai, Jing-Xiang Yao, and Jeng-Dao Lee, "Backstepping Fuzzy-Neural-Network Control Design for Hybrid Maglev Transportation System" IEEE Transactions on Neural Networks and Learning Systems, Vol. 26, no. 2, pp. 302-317, 2015.

[27] Dan Cho, Yoshifumi Kato, and Darin spilman "Sliding mode and classical controllers in magnetic levitation systems" IEEE Control Systems, Vol. 13, no. 1, pp. 42-48, 1993.

[28] S. S. Mishra, S. K. Mishra and S. K. Swain, "Coefficient diagram method (CDM) based PID controller design for magnetic levitation system with time delay", 2017 IEEE International Conference on Intelligent Techniques in Control, Optimization and Signal Processing (INCOS), Srivilliputhur, 2017, pp. 1-8.

[29] B. Tandon, S. Kaur and A. Kalra, "Stability analysis of feedback linearized magnetic levitation system using sum-of-squares method", 2017 4th International Conference on Signal Processing, Computing and Control (ISPCC), Solan, pp. 420-424, 2017.

[30] R. H. Subrata, J. L. Hardenberg and F. Gozali, "The use of pid controller to get the stable floating condition of the objects in magnetic levitation system", 2017 15th International Conference on Quality in Research (QiR): International Symposium on Electrical and Computer Engineering, Nusa Dua, pp. 321-324, 2017

[31] A. S. C. Roong, C. Shin-Homg and M. A. B. Said, "Position control of a magnetic levitation system via a PI-PD control with feedforward compensation", 2017 56th Annual Conference of the Society of Instrument and Control Engineers of Japan (SICE), Kanazawa, pp. 73-78, 2017

[32] R. E. Precup, C. A. Bojan-Dragos, E. L. Hedrea, M. D. Rarinca and E. M. Petriu, "Evolving fuzzy models for the position control of magnetic levitation systems",2017 Evolving and Adaptive Intelligent Systems (EAIS), Ljubljana, pp. 1-6, 2017.

[33] B. Singh and V. Kumar, "A real time application of model reference adaptive PID controller for magnetic levitation system", 2015 IEEE Power, Communication and Information Technology Conference (PCITC), Bhubaneswar, pp. 583-588, 2015.

[34] K. H. Su and C. Y. Li, "Supervisory fuzzy model control for magnetic levitation system", 2016 IEEE International Conference on Networking, Sensing, and Control (ICNSC), Mexico City, pp.1-6, 2016.

[35] Ahmed El Hajjaji and M Ouladsine, "Modeling and Nonlinear Control of Magnetic Levitation Systems", IEEE Transactions on Industrial Electronics, vol. 48, No. 4, pp. 831-838, 2001.

[36] Rong-Jong Wai, Jeng-Dao Lee, and Kun-Lun Chuang, "Real-Time PID Control Strategy for Maglev Transportation System via Particle Swarm Optimization", IEEE Transactions on Industrial Electronics, vol. 58, No. 2, pp. 629-646, February 2011.

[37] Kiyong Kim, Rao, P. and Burnworth, J., "Self-tuning of the PID controller for a Digital Excitation Control System," IEEE Transactions on Industry Applications, vol. 46, no. 4, pp. 1518-1524, July-Aug 2010.

[38] Muhammad Shafiq and Sohail Akhtar, "Inverse Model Based Adaptive Control of Magnetic Levitation System", 5th Asian Control Conference, vol. 3, pp. 1414-1418, July 2004.

[39] C. Wu and C. Zhu, "Implicit generalized predictive control of an active magnetic bearing system," in Proc. IEEE 17th International Conference on Electrical Machines and Systems, Hangzhou, China, pp. 2319 – 2323, 2014.

[40] S. Sgaverdea, C. A. Bojan-Dragos, R. E. Precup, S. Preitl and A. I. Stinean, "Model predictive controllers for magnetic levitation systems", 2015 IEEE 10th Jubilee International Symposium on Applied Computational Intelligence and Informatics, Timisoara, pp. 171-176, 2015.

[41] M. Ahsan, N. Masood and F. Wali, "Control of a magnetic levitation system using non-linear robust design tools", 2013 3rd IEEE International Conference on Computer, Control and Communication (IC4), Karachi, pp. 1-6, 2013.

[42] A. Rawat and M. J. Nigam, "Comparison between adaptive linear controller and radial basis function neurocontroller with real time implementation on magnetic levitation system", 2013 IEEE International Conference on Computational Intelligence and Computing Research, Enathi, pp. 1-4, 2013.

[43] I. Mizumoto and A. Minami, "Anti-windup adaptive PID control for a magnetic levitation system with a PFC based on time-

varying ASPR model", 2011 IEEE International Conference on Control Applications (CCA), Denver, CO, pp. 113-118, 2011.

[44] C. S. Chin, C. Wheeler, S. L. Quah and T. Y. Low, "Design, modeling and experimental testing of magnetic levitation system for conveyance applications", 2011 IEEE 2nd International Conference on Computing, Control and Industrial Engineering, Wuhan, pp. 174-179, 2011.

[45] C. S. Teodorescu, N. Sakamoto and S. Olaru, "Controller design for sine wave tracking on magnetic levitation system: A comparative simulation study", 2010 IEEE International Conference on Control Applications, Yokohama, pp. 2231-2236, 2010.

[46] J. H. Yang, Y. S. Lee and O. K. Kwon, "Development of magnetic force modeling equipment for magnetic levitation system", ICCAS 2010, Gyeonggi-do, pp. 29-33, 2010.

[47] Feng Li, K. Ishihata, Jianming Lu and T. Yahagi, "Perfect tracking control using multirate control in magnetic levitation system", 2005 IEEE International Symposium on Circuits and Systems, Vol. 5, pp. 4851-4854, 2005.

[48] A. Kumar, P. J. Gaidhane and V. Kumar, "A nonlinear fractional order PID controller applied to redundant robot manipulator," 2017 6th International Conference on Computer Applications In Electrical Engineering-Recent Advances (CERA), Roorkee, India, 2017, pp. 527-532.

[49] T. George and V. Ganesan, "Tuning performance of PID controller with advanced hybrid technology," 2017 International Conference on Intelligent Computing, Instrumentation and Control Technologies (ICICICT), Kerala State,Kannur, India, 2017, pp. 1698-1708.

[50] N. Kanagaraj, M. Al-Dhaifalla and K. S. Nisar, "Design of intelligent fuzzy fractional-order PID controller for pressure control application", 2017 International Conference on Intelligent Computing, Instrumentation and Control Technologies (ICICICT), Kerala State, Kannur, India, pp. 525-530, 2017.

[51] Q. Chen, Y. Tan, J. Li and I. Mareels, "Decentralized PID Control Design for Magnetic Levitation Systems Using Extremum Seeking", in IEEE Access, vol. 6, pp. 3059-3067, 2018.

[52] Xiaojia Li, Tingting Xiao, Fengwei Chen, Yingjuan Zhang and Weidong Wu, "A novel superconducting magnetic levitation method to support the laser fusion capsule by using permanent magnets" Matter and Radiation at Extremes, In press article, 2018.

[53] J.J. Hernandez-Casanas, M.A. Marquez-Vera and B.D. Balderrama Hernandez, "Characterization and adaptive fuzzy model reference control for a magnetic levitation system", Alexandria Engineering Journal, vol. 55, pp.2597–2607, 2016.

[54] T.T. Salim, V.M. Karsli, "Control of single axis magnetic levitation system using fuzzy logic control", International Journal of Advanced Computer Science and Applications, Vol.4, pp. 83–88, 2013.

[55] A. Senba, H. Kitahara, H. Ohsaki and E. Masada, "Characteristics of an electromagnetic levitation system using a bulk superconductor", in IEEE Transactions on Magnetics, vol. 32, no. 5, pp. 5049-5051, Sep 1996.

[56] Y. Jin, S. Wang, K. Qiu, P. Yu, P. Hao and H. Li, "Control and analysis of magnetic levitation device based on induced eddy current", 2017 IEEE International Magnetics Conference (INTERMAG), Dublin, pp. 1-1, 2017.

[57] L. Jin et al., "Effect of Eddy Current Damper on the Dynamic Vibration Characteristics of High-Temperature Superconducting Maglev System", in IEEE Transactions on Applied Superconductivity, vol. 27, no. 3, pp. 1-6, April 2017.

[58] Y. Fu, M. Takemoto, S. Ogasawara and K. Orikawa, "Investigation of a high speed and high power density bearingless motor with neodymium bonded magnet", 2017 IEEE International Electric Machines and Drives Conference (IEMDC), Miami, FL, pp. 1-8, 2017.

[59] B. Reutzsch and W. Schinkoethe., "Magnetic Levitation System for Linear Direct Drives based on Lorentz Forces", Innovative

Small Drives and Micro-Motor Systems: 9. GMM/ETG Symposium, Nuremberg, Germany, pp. 1-6, 2013.

[60] C. Elbuken, M. B. Khamesee and M. Yavuz, "Damping Control in Magnetic Levitation of Micro Objects", IECON 2006 -32nd Annual Conference on IEEE Industrial Electronics, Paris, pp. 4170-4175, 2006.

[61] J. J. Stickler, "A study of single-sided linear induction motor performance with solid iron secondaries", in IEEE Transactions on Vehicular Technology, vol. 31, no. 2, pp. 107-112, May 1982

[62] L. Zheng, J. Jin, Y. Guo and J. Zhu, "Design and characteristics analysis of long-primary single-sided linear induction motor", 2009 International Conference on Applied Superconductivity and Electromagnetic Devices, Chengdu, pp. 85-88, 2009.

[63] Yong-Joo Kim, Pan-Seok Shin, Do-Hyun Kang and Yun-Hyun Cho, "Design and analysis of electromagnetic system in a magnetically levitated vehicle, KOMAG-01", in IEEE Transactions on Magnetics, vol. 28, no. 5, pp. 3321-3323, Sept. 1992.

[64] K. Wang, L. Shi, Y. Li and J. He, "A Decoupling Control Scheme of Combined Levitation-and-Propulsion SLIM for Maglev Vehicle", 2008 IEEE Industry Applications Society Annual Meeting, Edmonton, Alta., pp. 1-5, 2008.

[65] Margaliot M., G. Langholz, "New Approaches in Fuzzy Modeling and Control", World Scientific Pub. Co., 2000.

[66] Luo, Y., Zhang, T., Lee, B., Kang, C., and Chen, Y. "Fractional-Order Proportional Derivative Controller Synthesis and Implementation for Hard-Disk-Drive Servo System" IEEE Transactions on Control Systems Technology, Vol. 22, no. 1, pp. 281 – 289, 2014.

[67] Fossen, T. I., and Strand, J. P., "Tutorial on Nonlinear Backstepping: Applications to Ship Control", Modeling, Identification and Control, Vol. 20, no. 2, pp. 83-134, 1999.

[68] Binglong Cong, Xiangdong Liu and Zhen Chen "Backstepping based adaptive sliding mode control for spacecraft attitude maneuvers", International Conference on Control, Cardiff, UK, 3-5 September, pp. 1046-1051, 2012.

[69] Yuanjin Yu, Zhaohua Yang, Chao Han, and Hu Liu, "Fuzzy Adaptive Back-Stepping Sliding Mode Controller for High-Precision Deflection Control of the Magnetically Suspended Momentum Wheel", IEEE Transactions on Industrial Electronics, vol. 65, no. 4, pp. 3530-3538, 2018.

[70] Pallav., S, K, Pandey., V, Laxmi., "PID control of magnetic levitation system based on derivative filter", Annual International Conference on Emerging Research Areas: Magnetics, Machines and Drives, pp. 1-5, 2014.

[71] Maria Hypiusova and Alena Kozakova, "Robust PID Controller Design for the Magnetic Levitation System: Frequency Domain Approach", International Conference on Process Control (PC), pp. 274-279, 2017.

[72] Witchupong Wiboonjaroen and Sarawut Sujitjorn "Stabilization of a Magnetic Levitation Control System via State-PI Feedback" International Journal of Mathematical Models and Methods In Applied Sciences, Vol.7, no.7, pp.717-727, 2013.

[73] Chang-Hyun Kim "Robust Control of Magnetic Levitation Systems Considering Disturbance Force by LSM Propulsion Systems", IEEE Transactions on Magnetics, Vol. 53, no. 11, 2017.

[74] Xin she yang "Nature-inspired metaheuristic algorithms", Luniver press, UK, Second edition, 2010.

[75] Marc. T. Thompson, "Eddy current magnetic levitation Models and experiments"IEEE Pottentials, pp.40- 44, 2000.

[76] Ebrahim, M. Khodabakhsh, M. and Vossough, G, "An Analytical 3-D Model for calculating eddy current damping force for a magnetic levitation system with permanent magnet," IEEE Transc. On Magnetics, Vol 48, No.9, pp. 2472-2478, Sept 2012

[77] H. A Sodano and J.S. Bae, "Eddy current damping in structures" the shock and vibration digest, Vol. 36, pp. 469-478, Nov 2004.

[78] Babak Ebrahimi, Mir Behard Khamesee and farid Golnaraghi,"a novel eddy current damper: theory and experiment",J. Phys. D: Appl. phys. 42, 2009.

[79] Gautam Sinha and S. S. Prabhu, "Analytical model for estimation of eddy current and power loss in conducting plate and its application", Phys. Rev. Special Topics-Accelerators and Beams, vol. 14, no. 6, p. 062401, Jun 2011.

[80] Chih-Hsien Lin, Shao kung hung, sang T sung, Li, and Li-chen fu, "High precision Eddy current damped electromagnetic positioner with flexure-Suspenssion" IEEE Multi conference on systems and control saint petersburg, pp.1568-1573, Jul 2009

[81] C.Elbuken, E.Shameli and M. B. Khamesee, "Modelling and analysis of eddy current damping for high precision magnetic levitation of a small magnet", IEEE Trans.Magn., vol. 43, no.1, pp. 26-32, Jan 2007.

[82] Hong song and Nathan Ida, "An Eddy current constrained formulation for 3D electromagnetic field calculations", IEEE Transactions on Magnetics, vol.27, no.5, Sept 1991.

[83] J. D. Jackson, "Classical Electrodynamics" New York, Wiley, 1999.

[84] J. Sung Bae, J. H. Hwang, J. Sam Park and D. Gi Kwag, "Modeling and experiments on eddy current damping caused by a permanent magnet in a conductive tube", Jornal of

Mechanical science and Technology, vol. 23, pp. 3024-3035, 2009.

[85] Hamid Yaghoubi, "Practivcal Applications of Magnetic Levitation Technology," Iran Maglev Tachnology, sep 2012.

[86] Cermak R., Barton L., Spal P., Bartak J. and Vavrik J., "Overview of Magnetic Levitation Principles and their application in Maglev systems, " Advanced Engineering, ISSN 1846-5900, 2008.

[87] M. Ono, S. Koga, and H. Ohtsuki, "Japan's superconducting maglev train", IEEE Instrum. Meas. Mag., vol. 5, no. 1, pp. 9–15, Mar 2002.

[88] Brooks, J.S. ; Reavis, J.A. ; Medwood, R.A. ; Stalcup, T.F. , "New opportunities in science, materials, and biological systems in the low-gravity (magnetic levitation) environment", IEEE Journal of Applied Physics, Vol. 87, no. 18, pp.6194-6199, June 2009.

[89] Arnie Heller, "Maglev on the Development Track for Urban Transportation" Lawrence Livermore National Laboratory, S&TR November 2003.

[90] Elbuken. C, Khamesee. M. B, and Yavuz. M, "Eddy current damping force for magnetic levitation: downscaling from macro micro levitation, " J. Appl. Phys. Vol 39, no. 18, pp. 3932-3938, Sept 2006.

[91] Ebrahim, M. Khodabakhsh, M. and Vossough, G, "An Analytical 3-D Model for calculating eddy current damping force for a magnetic levitation system with permanent magnet," IEEE Transc. On Magnetics, Vol 48, No.9, pp. 2472-2478, Sept 2012

[92] Maria Hypiusova and JakubOsusky, "PID controller design for magnetic levitation model", CIVB International Conference February 10 - 13, 2010.

[93] Hong song and Nathan Ida, "An Eddy current constrained formulation for 3D electromagnetic field calculations", IEEE Trans. on Magnetics, Vol. 27, no.5, Sept. 1991.

[94] H. A Sodano and J.S. Bae, "Eddy current damping in structures" the shock and vibration digest, Vol. 36, pp. 469-478, Nov. 2004.

[95] Jiang Dong, Yang Jia-xiang, Ma Ling-ling and Jiang Di, "Model building and simulating for hybrid magnetic levitation ball system," Mechanic Automation and Control Engineering (MACE), 2010 International Conference in Wuhan 26-28 June 2010, pp. 6105 – 6110.

[96] Suster. P, Jadlovska. A, "Modeling and control design of Magnetic levitation system," in Applied Machine Intelligence and Informatics (SAMI), Jan- 2012 IEEE 10th International Symposium, pp.295-299, ISBN online: 978-1-4577-0196-2.

[97]   Shunli Xiao, Yangmin Li and Jinguo Liu "A Model Reference Adaptive PID Control for Electromagnetic Actuated Micro-positioning Stage", the Eighth Annual IEEE International Conference on Automation Science and Engineering (CASE), August 20-24, 2012, Seoul, Korea, pp.97-102.

[98]   Astrom, K. J. and Wittenmark, B., Adaptive Control, Addison-Wesley, Reading, MA, 1995.

[99]   Hang, C. C. and Parks, P. C., 'Comparative studies in model reference adaptive control systems', IEEE Transactions on Automatic Control 18, 1973, 419–428.

[100] Oldham, K. B. and Spanier, J., The Fractional Calculus, Academic Press, New York, 1974.

[101] Podlubny, I., Fractional Differential Equations, Academic Press, San Diego, CA, 1999.

[102] Petras, I., 'The fractional-order controllers: Methods for their synthesis and application', Journal of Electrical Engineering 50(9–10), 1999, 284–288.

[103] Podlubny, I., 'Fractional-order systems and $PI^\lambda D^\mu$-controllers', IEEE Transactions on Automatic Control 44(1), 1999, 208–214

[104] Podlubny, I., Fractional Differential Equations, Academic Press, San Diego, CA, 1999.

[105] Debnath, L., Integral Transforms and Their Applications, CRC Press, Boca Raton, FL, 1995.

[106] Oustaloup, A., Sabatier, J., and Lanusse, P., 'From fractal robustness to CRONE control', Fractional Calculus & Applied Analysis 2(1), 1999, 1–30.

[107] Wong T. "Design of a magnetic levitation system - an undergraduate project", IEEE Transactions on Education, 29, 1986, 196-200.

[108] Wodson, H., and Melcher, j., Electromechanically Dynamics- Part 1: Discrete Systems (New York: Wiley) 1968.

[109] S. Xiao, Y. Li and X. Zhao, "Design and analysis of a novel flexurebased XY micro-positioning stage driven by electromagnetic actuators", Int. Conf. on Fluid Power and Mechatronics, Beijing, China, pp.953- 958, August 17-20, 2011

[110] M.A Henson and D.E. Seborg "critique of exact linearization strategies for processes control" Journal of process control, 1, pp.122-139, 1991.

[111] A. Isidori, "Nonlinear control systems", Springer-Verlag, New York, NY, 1989.

[112] J.C Kantor, "An overview of nonlinear geometrical methods for process control", shell Process control workshop, pp.225-250, London, 1987.

[113] C Kravaris and Y Arkun, "Geometric nonlinear control –An Overview", chemical process control IV, CACHE, AIChE, Austin, TX, 1991.

[114] C Kravaris andJ C Kantor, "Geometric methods for nonlinear process control: 1 Background" Ind. Eng. Chem Res., 29, pp.2295-2310, 1990.

[115] C Kravaris and J C Kantor, "Geometric methods for nonlinear process control: 2 Control Synthesis" Ind. Eng. Chem. Res., 29, pp.2310-2323, 1990.

[116] P.J Mclellan, T.J Harris and D.W. Bacon, "Error trajectory descriptions of nonlinear controller design" chem. Eng. Sci, 45, pp. 3017-3034, 1990.

[117] H Nijmeijer and a.J. Van der schaft, "Nonlinear Dynamical control systems", Springer-Verlag, New York, NY, 1990.

[118] A. Isidori, Nonlinear Control Systems, 3rd ed. Berlin, Germany: Springer-Verlag, 1995.

[119] H. K. Khalil, Nonlinear Systems, 3rd ed. Upper Saddle River, NJ, USA: Prentice-Hall, 2002.

[120] John Hauser, Shanker Sastry and Peter Kokotovic, "Nonlinear Control Via approximate input-output linearization: The ball and beam Example" IEEE Transactions on Automatic Control, vol.37, No.3, pp.392 -398, 1992.

[121] Ting-Li Chien, Chung-Cheng Chen, and Chiou-Jye Huang, "Feedback Linearization Control and Its Application to MIMO Cancer Immunotherapy" IEEE Transactions on Control Systems Technology, vol. 18, No. 4, pp.953-961, 2010.

[122] Jing Lei and Hassan, "Feedback Linearization for Nonlinear Systems with Time-Varying Input and Output Delays by Using High-Gain Predictors" IEEE Transactions on Automatic Control, vol. 61, no. 8, pp. 2262-2268, 2016.

[123] L. Yan, L. Hsu, R. R. Costa, and F. Lizarralde, "A variable structure model reference robust control without a prior knowledge of high frequency gain sign," Automatica, vol. 44, no. 4, pp. 1036–1044, 2008.

[124] T. R. Oliveira, A. J. Peixoto, E. V. L. Nunes, and L. Hsu, "Control of uncertain nonlinear systems with arbitrary relative degree and unknown control direction using sliding modes," Int. J. Adapt. Control Signal Process., vol. 21, no. 8/9, pp. 692–707, 2007.

[125] Shaocheng tong, Yue Li, Yongming Li and yanjun Liu, "Observer-Based Adaptive Fuzzy Backstepping Control for a Class of Stochastic Nonlinear Strict-Feedback Systems" IEEE Transactions on Systems, Man, and Cybernetics –Part B: Cybernetics, Vol.41, No.6, pp.1693-1704, 2011.

[126] A. R. Benaskeur and A. Desbiens, "Backstepping-based adaptive PID control", IEE Proceedings –Control Theory and Applications,vol.149,No.1, pp. 54-59,2002.

[127] Tarek Madani and Abdelaziz Benallegue "Backstepping Control for a Quadrotor Helicopter" IEEE Proceedings of the

International conference on Intelligent robots and systems, pp.3255-3260, Oct 2006.

[128] Ch.V.N. Raja, Ananthababu P, D. V. P Latha and K. R Sudha, "Design and analysis of position controlled eddy current based non-linear magnetic levitation system using LMI", pp.137-142, Nov 2015.

[129] Hyung-Woo Lee., Ki-Chan Kim., and Ju Lee., "Review of maglev train technologies," IEEE Transactions on Magnetics, vol. 42, no. 7, 2006, pp. 1917–1925.

[130] Adrian Vasile Duka., Mircea Dulau., and Stelian Emilian Oltean., "IMC based PID control of a Magnetic Levitation Systems," Procedia Technology, vol. 22, 2016, pp. 592-599.

[131] Z. Yang and G. Pedersen., "Automatic tuning of PID controller for a 1-D levitation system using a genetic algorithm - a real case study", Proceedings of IEEE International Symposium on Intelligent Control, Munich, Germany, 2006, pp. 3098-3103.

[132] Pallav., S, K, Pandey., V, Laxmi., "PID control of magnetic levitation system based on derivative filter," Annual International Conference on Emerging Research Areas: Magnetics, Machines and Drives, 2014, pp. 1-5.

[133] Maria, H., Alena, K., "Robust PID Controller Design for the Magnetic Levitation System: Frequency Domain Approach,"

International Conference on Process Control, June 2017, pp. 274-279.

[134] Witchupong, W., Sarawut, S., "Stabilization of a magnetic levitation control system via state-PI feedback," International Journal of Mathematical models and methods in applied sciences, 2013, vol.7, no.7, pp. 717-727.

[135] C, H, Kim., "Robust Control of Magnetic Levitation Systems considering Disturbance Force by LSM Propulsion Systems," IEEE Transactions on Magnetics, 2017, vol. PP, no.99, pp.1-1.

[136] Hongpo, Wang., Jie Li., Kun Zhang., "Optimizing Control Algorithms of the Magnetic Levitation System Based on the State Observer," Proceedings of the 6th World Congress on Intelligent Control and Automation, June 2006, Dalian, China, pp. 6508 -6512.

[137] R, J, Wai., J, D, Lee., K, L, Chuang., "Real-Time PID Control Strategy for Maglev Transportation System via Particle Swarm Optimization," IEEE Transactions on Industrial Electronics, vol. 58, no. 2, 2011, pp. 629-646.

[138] I, Ahmad., M, Shahzad., P, Palensky., "Optimal PID control of Magnetic Levitation System using Genetic Algorithm," IEEE International Energy Conference, Cavtat, 2014, pp. 1429-1433

[139] Wang F., He X-S., Wang Y., Yang SM., "Markov model and convergence analysis based on cuckoo search algorithm," Computer Engineering, vol. 38, no.11, 2012, pp.180–5.

[140] Civicioglu, P., Besdok, E., "A conception comparison of the cuckoo search, particle swarm optimization, differential evolution and artificial bee colony algorithms," Artif Intell Rev 2013, vol. 39 no.3, pp. 315–46.

[141] Dhivya, M., Sundarambal, M., Anand, LN., "Energy efficient computation of data fusion in wireless sensor networks using cuckoo-based particle approach (CBPA)" Int. J. of Communications, Network and System Sciences, 2011, vol. 4, no.4, pp. 249–55.

[142] Åström., Karl Johan., Tore, Hagglund., "PID controllers: theory, design, and tuning," Vol.2. Research Triangle Park, NC: Isa, 1995.

[143] Umenai, Y., Uwano, F., Tajima, Y., Nakata, M., Sato, H., Takadama, K., "A modified cuckoo search algorithm for dynamic optimization problems," Int. IEEE Congress on Evolutionary Computation (CEC), pp. 1757–1764, 2016.

[144] Xin-She, Y., Suash, D., "Cuckoo search via levy flight" International World Congress on Nature and Biologically Inspired Computing, NaBIC 2009, pp. 210–214.

[145] M. Mareli and B. Twala, "An adaptive Cuckoo search algorithm for optimisation", Applied Computing and Informatics, In press, 2017.

[146] X.S. Yang and S. Deb, "Engineering optimization by Cuckoo search", International Journal of Mathematical Modelling and Numerical Optimisation, Vol.1 no.4, pp.330-343, 2010.

[147] Amir Zare Bazghaleh, Mohammad Reza Naghashan, and Mohammad Reza Meshkatoddini "Optimum Design of Single-Sided Linear Induction Motors for Improved Motor Performance" IEEE Transactions on Magnetics, vol. 46, no. 11, pp.3939 – 3947, 2010.

[148] Yaghoubi, H. "The most important Maglev applications" Journal of Engineering, Vol. No. 2013, Article ID 537986, 19 pages, 2013.

[149] G. Kratz, (1979). Der Linearmotor in der Antriebstechnik. Technische Mitteilungen AEG-Telefunken, vol. 69, pp. 65–73.

[150] Poitout. S, and P. J. Costa Branco. (2006). Theoretical modeling and experimental tests of an electromagnetic fluid transportation system driven by a linear induction motor, IEEE Trans. Magn., vol. 42, no. 9, pp.2133–2151.

[151] Haghmaram, R. and Shoulaie, A. (2006). Transient modeling of multiparallel tubular linear induction motors, IEEE Trans. Magn., vol. 42, no. 6, pp. 1687–1693.

[152] Xu Qiwei, Cui Shumei, Zhang Qianfan, Song Liwei, Xiyuan Li Sensorless control research for linear induction motor based on sliding mode observer in electromagnetic aircraft launch system, IEEE International symposium on Electromagnetic launch Technology (EML), La Jolla, CA, pp.1-7, 2014.

[153] Nasar, S.A. and Boldea, I., (1987). Linear Electric Motors, Prentice-Hall, Inc., Englewood Cliffs, New Jersey.

[154] E.R. Laithwaite, (1965). Electromagnetic levitation, Proc. IEE, 12, pp. 2361 – 2375.

[155] I. K. Bousserhane, A. Boucheta, A. Hazzab, B. Mazari, M. Rahli, M.K. Fellah, (2009). Adaptive backstepping controller design for linear induction motor position control, U.P.B. Sci. Bull., Series C, Vol. 71, No. 3, pp. 171-186.

[156] Wei Xu, Jian Guo Zhu, Yongchang Zhang, Yaohua Li, Yi Wang, Youguang Guo. (2010). An Improved Equivalent Circuit Model of a Single-Sided Linear Induction Motor, IEEE Transactions on Vehicular Technology, vol. 59, No. 4, pp. 2277–2289.

[157] R. J. Wal, D. C. Liu, and F. J. Lin. (1999). Rotor time-constant estimation approaches based on energy function and sliding mode for induction motor drive, Elect. Power Syst. Res., vol. 52, pp. 229-239.

[158] J. F. Gieras, (1994) 'Linear Induction Drives' Oxford, U.K, New Clarendon Press.

[159] Poloujadoff, M., "Linear induction machines", Part II – Applications, IEEE Spectrum, March 1971, pp. 77-86.

[160] Del Toro, V., "Electric Machines and Power Systems", Prentice-Hall, Inc., Englewood Cliffs, New Jersey, 1985.

[161] S. A. Nasar and I. Boldea, "Linear motion Electric Machines", John Wiley and Sons., New York 1976.

[162] Stephen J. Chapman, "Electric Machinery Fundamentals", McGraw-Hill, 1999.

[163] Gieras, J.F., Linear Induction Drives, Oxford University Press, Inc., New York 1994.

[164] Pai, R.M., Boldea, I., Nasar, S.A., "A complete equivalent circuit of a linear induction motor with sheet secondary", IEEE Transactions on Magnetics, Vol. 24 , no. 1, pp. 639 – 654, 1988

[165] Nasar, S.A. and Boldea, I., Linear Electric Motors, Prentice-Hall, Inc., Englewood Cliffs, New Jersey, 1987.

[166] M. Jalili-Kharaajoo, M. M. Tousi, H. Bagherzadeh and A. E. Ashari, "Sliding mode control of voltage-controlled magnetic levitation systems," *Proceedings of 2003 IEEE Conference on Control Applications,* pp. 83-86, vol.1, Istanbul, Turkey, 2003

[167] A. K. Ahmad, Z. Saad, M. K. Osman, I. S. Isa, S. Sadimin and S. S. Abdullah, "Control of Magnetic Levitation System Using Fuzzy Logic Control," Second International Conference on Computational Intelligence, Modelling and Simulation, Tuban, pp. 51-56, 2010.

LIST OF PUBLICATIONS FROM RESEARCH WORK

1. Ananthababu, P., Ch. V. N. Raja., D.V.P Latha and Sudha, K.R., 'Design of fractional model reference adaptive PID controller to magnetic levitation system with permagnet', International Journal of Systems, Control and Communications (IJSCC), Inderscience Publishers, Vol.7 , No.1, pp.35-44, 2016

2. Ananthababu, P., Ch. V. N. Raja., D.V.P Latha and Sudha, K.R., 'Design, Implementation and Speed tracking of Linear Induction Motor for Maglev Transportation System', Springer Advances in Intelligent Systems and Computing Series, International Conference on Soft Computing, Intelligent Systems and Applications, 8th – 9th April 2016, Bangalore, pp.108-114, 2016

3. Ch. V. N. Raja., P. Ananthababu., D.V.P Latha and Sudha, K.R. 'Design and Analysis of Position Controlled Eddy Current Based Nonlinear Magnetic Levitation System Using LMI' International Conference on Control, Communication & Computing India, 19th–21st November 2015, Trivandrum, IEEE Conference Publication, pp.137-142, 2015

4. Ananthababu, P., Sudha, K.R., 'Backstepping Sliding Mode Control approach to Nonlinear Magnetic Levitation System', National Conference on Recent Advances in Power Electronics, Power and Control Systems Engineering (RAPEPCSE 2016), 6th – 7th Oct 2016, Visakhapatnam.

5. Ananthababu, P., Sudha, K.R., 'Optimal Control of Magnetic Levitation System based on Cuckoo Search Algorithm', International Journal of Computational Systems Engineering, Inderscience Publishers, 2017 (In Press)

6. Ananthababu, P., Sudha, K.R., 'Backstepping Based Fuzzy Sliding Mode Control for tracking nonlinear Maglev System', Journal of Engineering Science and Technology Review, 2017 (Under review)

APPENDIX

Reference	Technique
Ahmed El Hajiaji et al. [35]	A non-linear control law based on differential geometry
Bhawna T, et al. [29]	Sum of Squares (SoS) technique
Chang. Wu et al. [39]	Generalized predictive self-tuning control based on Controlled Auto-Regressive Integrated Moving-Average (CARIMA) model
Kim K et al. [37]	Indirect method for self-tuning PID controller gains
Rosalia H Subrata et al. [30]	PID controller to stabilize floating objects in Maglev systems
Sirsendu S. M, et al. [28]	Coefficient Diagram Method based PID controller
A. S. C. Roong et al. [31]	Model based feed forward PI-PD controller
R J Wai et al. [36]	PID controller based on particle swarm optimization
M Shafiq et al. [38]	Controller based on adaptive finite impulse response (FIR) filter
A. Rawat et al. [42]	Adaptive linear and neuro controller
I. Mizumoto et al. [43]	Almost Strict Positive Real (ASPR) based adaptive PID controller

Feng Li, K et al. [47]	Novel PTC method using multirate feed forward control
T.T Salim et al. [54] A.K. Ahmad et al. [167]	Fuzzy logic controller
R. E. Precup, et al. [32]	Takagi-Sugeno (T-S) fuzzy
K. H. Su et al. [34]	Fuzzy and supervisory fuzzy models based on gradient descent algorithm
Q. Chen et al. [51]	Designed a decentralized PID controller
N. Kanagara et al. [50]	Intelligent fuzzy fractional order PID Controller
Dan Cho, et al. [27] M. J. Kharaajoo et al. [166]	Sliding mode controller
T. George et al. [49]	Hybrid technique for tuning time delay system

Table A.1 Reference table